Department of Chemical Engineering

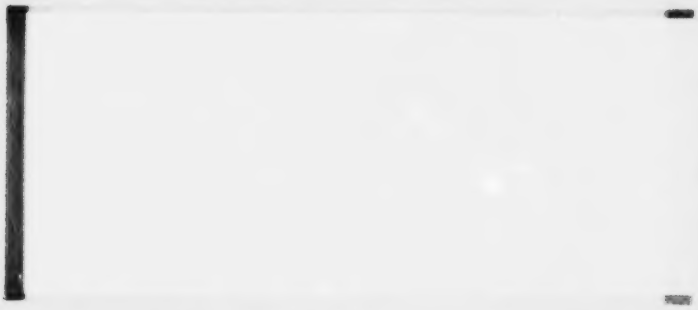

The University of Alberta
Edmonton, Alberta
Canada T6G 2G6

"ROLE OF CATALYSTS IN HETEROATOM REMOVAL DURING HYDROPROCESSING OF MODEL COMPOUNDS"

DSS File Number: 37 SV.23440-4-9261

CONTRACT SERIAL NO. 1SV84-00197

CONTRACTOR: University of Alberta

FINAL REPORT

"ROLE OF CATALYSTS IN HETEROATOM REMOVAL DURING HYDROPROCESSING OF MODEL COMPOUNDS"

DSS File Number: 37 SV.23440-4-9261

Principal Investigator:
I.G. Dalla Lana

Research Associates:
M. Konkin and W. Przystajko

Scientific Authority:
C. Fairbridge (EMR)

July 4, 1986

Department of Chemical Engineering
University of Alberta
Edmonton, Alberta
T6G 2G6

139 pp

OCT 14 1988
MICROMEDIA

SUMMARY OF RESULTS

1. Comment: An up-to date very extensive literature survey of considerable value to other researchers in this area has been completed. The critical evaluation and correlation of data from various sources is of special interest.

   Recommendation: This literature survey has been prepared in a form suitable for easy reproduction. It would be of value to issue these as "Information Circulars" in the EMR publications series.

2. Comment: A novel self-compensating pressure seal suitable for high-vacuum and high-temperature operations was developed. This design will be submitted as a short paper to Review of Scientific Instruments.

   Recommendation: Since the above was developed under the terms of the research contract with DSS, the possibility of patenting this self-compensating pressure seal should be examined before the above publication is released.

3. Comment: Construction of the IR cell-flow reactor is now underway at the Department of Chemical Engineering at the University of Alberta. In addition, the TPD-MS apparatus is being constructed and/or assembled.

   Recommendation: The applicability of the pressure seal to the IR cell-reactor will be demonstrated. The applicability of the apparatus to catalyst pre-treatment and catalytic activity studies will be tested. This work will be

reported to EMR as it develops because of its relevance to sulfidation and activation of HDS catalysts.

4. Comment: The many difficulties and delays in the experimental studies of H_2S uptake on MoO_3/Al_2O_3 catalysts were eventually hurdled. As a result, the data obtained are not as extensive as was earlier anticipated. The results are now being finalized and should be available before the summer of 1986 is over.

Recommendation: These results will be produced in the form of a manuscript to be submitted for publication. This manuscript will be provided to EMR for their information.

INTRODUCTION

Unconventional sources of hydrocarbons in Canada, such as bitumens, heavy oils, and coal-derived liquids, require the elimination of sulphur and nitrogen from their upgraded products. While studies of catalytic hydrodesulphurization are prevalent worldwide, the focus has largely been upon the role of Co-Mo/Al_2O_3 catalysts. Much less activity has been directed towards characterizing and elucidating the role of Ni-Mo/Al_2O_3 catalysts, and yet the latter is extensively, if not exclusively, used by Syncrude and Suncor in their operations for upgrading Athabasca bitumen. This research project was originally directed towards fundamental studies of the Ni-Mo/Al_2O_3 catalyst, with particular emphasis upon correlating catalytic reactivity (towards HDS of a model compound such as thiophene) with the nature of the catalyst as it proceeds from the original oxidic state to its activated sulphided form.

Upon commending the project, a literature survey revealed the complexity of the project; thus, its focus was narrowed towards elucidation of the Mo oxide-promoted alumina catalysts. This report, then, describes the major activities and results obtained for the period November 5, 1984 to February 28, 1986.

The report focuses upon the following actions:

A. Critical literature survey related to MoO_3 supported on alumina.

B. Preparation of appropriate catalysts including chemical analytical details.

C. Design and construction of apparatus appropriate for study of adsorption and surface reactions on the catalyst; and, for combining this capability with measurements of the steady-state catalytic reaction rate.

D. Progress in fundamental research on catalytic HDS with MoO_3/Al_2O_3 catalysts.

A. LITERATURE SURVEY

A-1. Introductory comments.

A-2. Molybdena-alumina catalysts.

A-3. Molybdenum disulfide.

A-4. Adsorption of O_2, NO and CO molecules on oxidic, reduced and sulfided catalyst- MoO_3/Al_2O_3.

A-5. Hydrodesulfurization on MoO_3/Al_2O_3 catalysts.

LITERATURE SURVEY

Introductory Comments

An immense amount of work has been done on catalytic hydrodesulfurization (HDS) and hydrodenitrogenation (HDN). Two broad subject areas have been studied in this field: i) the effects of catalysts on model compounds such as thiophene (along with related sulfur compounds and products), and pyridine and quinoline (along with their related nitrogen compounds and products), and ii) characterization of the catalysts themselves. If one can understand the catalytic behaviour in terms of a) metal loading; b) calcination temperature and time; c) support effects; and, d) preparation method, one may learn about the types of reactive sites and concentrations of these sites present upon the various catalysts. A knowledge of these sites can lead to a better understanding of the hydrogenation and hydrogenolysis reactions of model compounds on these catalysts.

To this end, numerous techniques have been applied: XRD; ESR and NMR; IR, UV-visible reflectance and laser Raman spectroscopies; XPS (or ESCA), ISS, EXAFS, Mössbauer spectroscopy; TEM and SEM; TPD and TPR; volumetric and gravimetric studies; chemical analyses; electrophoresis; and reactor studies (using some of the other techniques plus GC), and likely others as well.

This accumulated body of work is beginning to provide a more general understanding of the structure of some of these HDS and HDN catalysts. These catalysts include Mo-alumina, Ni-alumina, Co-alumina, Ni-Mo-alumina and Co-Mo-alumina (as well as W, Ni-W

variations) in oxidic and sulfided forms. In correlating results obtained using various techniques or from different workers using the same technique, difficulties arise because of the non-standardization of catalyst preparation methods and expression of results.

First, different groups often use different alumina supports (with varying surface areas, m^2/g) and different ways of expressing metal loading (i.e. wt% metal oxide, wt% metal, number of metal atoms/g or number of metal atoms/nm^2). At present it is probably most useful to express the metal loading as the number of metal atoms per unit area of original support (#metal atoms/nm^2), a surface density. This reduces confusion due to a wt% expression of metal or metal oxide loading on supports of varying BET surface areas (100 m^2/g to 300 m^2/g). It also allows one to form ideas on configurations and dimensions of molecules or groups of molecules on the surface based on a knowledge of bond lengths and dimensions of various model compounds.

Secondly, calcination times and temperatures also vary. These two parameters affect the types of compounds formed on the support as well as the sizes of any crystallites grown.

In studies of Mo-alumina, a loading range of 1.25-20wt% MoO_3 on 101 m^2/g Al_2O_3 leads to values of 0.53-10.4 Mo atoms/nm^2, whereas on 196 m^2/g Al_2O_3 the values for this range are 0.22-5.34 Mo atoms/nm^2. Now, depending upon metal loading and calcination, one can have the molybdenum in the forms of isolated molybdate units, molybdate clusters or aggregates, aluminum molybdate, molybdenum trioxide or combinations of the above. Molybdenum coordination may also be tetrahedral or octahedral. At some point below theoretical monolayer coverage multilayer formation may begin. Unless one standardizes the

support-loading expression the results of the studies will at first glance appear to conflict wherease in fact they support each other.

The results from some of these Mo-alumina studies suggest that results of IR work on differently loaded catalysts will not simply be proportional to the loading but will depend upon the surface species particular to that loading.

MOLYBDENA-ALUMINA CATALYSTS

Alumina supported molybdena catalysts are of great interest for hydrodesulfurization and hydrodenitrogenation. The catalyst is generally prepared by an impregnation technique in which the alumina support is wetted with a minimal amount of aqueous solution of ammonium heptamolybdate [$(NH_4)_6\ Mo_7O_{24}.4\ H_2O$] to give the desired molybdenum loading in the catalyst. After impregnation the material is usually dried for about 12 hours (or overnight) at 110°-120°C then calcined at temperatures of 400-700°C (usually 500-550°C) for times of 2-24 hours.

This review of molybdena-alumina catalysts will deal mainly with the effects of the molybdenum loading and to a lesser extent with the effects of calcination time and temperature. Various authors express the Mo loading in different ways: wt% MoO_3, wt%Mo, number of metal atoms/nm^2. Since, at its smallest, molybdena is in the form of molydate ion MoO_4^{2-} in the impregnation solution and will be deposited (and/or chemisorbed) primarily on the alumina surface (unlike Ni^{2+} or Co^{2+} which can easily diffuse past the first atomic layer of alumina), it is most convenient at this point to express molybdena loading as the number of Mo atoms present per unit area of alumina surface, - #Mo atoms/nm^2. This reduces confusion since different surface areas of aluminas can be taken into account. The area to be used in loading expression conversion calculations will be the original, unloaded alumina surface area usually expressed as m^2/g.

The following conversion calculation for wt% MoO_3 is used:

$$\frac{X}{M.W.} \cdot \frac{NA}{SA} = \text{number of Mo atoms/nm}^2 , \qquad X = \frac{\text{wt\% } MoO_3}{100 - \text{wt\% } MoO_3}$$

where x is the weight in grams of MoO_3 added to 1 gram Al_2O_3, MW is the molecular weight of MoO_3, NA is Avogadaro's number, and SA is the surface area of 1 gram of unloaded alumina. For example, 10 wt% MoO_3 on gamma-alumina with a 200 m^2/g surface area would yield

$$\frac{10 \times 6.02 \times 10^{23}}{90 \times 143.9 \times 200 \times 10^{18}} = 2.32 \text{ Mo atoms/nm}^2$$

This expression for molybdenum loading in no way implies that the Mo is uniformly distributed over the alumina surface. At a certain point, well under theoretical monolayer coverage (5 Mo/nm^2) aggregation starts to occur as will be shown below.

We look at the work of authors who have used the impregnation technique but with no pH adjustment to the impregnating solution of water and ammonium heptamolybdate (pH 5-6). Adjustment of pH alters the state of aggregation of Mo in solution from MoO_4^{2-} at high pH to $Mo_8O_{26}^{4-}$ at low pH [1]. This seems to

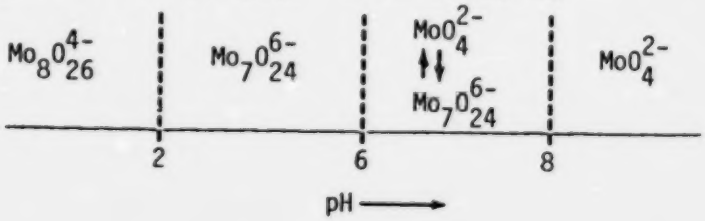

have a bearing on the form of molybdenum in the catalyst and will be dealt with later.

As already mentioned the molybdenum is not always uniformly dispersed on the alumina surface but may exist in several forms depending upon loading. These include: isolated molybdate tetrahedra MoO_4, aggregated or polymeric molybdate groups or clusters, MoO_3, and $Al_2(MoO_4)_3$.

The first tool for studying molybdenum on alumina that we will look at is x-ray diffraction (XRD). This will detect crystalline material of $\geq$ 40A° in size. Looking for crystalline MoO_3 and $Al_2(MoO_4)_3$, the following information is available with respect to different Mo loadings.

Ref.	Alumina	SA	Calcination
[2]	gamma-alumina	175 m^2/g	20 h @540°C
wt%Mo	#Mo/nm^2	MoO_3	$Al_2(MoO_4)_3$
8	3.12	-	
10	3.99	-	
25	11.95	X	
[3]	gamma-Al_2O_3	216 m^2/g	8 h @500°C
wt% MoO_3	#Mo/nm^2	MoO_3	$Al_2(MoO_4)_3$
10	2.15	-	-
15	3.41	-	-
20	4.85	-	-
25	6.45	X	-
30	8.29	X	X

[4] gamma-Al_2O_3 216 m^2/g, various times and temperatures

wt%MoO_3	#Mo atoms/nm^2	MoO_3	$Al_2(MoO_4)_3$
10	2.15	-	-
15	3.41	-	X (700°C min)
20	4.85		X (700°C)
25	6.45	X (450,500°C)	X (450,500,700)
30	8.29	X (350,450,500,700)	X (450,500,700 max.)

Note: pH 3.9-4.9 with H_2O and H_2O_2

---

[5] gamma-Al_2O_3 183 m^2/g

wt%Mo	#Mo/nm^2	MoO_3	$Al_2(MoO_4)_3$
4.7	1.69	-	-
7.8	2.80	-(500,750°C)	-(500,750°C)
7.6	2.82	-(500,750°C)	-(500,750°C)

---

[6] gamma-Al_2O_3 213 m^2/g 2h @ 550°C

#Mo/nm^2	MoO_3	$Al_2(MoO_4)_3$
4.48	-	-
4.68	-	-

ALON, gamma-alumina 100 m^2/g 6 h @550°C. Used in this laboratory as received.

#Mo/nm^2	MoO_3	$Al_2(MoO_4)_3$
5.97	X	X
4.86	-	X
3.74	-	-

These results indicate that below 5 Mo/nm^2, 40A° size MoO_3 crystallites are not detected, whereas above 6 Mo/nm^2 they are definitely present. $Al_2(MoO_4)_3$ is also detected, but its presence is a strong function of both calcination temperature and time, as well as loading. Higher calcination temperatures are conducive to its formation. At 700-750°C, it is not seen at 2.82 Mo/nm^2 but is detected at 3.41 Mo/nm^2 and above. At 500°C, however, it is not seen until ~6.5 Mo/nm^2 and above. Note that the lowered pH of [4] as opposed to [3] may have favored $Al_2(MoO_4)_3$ formation.

Next we will turn our attention to Laser Raman Spectroscopy (LRS). Spectra of reference compounds observed using LRS are presented by Zingg et al. [7] and include $(NH_4)_6 Mo_7O_{24}\cdot 4H_2O$, MoO_3, gamma-Al_2O_3 and $Al_2(MoO_4)_3$. Present predmoninantly at low concentrations is the so called interaction species, characterized by a broad skewed band peaking at about 950-980 cm^{-1}. This represents molybdate eithe in monomeric or aggregate (polymeric) form interacting with the alumina. Characteristic peaks for MoO_3 are 996, 822 and 667 cm^{-1}, and for $Al_2(MoO_4)_3$, 1030, 1006 and 380 cm^{-1}.

[8] gamma-alumina 240 m^2/g 19 h @600°C in O_2

wt% MoO_3	#Mo/nm^2	MoO_3	$Al_2(MoO_4)_3$
15	3.08	-	-
20	4.36	-	-
25	5.81	-	trace
30	7.47	-	trace
2 h @600 only	7.47	X	X

---

[8] gamma-alumina 80 m^2/g 2 h @600°C in air

wt% MoO_3	#Mo/nm^2	MoO_3	$Al_2(MoO_4)_3$
6	3.84	-	-
9	5.18	trace	X
12	7.14	trace	X
15	9.23	X	X

---

[9] gamma-alumina 101 m^2/g 6 h@500°C

wt%MoO_3	#Mo/nm^2	MoO_3	$Al_2(MoO_4)_3$
5	2.18	-	-
7.5	3.36	estimated threshold	
10	4.60	X	-
15	7.30	X	-
20	10.35	X	-

[7] gamma-alumina 196 m^2/g 16h @500°C

wt% MoO_3	#Mo/nm^2	MoO_3	$Al_2(MoO_4)_3$
9	2.11	N/A*	N/A
11	2.64	N/A	N/A
15	3.77	X1-6 h 500°C	trace>16h @500°C
20	5.34	X	trace 500 X 600,700°C
25	7.12		X
30	9.14	X	- 500°C

*N/A data not available.

From these results, we see that MoO_3 can be detected first at about 3.4 Mo/nm^2 after a short, lower temperature (500°C) calcination. Higher temperatures (>600°C) and longer times make detection more difficult since $Al_2(MoO_4)_3$ formation is then favored at the expense of the MoO_3 starting at about 3.8 Mo/nm^2 (according to these results). Zingg et al. [7] illustrate the effects of calcination time and temperature upon a 20 wt% MoO_3/Al_2O_3 sample (5.34 Mo/nm^2).

A comparison of XRD and Laser Raman Spectra (LRS) results for 500°C calcinations shows that LRS detected MoO_3 at a lower value, 3.4 Mo/nm^2, than XRD with 5-6 Mo/nm^2. Similarly, at 500°C LRS shows the presence of $Al_2(MoO_4)_3$ at 3.8 Mo/nm^2 whereas XRD does not show it until about 6.5 Mo/nm^2. At 700°C XRD will detect $Al_2(MoO_4)_3$ as low as 3.4 Mo/nm^2 but this cannot be compared with LRS because studies at 700°C for this type of loading are not available.

Another LRS study of MoO_3/alumina should be noted. This work of Brown et al [10] is quite anomalous in that only at 14.9 Mo/nm^2 is MoO_3 seen and at 10.2, 6.22 and 2.69 Mo/nm^2, $Al_2(MoO_4)_3$ is seen although not identified as such. These very high aluminum molybdate levels are very unusual in view of a 16 h at 500°C calcination time and impregnation loading. In a later work [11] the same high area alumina (claimed to be gamma-alumina) is used but the 1/32" pellets were ground up and calcined at 500°C for 1 h before Mo impregnation. Results for a 15 wt% MoO_3/Al_2O_3 (3.51 Mo/nm^2) sample show only the interaction species with no apparent MoO_3 or $Al_2(MoO_4)_3$. This conforms with the majority of published data. Perhaps the 90°C drying temperature (as opposed to 120°C) or some amorphous character in the original alumina caused the predisposition to extensive $Al_2(MoO_4)_3$ formation.

Using Extended X-Ray Absorption Fine Structure (EXAFS), two studies [12,13] one with Mo/ Al_2O_3 (2.36 Mo/nm^2) and the other with Co-Mo/ Al_2O_3 (2.34 Mo/nm^2) showed no evidence for crystalline MoO_3. Rather, the results suggested a large degree of disorder, very small crystallites (<10A°) or small patches of crystalline compound with the alumina substrate. Hence, on the basis of these studies (XRD, LRS and EXAFS), a large degree of ordering (>10A°) is not seen below roughly 2.4 Mo/nm^2.

At loadings below which MoO_3 and $Al_2(MoO_4)_3$ are detectable the "interaction species" molybdenum is present in either tetrahedral or octahedral coordination. Work by Chung and Massoth [5] suggests that

molybdenum in tetrahedral coordination Mo[T] is predominant at $\leq$0.7 Mo/nm^2, whereas when the loading reaches 2.8 Mo/nm^2 both octahedral Mo[O] and tetrahedral Mo[T] are present. Results of Zingg et al [7] show Mo[T] to be almost the exclusive species at 0.9 Mo/nm^2 and then increasing simultaneously with Mo[O] for a maximum 1.9 Mo/nm^2 Mo[T] concentration while Mo[O] continues to rise until the loading reaches 4.5 Mo/nm^2. At the low loadings, the Mo[T] are thought to exist in isolation while Mo[O] is thought to exist in octahedral sites or in association with other Mo groups.

To define a beginning of aggregation is difficult although an X-Ray Photoelectron Spectroscopy (XPS) study may help. The work of Edmonds and Mitchell [14] suggests that multilayer or aggregated molybdate can become dispersed with calcination. The following results as given:

wt%Mo	#Mo/nm^2	multilayer or aggregation with drying	monolayer after calcination, 24 h @500°C
2	0.43	X	X
3	0.65	X	X
4	0.87	X	X
9	2.07	X	not completely
15	3.69	X	not completely

This suggests that between 0.9 and 2.0 Mo/nm^2 one has aggregation on the calcined catalyst. If one also looks at a plot of minimum crystallite size of MoO_3 with respect to Mo loading for the XRD and EXAFS results and then extrapolates to zero of crystallite size, one obtains values of 1.2 - 2.0 Mo/nm^2 for the beginning of aggregation on a calcined catalyst. This plot is shown on the following page.

The beginning of aggregation would be expected to follow the formation of Mo-O-Mo bridges. Raman spectroscopy detects a band at about 220 cm^{-1} attributed to Mo-O-Mo deformation [15-17] although Stencel et al [18], suggest it may be due to an O...Mo...O symmetric stretching mode in sixfold coordinated Mo. At any rate, assuming that this band indicates aggregation, one obtains the following results for LRS studies that show sufficient resolution in the 200-400 cm^{-1}

[15] gamma-alumina 210 m^2/g 5 h @550°C in air

wt%MoO_3	#Mo/nm^2	220 cm^{-1} (Mo-O-Mo)
4	0.83	-
8	1.73	-
12	2.71	X
16	3.79	X
20	4.98	X

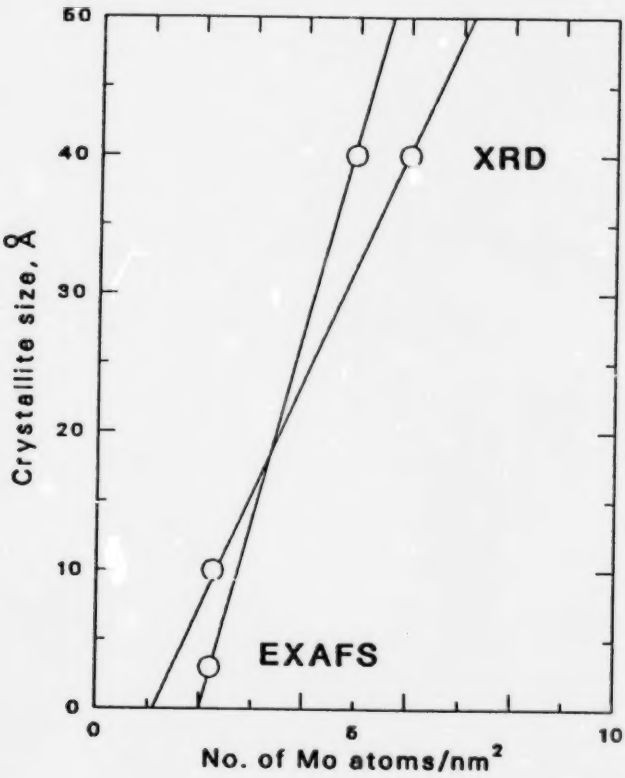

Crystallite size (Å) as a function of Mo loading
(#Mo/nm^2)

[16] gamma-alumina 100 m^2/g 8 h(?) @500°C in O_2

wt%Mo(per 100g Al_2O_3)	#Mo/nm^2	220 cm^{-1} (delta Mo-O-Mo)
1	0.63	-
2	1.26	-
4	2.51	?
6	3.76	X
8	5.02	X

[17] gamma-alumina 158 m^2/g 2 h @500°C in air

wt% MoO_3	#Mo/nm^2	220 cm^{-1}(delta Mo-O-Mo)
3	0.82	-
8	2.30	X(weak)

[18] gamma-alumina 200 m^2/g overnight (16 h?) @500°C in air

wt%MoO_3	#Mo/nm^2	220 cm^{-1} (O...Mo...O)
3	0.65	-
5	1.10	-
10	2.32	X
15	3.38	X
20	5.22	X

From these data it is seen that the 220 cm^{-1} band is not observed below 1.7 Mo/nm^2, while above 2.3 Mo/nm^2 it is present. Adequate LRS data for the region in between these limits have not been found. The previously mentioned XPS study [14] suggests aggregation at 2.1 Mo/nm^2 but not at 0.9 Mo/nm^2. Therefore, based on these studies, aggregation seems to begin at loadings between 1.7 and 2.1 Mo/nm^2 for calcined catalysts.

We now look at the effects of solution pH during catalyst preparation. The pH effects studied in the literature can be divided into two categories: 1) adsorption of a maximum amount of molybdenum from a large volume of ammonium molybdate solution of given pH, and 2) impregnation of a given amount of molybdenum at a certain pH. In the first case, the amount loaded is primarily due to adsorption, while in the second case, any excess molybdenum present that would ordinarily not be adsorbed is deposited on the alumina, with the pH supposedly determining the types of species adsorbed and deposited.

The first method, called equilibrium adsorption [1], involves the adsorption of molybdate from a volume of solution relatively large as compared to the alumina volume. Depending on the pH of the solution, different loadings of molybdenum are obtained, with higher loadings for lower pH values. The pH of the aqueous ammonium heptamolybdate solution (normally pH6) is usually adjusted with HNO_3 or NH_4OH. As mentioned before, the type of molybdate species present in solution varies with respect to pH [1].

The results of studies conducted by Wang and Hall [1], Kasztelan et al [19] and related earlier work by Sonnemans and Mars [20] are compared in the following graph of pH versus Mo uptake. As can be seen the results of Wang and Hall [1] and Kasztelan et al [19] are quite similar. The results of Sonnemans and Mars [20] agree with respect to the maximum and minimum values of loading as well as agreeing in the region above pH6. However, in the region of pH 2-6, their loading is higher than that of the other two works cited, although it never exceeds their maximum. This is likely due to the different conditions employed in this earlier work.

All curves do show similar "plateau" regions for pH 2-6 and pH 9-11 as well as a steep decrease at pH 5-9. The minimum loading is about 0.3 Mo/nm^2 (monomer species region) and the "plateau" region at pH 2-6 (for the two recent works) has values of 2 to 2.6 Mo/nm^2 which is 7 to 8 times the minimum value ((7 or 8) x 0.3 = 2.1 to 2.4). This is the region of heptamer and octamer forms. The step at pH 6-8 corresponds to the transition of $Mo_7O_{24}^{6-}$ to MoO_4^{2-}.

The presence of different species on the catalysts is shown by the ultraviolet-visible reflectance spectra of Wang and Hall [1] which show only tetrahedrally coordinated Mo at pH 8.6 (i.e. monomer MoO_4^{2-} only) while octahedrally coordinated Mo is seen at values of pH 3.9 and pH 1, suggesting the presence of polymeric species.

Turning now to the second case, we find a few studies that have dealt with the influence of impregnation solution pH on the characteristics of the catalysts produced [9,17,21]. In all of these studies pH was adjusted with either HNO_3 or NH_4OH, the pH of the aqueous heptamolybdate solution itself being pH 5-6.

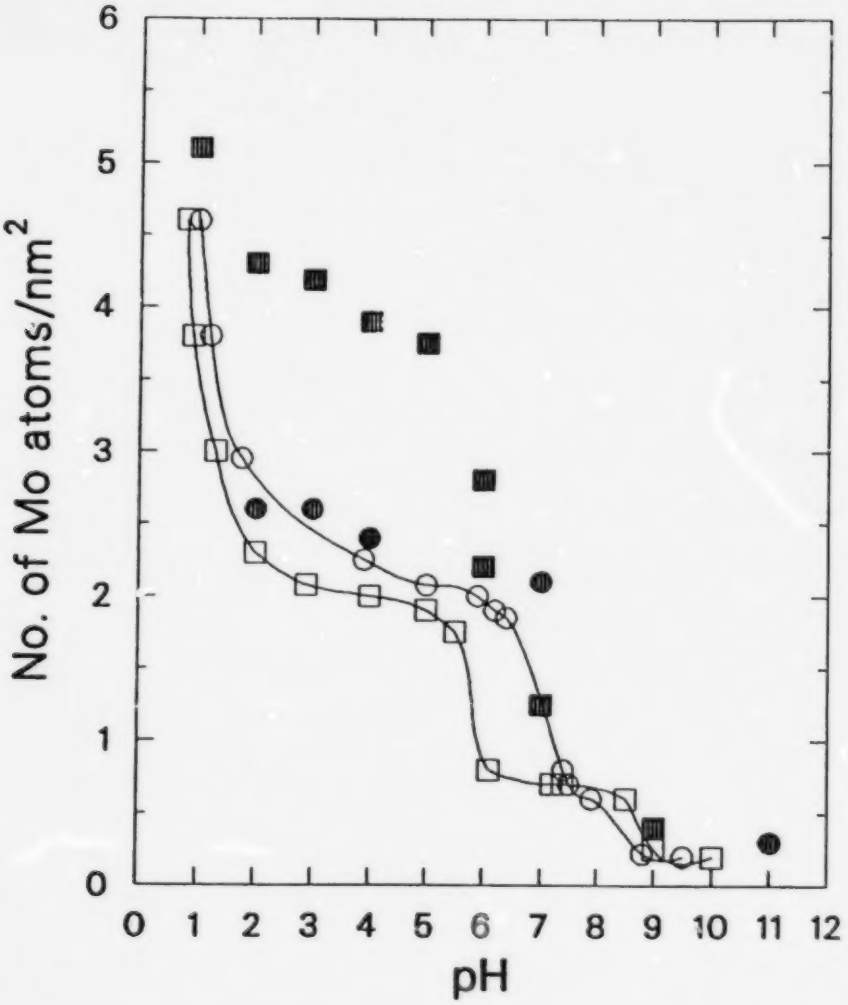

Influence of pH upon Mo loading:

- ○ [1] final pH } equilibrium adsorption method
- □ [1] initial pH }
- ● [19] pH regulated using HNO_3 or NH_4OH
- ■ [20] solution circulated through catalyst bed until final pH = initial pH

Laser Raman work by Cheng and Schrader [9] using a molybdenum loading of 4.60 Mo/nm^2 (10 wt% MoO_3 on 101 m^2/g gamma-alumina calcined 6 h at 500°C) showed prominent MoO_3 bands (as expected) at pH values of 4,7 and 9. The only major changes in the spectra with respect to pH were an increase in the "interaction species" peak at 950 cm^{-1} with an increasing pH and an increase in MoO_3 peaks with decreasing pH.

Another LRS work, one by Jeziorowski and Knozinger [17] showed spectra for samples prepared at pH 6 and pH 11 with loadings of 2.30 Mo/nm^2 and 0.82 Mo/nm^2 (8 and 3 wt% MoO_3 on 158 m^2/g gamma-alumina calcined 2 h at 500°C). In addition, Raman spectra of $Mo_7O_{24}^{6-}$ and MoO_4^{2} anions in aqueous solution were shown [17].

The 2.30 Mo/nm^2 samples both showed evidence of MoO_3 (that at pH 6 showing stronger bands) as well as bands at 334 and 222 cm^{-1} indicative of polymeric species, although for the pH 11 sample only monomeric molybdate is expected to be adsorbed and deposited. In the case of the 0.82 Mo/nm^2 samples, a broad band only at about 330 cm^{-1} (none at 220 cm^{-1}), indicative of the monomeric species, is present in both samples although at pH 6 one expects adsorption of polymeric $Mo_7O_{24}^{6-}$. Oddly enough, this pH 6 sample shows a trace of MoO_3. This seems very strange since the loading is only 0.82 Mo/nm^2.

As determined previously, aggregation is expected to occur at 1.7 to 2.1 Mo/nm^2. The 0.82 Mo/nm^2 loading, which shows momeric molybdate, agrees with this despite what might be expected because of the impregnation pH. Similarly, the 2.30 Mo/nm^2 samples showed the bands indicative of aggregation, regardless of impregnation pH. However, one noticeable effect, present in both LRS studies, is the increase in MoO_3 content with decreasing pH for a given loading level and calcination conditions.

A study by Houalla et al [21] using x-ray photoelectron spectroscopy (XPS) and ion scattering spectroscopy (ISS) correlated with thiophene hydrodesulfurization (HDS) activities was conducted using 2.89 Mo/nm^2 Mo/Al_2O_3 catalysts prepared at pH's 4.0, 5.4, 7.1 and 11.0 (8.1 wt% Mo on 200 m^2/g gamma-alumina calcined 16 h @500°C). Their results suggest that while the pH changes have no dramatic effect on the structure of the final catalysts, an improvement in dispersion is achieved. Secondly, HDS activity is better for pH 4.0 and 5.4 catalysts as opposed to those of pH 7.1 and 11.0 (by a factor of 1.3 in the rate constant measured after 25 h). We also note that adjustment of pH with nitric acid for the pH 4 sample was observed to induce a slight precipitation of the polymolybdate salt.

Taken altogether, the results of the three studies show that no dramatic changes occur in catalysts prepared at different pHs. An increase in MoO_3 LRS band intensities with decreasing pH, as well as an increase in HDS activity are noted. Whether these two observations have a direct bearing on each other is difficult to say due to a lack of other studies in this area. If the main effect of impregnation pH is to affect the MoO_3 content and molybdena dispersion, then this can also be accomplished by alteration of calcination time and temperature. It would also appear [21] that the HDS activity of the unadjusted pH 5.4 catalyst is optimal when compared to the other catalysts that had pH adjustment. More studies on all these aspects would be useful.

In terms of pH control, some work has been done using H_3PO_4 for creating low pH [22]. Claims for pH effects with these catalysts must be viewed with caution since the phosphate competes with molybdate for binding sites during impregnation and also remains as part of the catalyst after calcination, where it acts as a promoter [23].

To summarize the work on molybdenum/alumina oxidic catalysts, several points can be made:

1) The Mo loading on the alumina (Mo/nm^2) plays the initial role in determining the nature of the final catalyst.
2) Calcination time and temperature play an important role in terms of determining the distribution of Mo species present at a given loading (i.e. "interaction species", MoO_3, $Al_2(MoO_4)_3$, etc.) but their effects have not really been dealt with through systematic studies. In general, it has been found that lower temperatures (500°C as opposed to 700°C) and shorter calcination times (about 8 h as opposed to 30 h) favor the presence of MoO_3 as opposed to $Al_2(MoO_4)_3$. Calcination is, however, required in order to form MoO_3 for it is not observed in catalysts dried at 110-120°C, regardless of loading. Also, the catalysts without excess $Al_2(MoO_4)_3$ seem to be more active.
3) At this time, impregnation solution pH does not seem to have a major effect on final catalyst results.
4) The effects of alumina particle pore structure or changes in catalyst surface area with respect to Mo loading and calcination parameters were not included in this review.

REFERENCES

1. L. Wang and W.K. Hall, J. Catal. 77, 232 (1982).
2. F.E. Massoth, J. Catal. 30, 204 (1973).
3. N. Giordano, J.C.J. Bart, A. Castellan, A. Vaghi, J. Less Common Met. 36, 367 (1974).
4. N. Giordano, J.C.J. Bart, A. Vaghi, A. Castellan, and G. Martinotti, J. Catal. 36, 81 (1975).
5. K.S. Chung and F.E. Massoth, J. Catal. 64, 320 (1980).
6. R. Thomas, E.M. Van Oers, V.H.J. deBeer, J. Medema and J.A. Moulijn, J. Catal, 76, 241 (1982).
7. D.S. Zingg, L.E. Makovsky, R.E. Tischer, F.R. Brown and D.M. Hercules, J. Phys. Chem. 84, 2898 (1980).
8. J. Medema, C. van Stam, V.H.J. deBeer, A.J.A. Konings, and D.C. Koningsberger, J. Catal. 53, 386 (1978).
9. C.P. Cheng and G.L. Schrader, J. Catal. 60, 276 (1979).
10. F.R. Brown, R. Tischer, L.E. Makovsky and K.H. Rhee, Prepr., Div. Pet. Chem., Am. Chem. Soc., 23, 65 (1978).
11. L.E. Makovsky, J.M. Stencel, F.R. Brown, R.E. Tischer and S.E. Pollack, J. Catal. 89, 334 (1984).
12. B.S. Clausen, H. Topsoe, R. Candia, J. Villadsen, B. Lengeler, J. Als-Nielsen and F. Christensen, J.Phys. Chem. 85, 3868 (1981).
13. T.G. Parham and R.P. Merrill, J.Catal. 85, 295 (1980).
14. T. Edmonds and P.C.H. Mitchell, J.Catal. 64, 491 (1980).
15. B. Sombret, P. Dhamelincourt, F. Wallart, A.C. Muller, M. Bouquet and J. Grosmangin, J. Raman Spectrosc. 9, 291 (1980).
16. E. Payen, J. Barbillat, J. Grimblot and J.P. Bonnelle, Spectrosc. Letter. 11, 997 (1978).

References - cont'd

17. H. Jeziorowski and H. Knözinger, J. Phys. Chem. 83, 1166 (1979).

18. J.M. Stencel, L.E. Makovsky, T.A. Sarkus, J. deVries, R. Thomas, and J.A. Moulijn, J. Catal. 90, 314 (1984).

19. S. Kasztelan, J. Grimblot, J.P. Bonnelle, E. Payen, H. Toulhoat, and Y. Jacquin, Appl. Catal. 7, 91 (1983).

20. J. Sonnemans and P.Mars, J. Catal. 31, 209 (1973).

21. M. Houalla, C.L. Kibby, L. Petrakis and D.M. Hercules, J. Catal. 83, 50 (1983).

22. H. Jeziorowski and H. Knözinger, Appl. Surface Sci. 5, 335 (1980).

23. K. Gishti, A. Iannibello, S. Marengo, G. Morelli and P. Tittarelli, Appl. Catal. 12, 381 (1984).

MOLYBDENUM DISULFIDE

Molybdenum disulfide is believed to be the major active component in hydrodesulfurization catalysts. Because of this, some time will be spent investigating its characteristics in both supported and unsupported forms as well as examining some evidence for its presence in supported HDS catalysts.

Bulk MoS_2 is a dichalcogenide layer compound of molecular weight 160.07 and density 4.80 g/cm^3. The basic coordination unit for MoS_2 is the trigonal prism: the molybdenum atom at the enter of the prism is coordinated with six sulfur atoms at the corners. A layer consists of alternately occupied prisms placed side by side.

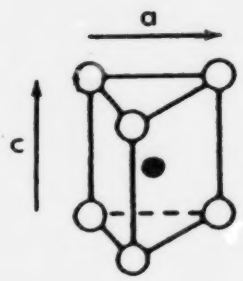

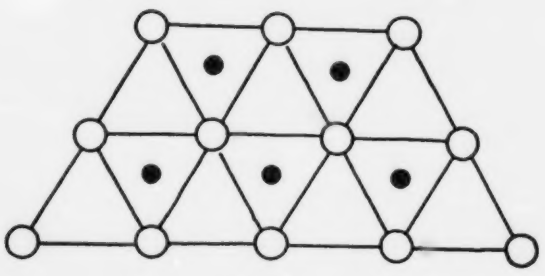

top view of MoS_2 layer (basal plant) ●Mo ⊙S

Each sulfur atom shares itself with three molybdenum atoms in the same layer with no strong bonds extending across the gap between the layers. This accounts for the easy mechanical cleavage along the basal plane of MoS_2.

Although the layers are structurally identical, variation in the stacking sequence results in the formation of the polytypes, rhombohedral and hexagonal. Hexagonal molybdenite, in which we are interested, is a uniaxial crystal belonging to the space group D^4_{6h} ($P6_3/mmc$). The repeat unit in the c direction contains two layers (1 and 2) with the sulfur atoms in one layer being directly above the molybdenum atoms in the next. This polytype is referred to as MoS_2(2 H)(2 layers, hexagonal). Two molecular units lie within the primitive cell for which the magnitudes of the translation vectors are

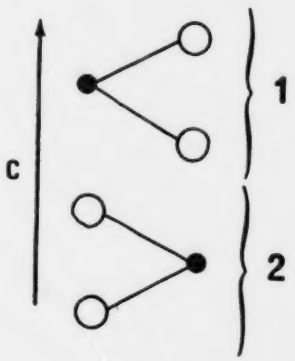

$a_1=a_2=a_3=3.160$Å (S-S or Mo-Mo distance in the basal plane) and c = 12.29 Å [1]. Other useful dimensions are the interlayer gap (2.96Å), the Mo-S bond length (2.41Å), and the S-S distance across the gap (3.47Å).

As already hinted, the short range forces between atoms <u>within</u> a layer are strong by comparison with the van der Waals forces <u>between</u> layers. Measurements of the lattice vibrations of crystalline hexagonal MoS_2 using IR reflectance and Raman spectroscopies give the following results [2]:

Activity	Polarization of Vibration	Ions Involved	Frequency (cm^{-1})
IR($E \parallel c$)	c-axis	Mo+S	466
IR($E \perp c$)	basal plane	Mo+S	384
Raman	c-axis	S	409 (s)
Raman	basal plane	Mo+S	383 (m)
Raman	basal plane	S	287 (m-w)

Small values of oscillator strengths for the IR-active modes of MoS_2 suggest that the bonding between the Mo and S atoms is largely covalent.

The normal vibrations of MoS_2 are essentially those of a single layer since the interatomic forces within a single layer are sufficient to account for the lattice dynamics of MoS_2 as shown by Bromley [3]. Considering a single layer of crystal structure with hexagonal symmetry, the following results were obtained.

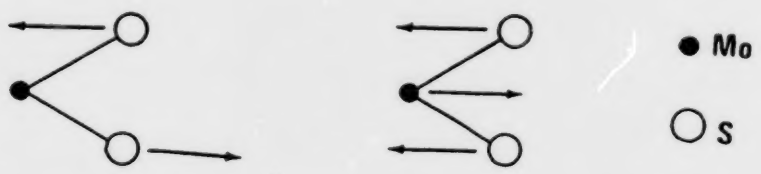

Homopolar $\quad\quad$ **Dipolar**

$w_H(x,y) = 286\ cm^{-1}$ $\quad\quad$ $w_D(x,y) = 383\ cm^{-1}$

$w_H(z) = 409\ cm^{-1}$ $\quad\quad$ $w_D(z) = 466\ cm^{-1}$

These are in agreement with measurement [2].

Further characteristics of the MoS_2 transition metal dichalcogenide, which is extremely anisotropic in its physical properties and is essentially a two-dimensional solid, are given in [1] and [4].

In terms of poorly crystalline MoS_2, Chang and Chan [5] measured sharp IR bands at 385 (s) and 470 (m) cm^{-1}, as well as sharp Raman bands at 384 and 408 cm^{-1}. These values concur with those for the well-crystallized MoS_2 except that the weak Raman band at 287 cm^{-1} is missing.

The presence of MoS_2 on a supported catalyst has been confirmed by Brown and Makovsky [6] for a sulfided $CoO(3\%)$-$MoO_3(15\%)/SiO_2(5\%)$-Al_2O_3 catalyst. The presence of bands of MoS_2 as well as the absence of any molybdenum oxide bands is quite evident in their LRS spectra. The presence of MoS_2 was also confirmed by x-ray diffraction measurements.

Medema et al [7], using Raman spectroscopy, again showed the presence of MoS_2 (and absence of molybdenum oxide) for Mo/Al_2O_3 and $Co\text{-}Mo/Al_2O_3$ samples sulfided for two hours at 400°C and atmospheric pressure in an H_2S/H_2 flow (volume ratio 1:6; flow rate, 50 cm^3/min). The molybdenum loading was about 2.4 Mo/nm^2 (12 wt% MoO_3 on 240 m^2/g gamma-alumina).

Schrader and Cheng [8], using laser Raman spectroscopy investigated the sulfiding of MoO_3/gamma-Al_2O_3 catalysts with loadings of 2.18, 3.36, 4.60 and 7.30 Mo/nm^2 (5,7.5,10 and 15 wt% MoO_3 on 101 m^2/g gamma-Al_2O_3) and various sulfiding conditions. For sulfiding 2 hours at 400°C in 10% H_2S/H_2, Raman bands for MoS_2 were seen for all loadings with no bands attributable to other species present. Sulfiding at the lower temperatures of 150, 250 and 350°C allowed them to monitor the oxide to sulfide transformation in these catalysts.

In a subsequent work on the sulfiding of Co-Mo/gamma-Al_2O_3 catalysts Schrader and Cheng [9] again observed strong MoS_2 bands at 386 and 407 cm^{-1} for all samples sulfided 2 hours at 400°C in a 10% H_2S/H_2 gas mixture. The loadings were again 5, 7.5, 10 and 15 wt% MoO_3 with 3 wt% CoO on 101 m^2/g gamma-Al_2O_3. Again, intermediate stages of sulfiding were observed by sulfiding the samples at 150, 250 and 350°C.

X-ray diffraction (XRD) has also been used to investigate the presence of MoS_2 in supported and unsupported catalysts. An illustration of the XRD pattern for well crystallized MoS_2 as well as poorly crystallized MoS_2 and Co-MoS_2 unsupported catalyst samples are shown by Candia et al. [10]. The most prominent reflection is that of the (002) plane with a corresponding interplanar spacing value of d=6.15A°. For the (100) and (110) planes which are also prominent in the poorly crystallized samples, d=2.74 and 1.58 A°, respectively. A broad peak for the (103) plane and slight shoulder for the (105) plane of these unsupported materials is also seen.

In studying preparations of poorly crystalline and amorphous MoS_2, Chianelli et al [11] describe a rag structure of MoS_2. The rag consists of several stacked but highly folded and disordered MoS_2 layers. Although 20-30 A° thick in the stack direction, the layers may extend several thousand A° perpendicular to the stack direction. It was found that poorly crystalline MoS_2 consisted mostly of rags containing at least two layers and gave rise to a well defined (002) x-ray reflection as well as (100), (103) and (110) peaks. The absence

of the (002) reflection in the XRD pattern of amorphous MoS_2 indicated that the rags, if present at all, were mostly individual layers. Using line-broadening analyses, Pecoraro and Chianelli [12] suggested an average x-ray crystallite size of 28A° in the "c" direction and 78A° in the "a" direction for the MoS_2.

Chang and Chan [5] also showed an XRD pattern for poorly crystalline MoS_2 prepared at 400°C. The 2Θ values (using CuK_α radiation were 14,33,40 and 59° corresponding to (002), (100), (103) and (110) reflections in agreement with others [10,11].

Looking now at supported MoS_2, the XRD study by Pollack et al [13] found that the crystallinity of MoS_2 in a Co-Mo/Al_2O_3 catalyst depended on the severity of sulfiding. For a commercial Harshaw catalyst of composition CoO(3%)-MoO_3(15%)/SiO_2(5%)- gamma-alumina used in coal hydrodesulfurization, XRD lines were assigned to poorly crystalline MoS_2. Samples had received the following treatments: A) sulfidation at 450°C in 10%H_2S/H_2 for 1 h at 1650-1960 psi, B) treatment at the inlet, or C) outlet of a reactor run under the conditions of 450°C at 4000 psi for 1068 h and processing about 12 tons of coal material. The lines had 2Θ values (CuK_α radiation) of 14.2, 33.0, 33.6 and 58.6° which correspond to d=6.15, 2.71, 2.67 and 1.57 A° spacings for the (002), (100), (101) and (110) planes of MoS_2. For the sample (A) that was sulfided only, the 6.15 A° (002) line was very weak, while in the spent catalyst, either from the reactor inlet or its outlet, the line was stronger and somewhat sharper. From diffraction line half-widths, crystallite sizes were estimated.

Crystallite Size (Å)

Sample	L_c	L_a
Unused	NP	NP
Sulfided 1 h @450°C and 1 atm.	NP	80
Sulfided 1 h @450°C @1650-1960 psi	57	92
Spent catalyst from reactor inlet	53	132
Spent catalyst from reactor outlet	66	142

L_c = dimension perpendicular to basal plane.

L_a = dimension in the basal plane.

NP = not present.

The MoS_2 crystallite dimension was greater in the basal plane than in the perpendicular plane. As the severity of sulfiding increased, so did the perpendicular dimension L_c, with the number of MoS_2 layers in the spent catalyst being 9 to 11. The most active form of MoS_2 was a 2-D layer; formation of the 3-D layer, accompanied by a decrease of surface area of the active components, results in catalyst deactivation.

Li and Hercules [14] also looked at unsupported MoS_2 as well as supported MoS_2/Al_2O_3 (Mo loading of 3.65 Mo/nm^2) formed from the decomposition of $(NH_4)_2$ MoS_4/Al_2O_3 and supported MoS_2/Al_2O_3 (3.76 Mo/nm^2) from MoO_3/Al_2O_3 sulfided at 350°C for 2 h in a flow of 15% H_2S/H_2 (50 mL/min). For the MoS_2/Al_2O_3 from $(NH_4)_2$ MoS_4 decomposition the (002), (100) and (110) lines of MoS_2 were seen while for the mildly sulfided MoO_3/Al_2O_3 sample only a trace, perhaps, of the (100) and (110) lines were visible but not clearly. Evidence for the (002) line was lacking.

Previously, deBeer et al. [15] had used XRD to study sulfided Co-Mo/Al_2O_3 and Co-Mo/SiO_2 catalysts. The strongest diffraction line of MoS_2 at 2θ=14.2° or d=6.15A° was observed for two of the silica-supported, but none of the alumina-supported catalysts. The alumina catalysts had loadings of 4.30 Mo/nm^2 (16% MoO_3 on 181m^2/g gamma-alumina) and 5.17 Mo/nm^2 (16% MoO_3 on 154m^2/g gamma-alumina). For these samples, sulfidation was carried out at atmospheric pressure for 2 h at 400°C in a H_2S/H_2 flow of volume ratio 116 and flow rate 50 cm^3/min. The lack of conclusive evidence for XRD lines of MoS_2 is thus in accordance with the other results on mildly sulfided catalysts.

The effect of the severity of sulfiding was also illustrated by Candia et al. [16]. Sulfidation of samples in 2% H_2S/H_2 for 4 h at temperatures from 675-1175 K(400-900°C) was studied for Mo/gamma-Al_2O_3 and Co-Mo/gamma-Al_2O_3 catalysts with Mo loadings of about 2.5 Mo/nm^2 (8.6% Mo on 250m^2/g gamma-Al_2O_3) and calcined for 2 h @500°C in air.

Their results show no diffraction lines due to MoS_2 after sulfiding a Co-Mo/Al_2O_3 catalyst at 400°C, whereas sulfiding temperature to 700°C resulted in the appearance of the (100) line of of MoS_2 while the (002) reflection was still absent. After sulfiding at 900°C, the x-ray pattern then very clearly showed the presence of the (002) reflection. From the width of this line, an average crystallite size along th c-direction of 30A° was estimated implying MoS_2 crystals consisting of 4-5 slabs. The catalysts sulfided at 900°C also showed sharper diffraction lines than those treated at 700°C indicating larger and more well-ordered MoS_2 crystallites.

Computer calculations of XRD scattering intensities for disordered molybdenum sulfide by Chien et al [17] have shown the effects of the number of MoS_2 layers and of disorder between layers upon the XRD pattern of poorly crystalline MoS_2. Their patterns are similar to those of Candia et al. [10] shown earlier in this section. The sharpening and greater resolution of peaks support that the crystallinity of MoS_2 improves as preparation temperature is increased.

Their computer-calculated spectra show XRD patterns of N/(6x6) or 20 A°x20 A° sized crystallites of N=1 to 4 layers in thickness. As expected, no (002) peak is seen for the single layer crystallite, although the (100) and (110) peaks are quite evident. These calculations, however, do not explain the (103) and (105) broadening present in samples of more than one layer in thickness (as evidenced by the presence of a (002) reflection).

To simulate a defect in layer stacking, calculations were made for a two-layer structure in which the layers were rotated about the c-axis with respect to each other through angles of 0.00, 0.02, 0.04, 0.08 and 0.10 radians. This seems to provide the required peak broadening and a comparison between calculated and experimntal results also provided.

Having seen that MoS_2 can be detected on supported catalysts by Raman spectroscopy and x-ray diffraction, we also find evidence for its existence from electron microscopy.

Using transmission electron microscopy, Delannay et al [18] studied unsupported Co, Fe or Ni promoted MoS_2 which was sulfided at 1000°C to obtain well crystallized samples. High resolution transmission electron micrographs of ultramicrotome sections of MoS_2 crystallites from Co-Mo r=0.02 and r=0.25 [r=Co/(Co+Mo) ratio] samples showed quite clearly a layer structure in which layer spacings of 0.615nm (0.615 nm = 1/2c for MoS_2) were clearly resolved. The crystallite edges were not cleavage planes but resulted rather from the uneven termination of the individual layers.

In a study of unsupported MoS_2 by Sanders and Pratt [19], samples of MoO_3, NiO and co-precipitated NiO-MoO_3 were sulfided in 20% H_2S/H_2 and then used for hydrogenolyzing thiophene at 322°C for about 8 hours. Their electron micrographs show quite clearly the layer structure of MoS_2 on sulfided MoO_3 as well as sulfided NiO-MoO_3 crystallites. Again fringe spacings of 0.615 nm were evident.

High resolution transmission electron microscopy work by Sorensen et al [20] on unsupported MoS_2 and Co-MoS_2 again shows the layer structure of MoS_2. Note that no individual layer appears to be more than 100A° long and that in disordered regions the stack thickness ranges from 3-10 layers (about-20-60A°).

Looking now at supported MoS_2, Delannay et al. [21] investigated supported Co-Mo/gamma-Al_2O_3 catalysts with the following loadings:

A1-0.00 4.52 Mo/nm^2 (14.80% MoO_3, 0% Co_3O_4 on 160m^2/g gamma-alumina)

A1-0.25 3.69 Mo/nm^2 (12.08% MoO_3, 2.52% Co_3O_4)

A1-0.75 1.88 Mo/nm^2 (6.03% MoO_3, 9.95% Co_3O_4)

A1-1.00 0.0 Mo/nm^2 (14.46% Co_3O_4)

The samples were first sulfided for 6 h at 600°C using a 15% H_2S/Ar gas mixture and then subjected to a catalytic reaction at 305°C and 30 bar pressure in cyclohexene (30 wt%) and cyclohexane (70 wt%), to which 5000 ppm thiophene was added. Their high resolution electron microscopy pictures of the samples after this treatment shows doubly and triply stacked MoS_2 layers for the various Mo loadings, with none present in the pure cobalt sulfide sample. The layers reach a maximum length of about, 100A° with the number of layers seen, increasing with Mo loading.

Work on Co-Mo/Al_2O_3 catalysts by Sanders et al. [22] showed an electron micrograph of the catalysts after use in reactor tests (using coal material) carried out at 527°C and high pressure (15 MPa) for periods up to 480 hours. Their micrographs show individual sheets of dispersed MoS_2 on the support as thin black lines 50-100A° in length. Examined by XRD, the used catalyst showed evidence for MoS_2 as well as Co_9S_8 and Al_2O_3.

Millward and Thomas [23] showed pictures for Ni-Mo/gamma-Al_2O_3 catalysts sulfided by H_2S in the laboratory and sulfided in a commercial reactor.

The laboratory-sulfided sample yielded short (about 50A°) crystallites up to 4 or 5 layers thick whereas MoS_2 seen after reactor usage appears as singly and doubly layered strands of roughly 100A° in length, similar in appearance to the previous picture [22] of a used Co-Mo/gamma-Al_2O_3 catalyst.

A work by Pollack et al [24] on Co-Mo and Ni-Mo/Al_2O_3 catalysts showed some very fine pictures of MoS_2 structures induced under various conditions and treatments.

Results of Candia et al [16] show the changes which take place as the severity of sulfiding is increased for Co-Mo/Al_2O_3 catalysts with a 2.5 Mo/nm^2 loading (8.6% Mo on 250m^2/g gamma-Al_2O_3). Sulfidation was carried out in a 2% H_2S/H_2 mixture at 400-900°C for 4 hours. High resolution electron micrographs of Co-Mo/Al_2O_3 catalysts (Co/Mo=0.27) sulfided at 400°C failed to show any MoS_2 layers. This is likely due to the MoS_2 being in the form of very small crystallites which EXAFS measurements estimate to be near 10A° [25]. An increased sulfiding temperature of 700°C leads to the growth of the MoS_2 layers, while at 900°C the presence of MoS_2 is much more extensive.

Extended x-ray absorption fine structure (EXAFS) studies allow one to probe the structure of the catalyst below XRD and EM detection limits. One such study, by Clausen et al. [25] showed the presence of MoS_2 crystallites on domains of roughly 10A° size for both Mo/Al_2O_3 and Co-Mo/Al_2O_3 catalysts with about 2.5 Mo/nm^2 loadings (8.6% Mo on 250 m^2/g gamma-Al_2O_3), that were sulfided in 2% H_2S/H_2 for 4 h at 400°C. No evidence for MoO_3 was seen for the sulfide samples, which agrees with [8].

Another EXAFS study, this time by Parham and Merrill [26] using Co-Mo/gamma-Al_2O_3 with a 2.3 Mo/nm^2 loading (15.4 wt% MoO_3,3.2 wt% CoO on 310 m^2/g gamma-Al_2O_3) showed similar results. Sulfiding was carried out in a H_2S/H_2 (1:9) mixture for 4 hours at various temperatures. At 100°C evidence for Mo-O as well as Mo-S bonding was present, in agreement with [8,9). At 300°C however, no Mo-O was present and the

results supported the existence of MoS_2 as crystallites of size <30A°. At 500°C MoS_2 was again solely present but as slightly larger crystallites. Parham and Merrill concluded that the size of the MoS_2 crystallites increased with increased sulfiding temperature. This is supported by the work we have already seen, particularly that of Candia et al [16].

To briefly summarize the Raman, XRD, EM and EXAFS results, it can be said that MoS_2 crystallites do exist on supported, promoted (by Co or Ni) and unpromoted, molybdena-alumina catalysts which have been sulfided either mildly or severely. By mild sulfiding we refer to conditions of 300-400°C in H_2S/H_2 mixtures with nearly 15% H_2S, atmospheric pressure, and 4 hours. Under these mild conditions Raman spectroscopy and EXAFS show ample evidence for MoS_2 on Co-Mo, Ni-Mo or Mo/Al_2O_3 catalysts with Mo loadings of 2-5 Mo/nm^2 while XRD and EM do not, due to the smallness of the MoS_2 domains (10-30A°). Increased severity of sulfiding, either at higher temperatures or in reactors, allows XRD and EM to reveal the presence of MoS_2; both of which methods then show crystallites to range in thickness from 1 to 10 layers, with lengths of 50-100A° or more. Similarities in results for supported and unsupported MoS_2, both promoted and unpromoted, suggests that Ni and Co do not interact with the bulk of the MoS_2 crystallite but rather with the edges or in some other way.

Having seen that MoS_2 does indeed exist on sulfided molybdenum oxide/alumina catalysts, a look at some of its surface properties is of interest. Bulk MoS_2 will be the starting point.

Several studies have looked at the reactivity of the MoS_2 basal plane. Since the chemical bonds within each molecular layers are all saturated, the basal surface should be extremely inert. On the other hand, an edge (non-basal surface) is much more reactive because it has many broken bonds.

LEED studies by Williams and McEvoy [27] showed that a MoS_2 crystal cleaved in vacuum (10^{-10} torr) to expose a fresh basal plane surface exhibited spot patterns of good quality with hexagonal symmetry. These patterns did not visibly change in any way after exposing the surface to dry air at atmospheric pressure and room temperature followed by evacuation to 10^{-8} torr.

Using basal surfaces prepared by cleavage Williams et al [28] studied the effect of introducing defects in a controlled manner by low energy argon ion bombardment. Auger electron spectroscopy was used to monitor the changes. As before [27], no effect was seen upon exposing the cleaved surface to atmosphere. After argon ion bombardment, the sulfur peak was reduced in size and the molybdenum one increased. Subsequent exposure to atmosphere led to both Mo and S decreases but also to a large increase in oxygen. In fact, oxygen was readily detectable even after an exposure of a few hours at 10^{-3} torr. The oxygen was tightly bound to the surface and could not be removed by heating in high vacuum at 200°C. Following ion bombardment, an increase in the reactivity of the basal surface with oxygen by $\geq 10^8$, was estimated. They concluded that the creation of defects on the basal plane of this layer structure led to a dramatic increase in the chemical reactivity of that face. Indeed, the results were in accordance with the observation that defects such as

vacancies, vacancy clusters and dislocations are of the utmost importance in determining the high temperature oxidation properties of MoS_2 [29].

A study of the reactivity of some molecules of interest in hydrodesulfurization was conducted by Salmeron et al [30]. Using the basal plane of MoS_2 single crystals, the adsorption of thiophene, butene and H_2S was studied in the temperature range of 77-300K. Only at the lowest temperatures did thiophene adsorb, using a partial pressures of 10^{-6} torr. It then desorbed intact at 165K. Both H_2S and butene behaved similarly and all these molecules had binding energies of 8 to 10 kcal/mole. It was thus shown that basal plane MoS_2 exhibited very little chemical activity when exposed to thiophene (C_4H_4S), 1,3-butadiene (C_4H_6) or H_2S at low pressures. Based on this, they concluded that the edge planes of MoS_2 are more likely to be HDS sites, but noted that at high reactant pressures, especially in the presence of excess hydrogen, the basal plane could become reactive if it lost sulfur.

A recent work by Davis and Carver [31] showed that under appropriate conditions, sulfide vacancy defect sites could be produced in basal plane MoS_2 surfaces and that these sites indeed display high activity for oxygen chemisorption.

Low energy helium ion scattering (LEIS) was used to investigate oxygen chemisorption on single crystal MoS_2 basal plane surfaces as a function of defect site concentration. Defect vacancy sites were artificially created by brief sputtering in UHV with Ne^+. The results tended to confirm that oxygen uptake correlated well with vacancy concentration (proportional to Ne^+ ion dose).

Molybdenum Disulfide - References

1. J.A. Wilson and A.D. Yoffe, Advan. Phys. 18, 193 (1969).
2. T.J.Wieting and J.L. Verble, Phys.Rev. B3, 4286 (1971).
3. R.A. Bromley, Phil. Mag. 23, 1417 (1971).
4. A.D. Yoffe, Festkorperprobleme, 13, 1(1973).
5. C.H. Chang and S.S. Chan. J. Catal. 72, 139 (1981).
6. F.R. Brown and L.E. Makovsky, Appl. Spectroscopy, 31, 44 (1977).
7. J. Medema, C. van Stam, VHJ deBeer, A.J.A. Konings, and D.C. Koningsberger, J. Catal, 53, 386 (1978).
8. G.L. Schrader and C.P. Cheng, J. Catal. 80, 369 (1983).
9. G.L. Schrader and C.P. Cheng, J. Catal. 85, 488 (1984).
10. R. Candia, B.S. Clausen, and H. Topsøe, Bull.Soc. Chim.Belg. 90, 1225 (1981).
11. R.R. Chianelli, E.B. Prestridge, T.A. Pecoraro, and J.P. DeNeufville, Science 203, 1105 (1979).
12. T.A. Pecoraro and R.R. Chianelli, J. Catal. 67, 430 (1981).
13. S.S. Pollack, L.E. Makovsky and F.R. Brown, J. Catal. 59, 452 (1979).
14. C.P. Li and D.M. Hercules, J. Phys. Chem. 88, 456 (1984).
15. V.H.J. deBeer, M.J.M. van der Aalst, C.J. Machiels and G.C.A. Schuit, J.Catal. 43, 78 (1976).
16. R. Candia, O. Sørenson, J. Villadsen, N.-Y. Topsøe, B.S. Clausen and H. Topsøe, Bull.Soc.Chim.Belg. 93, 763 (1984).
17. F.Z. Chien, S.C. Moss, K.S. Liang and R.R. Chianelli, J. dePhys. 42, C4-273 (1981).
18. F. Delannay, D.S. Thakur and B. Delmon, J. Less Common Metals, 63, 265 (1979).

References - continued

19. J.V. Sanders and K.C. Pratt, J. Catal. 67, 331 (1981).

20. O. Sørensen, B.S. Clausen, R. Candia and H. Topsøe, Appl. Catal. 13, 363 (1985).

21. F. Delannay, P. Gajardo, P. Grange and B. Delmon, J.C.S. Faraday I. 76, 988 (1980).

22. J.V. Sanders, J.A. Spink and S.S. Pollack, Appl. Catal. 5, 65 (1983).

23. G.R. Millward and J.M. Thomas in "Surface Properties and Catalysis by Non-Metals" (Eds. J.P. Bonnelle et al) pp.197-216 (1983) Reidel, Dordrecht.

24. S.S. Pollack, J.V. Sanders and R.E. Tischer, Appl.Catal.8, 383 (1983).

25. B.S. Clausen, R. Candia, J. Villadsen, B. Lengeler, J.Als-Nielsen and F. Christensen, J. Phys. Chem. 85, 3868 (1981).

26. T.G. Parham and R.P. Merrill, J. Catal., 85, 295 (1984).

27. R.H. Williams and A.J. McEvoy, J. Phys. D4, 456 (1971).

28. R.H. Williams, I.G. Higginbotham and M.A.B. Whitaker, J. Phys. C5, L191 (1972).

29. O.P.Bahl, E.L. Evans and J.M. Thomas, Proc.Roy.Soc. A306 , 53 (1968).

30. M.Salmeron, G.A. Somorjai, R.Chianelli and K.S. Liang, Chem. Phys. Lett. 90, 105 (1982).

31. S.M. Davis and J.C. Carver, Appl.Surf.Sci. 20, 193 (1984).

ADSORPTION OF O_2,NO AND CO MOLECULES ON OXIDIC, REDUCED AND SULFIDED CATALYST - MoO_3/Al_2O_3

Much work in the literature has been devoted to studying the chemisorption of various gas molecules on MoO_3/Al_2O_3 catalysts in an attempt to characterize catalyst properties and adsorption sites. Foremost among the various probes are O_2, NO and CO which will be dealt with exclusively in this report. As before, attempts will be made to correlate the chemisorption of these molecules (micromole/g) with catalyst loading (#Mo/nm^2) for catalysts in oxidic, reduced and sulfided states. Effects due to sintering and the extent of catalyst reduction will also be mentioned.

Various methods, static (difference between two isotherms) or dynamic (pulse method), have been used to determine the amount of gas chemisorbed by a sample. In the difference between two isotherms method, an initial isotherm is measured at a given temperature T_o to determine the total adsorption, both physical and chemical. The sample is then pumped off at a higher temperature ($T>T_o$) for about one hour (to drive off the physisorbed gas) after which the reversible part of the adsorption is measured (at T_o). The difference between the two isotherms gives the irreversible or chemisorbed amount of gas. In the pulse method, small quantities (about 1 ml) of the chemisorbing gas are injected at certain time intervals (minutes) into an inert carrier gas (He or Ar) flowing through the sample. This is continued until no portion of the pulse is irreversibly adsorbed anymore (about 6 pulses). By measuring the amount of gas adsorbed in each pulse, the total amount of chemisorbed gas can be determined.

O_2, NO and CO on Al_2O_3

To begin, we shall examine the uptake of O_2, NO and CO on the alumina support itself. No chemisorption of CO or O_2 was observed for pure alumina at -195°C [1], nor for NO at room temperature [2]. O_2 chemisorption was nil on reduced alumina at -78°C [3] as well as on sulfided alumina at -78, 27 and 60°C [4,5,6]. However, on sulfided alumina at 27°C some irreversible NO uptake was observed [5]. Coked alumina at -78°C showed O_2 uptake [4].

O_2 on Oxidic MoO_3/Al_2O_3

Turning now to alumina-supported molybdena catalysts, O_2 chemisorption will be examined first. In general, the oxidic MoO_3/Al_2O_3 catalysts did not chemisorb O_2 [7,8]. Only upon reduction or sulfidation did O_2 chemisorption occur.

O_2 on reduced MoO_3/Al_2O_3

Many studies of O_2 chemisorption on reduced MoO_3/Al_2O_3 catalysts have been carried out. Using hindsight, it is apparent that the irreversible O_2 uptake at a given Mo loading is strongly dependent upon the extent of reduction of the catalyst. The following data of Millman and Hall [7] taken from their graph illustrates this well. Here the catalyst was reduced to various extents [9]. O_2 uptake was measured using a pulse technique of O_2 in He (-195°C) with the temperature then raised to -78°C to catch and measure the reversible fraction of O_2. Data is given in original units (cc[STP]/g) as well as micromole O_2/g and the ratio of O atoms to Mo atoms (O/Mo).

8.0% Mo/Al_2O_3 ($192 m^2/g$ Ketjen CK-300) - 2.97 Mo/nm^2

Extent of Reduction e/Mo	vol O_2 [cc(STP)/g]	O_2 micromole/g	O/Mo
2.0	3.0	133.8	.32
1.91	2.7	120.3	.29
1.85	2.0	89.2	.21
1.7	1.3	57.9	.14
1.5	0.9	40.2	.096
1.2	0.42	18.7	.045
0.7	~0.1	4.5	.011
0.4	~0.05	2.3	.006

The data are plotted on the next page.

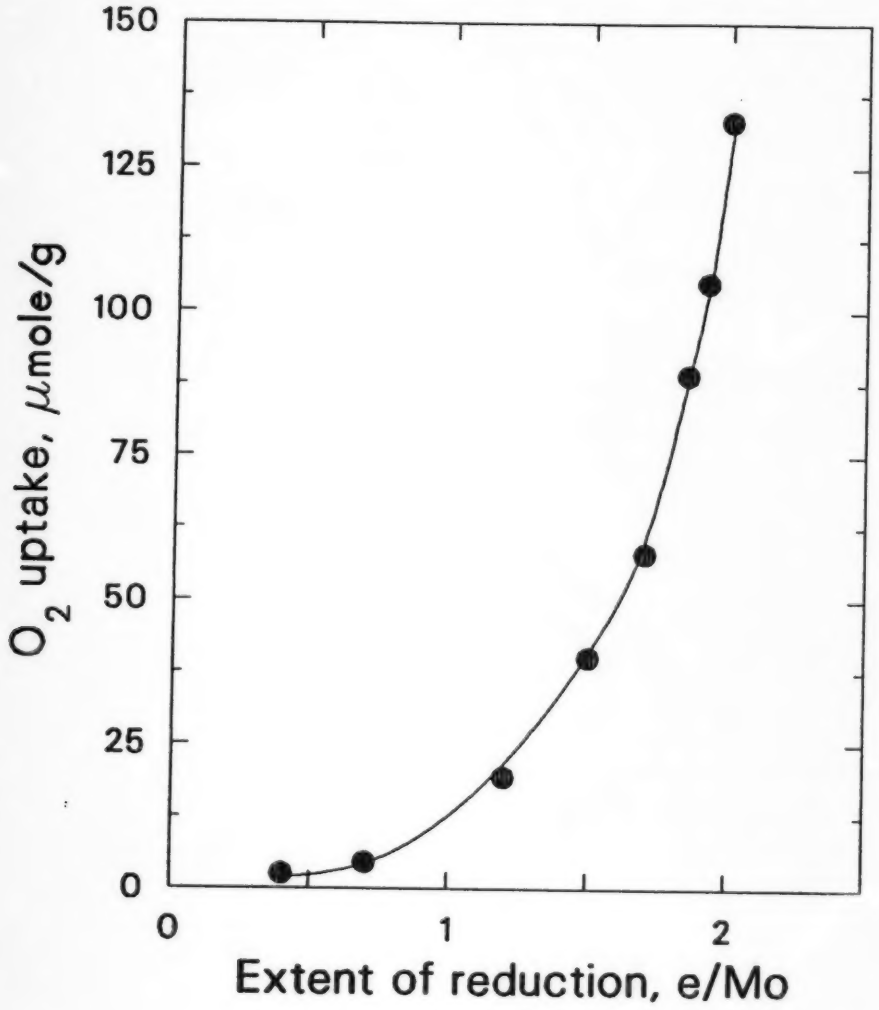

Oxygen uptake versus extent of reduction for 8% Mo/Al_2O_3 (3.0 Mo/nm^2) catalyst.

As shown in this work, the extent of reduction plays an important role in O_2 uptake. Bearing this in mind, we shall now look at a collection of data in which the same catalyst reduction procedure is used (unless otherwise specified). These data, by Weller and various coworkers explore the effects of catalyst sintering, different methods of O_2 uptake measurement and the effect of Mo loading level.

[10] 15% MoO_3/Al_2O_3 (170 m^2/g Corning) dry 2 h @110°C; calcination 24 h @550°C.

- reduction H_2 6 h @500°C; vacuum pumped 1 h @550°C
- difference between two isotherms @-195°C
- 1 ml O_2 (STP) = 44.6 micromole O_2

#Mo/nm^2	T(°C)	vol O_2 (ml[STP])/g	O_2 micromole/g	O/Mo
4.34	-195°C	2.9	129.5	.25

---

[11] 11.5% MoO_3/Al_2O_3 (158 m^2/g Houdry 200S) dry 110°C; calc. 6 h @550°C

- reduction H_2 6 h @500°C; 1 h @550°C vacuum
- difference between two isotherms @ -195°C

#Mo/nm^2	Sintering Temp. (°C)	BET area (m^2/g)	Vol O_2 ml[STP]/g	O_2 mole/g	O/Mo
3.44	550	127	1.5	66.9	.17
3.44	800	63	1.2	53.6	.13
3.44	850	20	0.8	35.7	.09
3.44	925	7.7	0.1	4.5	.01

These data show that sintering results in decreased O_2 chemisorption.

[12] 15% MoO_3/Al_2O_3 (158m^2/g Houdry 200S) dry 4 h @110°C; calc 12 h @500°C

- reduction H_2 6 h @500°C; 1 h @500°C vacuum, static measurements
- reduction H_2 6 h @500°C; 1 h @500°C in He(100 cm^3/min), dynamic measurement
- difference between two isotherms, @-195°C and -78°C

O_2 static chemisorption

#Mo/nm^2	reduction time	T(°C)	Vol O_2 (ml[STP]/g)	O_2 micromole/g	O/Mo
4.67	6	-78	1.4	62.5	.12
4.67	1	-78	0.8	35.7	.07
4.67	6	-195	1.5	66.9	.13

A dynamic method for O_2 adsorption (@-78°C) was said to give identical results to the static measurements. With regard to the static results, little difference is evident between the measurement taken at -195°C and that at -78°C. Also, a reduction period of only 1 hour as opposed to 6 hours resulted in less O_2 uptake suggesting a lesser extent of reduction.

[3] various $\%MoO_3/Al_2O_3$ (144 m^2/g Houdry 200S) vacuum dry 110°C; calcined 12 h @500°C

- reduction H_2 6 h @500°C (40 cm^3/min); 1 h @500°C vacuum.
- difference between two isotherms @-78°C.
- O_2 chemisorption data is taken from their graph.

wt%MoO_3	#Mo/nm^2	Vol O_2 (ml[STP]/g)	O_2 micromole/g	O/Mo
0	0	~0	-	-
3.9	1.18	.3	13.4	.10
5.7	1.75	(.2)	(8.9)	-poor value
7.5	2.36	.4	17.8	.07
10.8	3.52	1.4	62.4	.17
11.4	3.74	1.5	66.9	.17
13.2	4.42	1.5	66.9	.15
14.9	5.08	2.7	120.3	0.23

As can be seen, O_2 uptake tends to increase as a function of catalyst loading. Collecting all of the Weller data (excluding >550°C sintering and the 1 h reduction data), we have the following results as a function of catalyst loading:

wt%MoO_3	#Mo/nm^2	Vol O_2 (ml[STP]/g)	O_2 mole/g	O/Mo
0	0	~0	-	-
3.9	1.18	.3	13.4	.10
5.7	1.75	(.2)	(8.9)	-
7.5	2.36	.4	17.8	.07
10.8	3.52	1.4	62.4	.17
11.4	3.74	1.5	66.9	.17
11.5	3.44	1.5	66.9	.17[11]
13.2	4.42	1.5	66.9	.15
15	4.34	2.9	129.5	.25[10]
15	4.67	1.4,1.5	62.5,66.9	.12,.13[12]
14.9	5.08	2.7	120.3	.23

This compilation shows some disagreement between the results of [12] with and those from the other three sets. Reduction conditions were identical for all four data sets, and although calcination time varied from 6 to 24 h and temperature from 500 to 550°C, this does not seem to be the cause of the discrepancy.

Work by another group has produced the following results for reduced catalysts.

[13] various % MoO_3/Al_2O_3 (188 m^2/g Girdler T-126) dry 80°C; heat 2-1/2 h @ 380°C; calcined 4-1/2 h @550°C

- reduction H_2 overnight @430°C; evac. 4 h @430°C
- difference between two isotherms (-195°C)

% MoO_3 per dry Al_2O_3	#Mo/nm^2	ΔmO_2 (mg/g)	O_2 micromole/g	O/Mo
1.0	.22	0.86	26.8	.78
6.9	1.54	3.51	110	.49
8.2	1.83	4.28	134	.51
8.2	1.83	4.46	139	.53
11.3	2.51	6.90	215	.62
14.3	3.18	8.36	261	.60

These values are certainly much higher than those of Weller or Hall. They do however show an increase of O_2 uptake with Mo loading.

A recent work by Nag [14] gives results more consistent with those of Weller and Hall. Here the conversions are made assuming a loading expressed as micromol/original Al_2O_3 surface area.

[14] various %MoO_3/Al_2O_3($204m^2$/g Harshaw) dry 16 h @120°C; calc 16 h 540°C

- reduction H_2 6 h @ 500°C (40 ml/min); 2 h @ 500°C vacuum; 2 h @-78°C vacuum

- difference between two isotherms (-78°C). (Data taken from their graph).

micromole Mo/nm^2	#Mo/nm^2	O_2 10^2xmicromole/m^2	O_2 micromole/g	O/Mo
1	.60	8	15.8	.15
2	1.21	13	25.0	.12
3	1.81	19	35.5	.115
3.6	2.17	25	46.2	.105
5.2	3.13	28	49.6	.08
6.6	3.97	29	49.6	.075

The following graph compares data from the various groups.

In general, the amount of chemisorbed O_2 increases as molybdenum loading increases for a given reduction procedure. Weller and Nag who used the same reduction procedure report uptakes that are similar when compared to those of Garcia Fierro although the shapes of their curves differ. The uptake of O_2 on reduced MoO_3/Al_2O_3 catalysts seems to tell little at this point in time except that loading is important as is the extent of reduction which is not quantified in any systematic way among all the data sets.

O_2 on sulfided MoO_3/Al_2O_3

We next turn our attention to O_2 chemisorption on sulfided MoO_3/Al_2O_3 samples. This is of special interest since these are the actual hydrodesulfurization catalysts. As above some details of catalyst preparation, sulfidation and O_2 measurement technique are given along with the data.

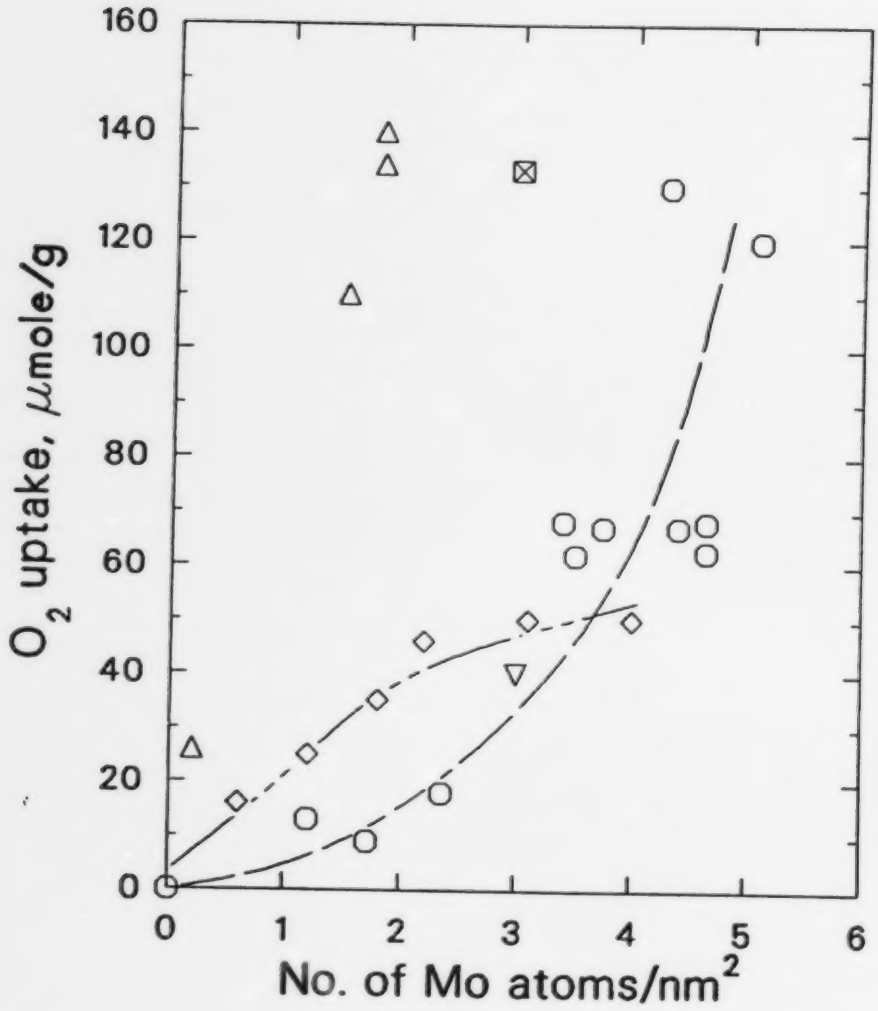

Comparison of O_2 uptake results: ○ Weller [3,10,11,12], △ Garcia Fierro [13], ◇ Nag [14], ▽ Hall [7], e/Mo = 1.5 and ⊠ , e/Mo = 2.0 .

[5] various % MoO_3/Al_2O_3 (231 m^2/g American Cyanamid) dry; calcined 1 h @ 600°C

- sulfided 1 h @ 400°C 10% H_2S/H_2 (50 cc/min); purged 1/2 h He @ 400°C

- measured with pulse technique @ 27°C.

% MoO_3	#Mo/nm^2	O_2 micromole/g	O/Mo
0	0	0	-
2	.37	11	.16
4	.75	20	.15
6	1.16	29	.14
8	1.57	37	.13
10	2.01	43	.12
12	2.47	57	.14
14	2.95	56	.11
16	3.44	59	.11
20	4.53	65	.09

These catalysts show an increase of O_2 uptake with respect to loading of the same order of magnitude as did the reduced catalysts in the previous section.

[15] various %MoO_3/Al_2O_3 ($244 m^2/g$ Ketjen 00039) rotation dry 80°C; calc 4 hr @ 500°C

- sulfided 1 h @ 380°C 10% H_2S/H_2 ($4000\ cm^3/(h)(gcat)$); cooled while maintaining flow.

- O_2 pulse technique; flushed 1/2 h with He ($5000\ cm^3/(h)(gcat)$) before start of O_2 pulses (room temperature measurement).

- data taken from their graph.

% Mo	#Mo/nm^2	O_2 mmol/mol Mo	O_2 micromole/g	O/Mo
5	1.39	113	59	.22
9.5	2.84	90	89	.18
10	3.03	88	92	.18
14	4.56	70	104	.14
18	6.34	56	105	.11

also,

1.040 mmol Mo/g-cat = 2.56 Mo/nm^2, 88 micromole O_2/g, 0.17 O/Mo ratio

These data show a similar trend to those of Jung et al. [5] with respect to loading.

[16] 8%MoO_3/Al_2O_3 (188m^2/g Girdler T-126), dry 77°C; heat 2-1/2 h @370°C; calcined 4-1/2 h @550°C

- sulfided 2 h @400°C 2% H_2S/H_2 (160 cm^3/min); 1/2 h flush He @400°C; outgas 1 h @500°C.
- after NO chemisorption, samples outgassed 2 h @500°C high vacuum; cooled to-78°C for O_2 uptake - difference between two isotherms.
- data from their graph.

#Mo/nm^2	O_2 mmole/g	O_2 micromole/g	O/Mo
1.78	.005	5	.01

This value is very low compared to the earlier data sets and may be perhaps attributed to a different measurement method or an irreversible chemical reaction of NO with the sample before the O_2 uptake measurement.

We now consider three sets of data by Bachelier et al. In the first set, a small range of O_2 chemisorption temperature dependence is shown.

[17] 6.5% MoO_3/Al_2O_3 (238 m^2/g Rhône Poulenc) dried; calcined 2 h @500°C

- sulfided H_2 (700 torr) thiophene (60 torr) 24 h @420°C (30 ml/min)/flushed 2 h @ 420°C with Ar; cooled.
- pulse technique/data from a graph.

#Mo/nm^2	T(°C)	O_2 ml/g	O_2 micromole/g	O/Mo
1.22	-80	.45	20	.09
1.22	0	.8	36	.16
1.22	25	.9	40	.18
1.22	60	1.8	80	.35

We see that O_2 chemisorption is quite dependent upon measurement temperature. Above 60°C, SO_2 was formed in the sample; consequently, Bachelier et al have used the temperature of 60°C to carry out their measurements, this being the temperature for maximum O_2 chemisorption before other chemical reactions occur.

[6] various MoO_3/Al_2O_3 (238 m^2/g Rhône Poulenc) dry 12 h @110°C in air/calciined 2 h @500°C in air plus 2 h @500°C before use.

- sulfided 24 h @420°C in thiophene (60 torr)/H_2(700 torr) 30 cm^3/min; flushed 2 h @420°C with Ar; cooled to 60°C.

- pulse technique @ 60°C

wt%MoO_3	#Mo/nm^2	10^4N_o(mol/g)	O_2 micromole/g	O/Mo
3.1	.56	.31	15.5	.14
4.5	.83	.91	45.5	.29
7.0	1.33	1.79	89.5	.37
8.0	1.53	2.53	126.5	.46
13.3	2.69	3.32	166.0	.36
15.7	3.27	3.56	178.0	.33
19.3	4.20	3.58	179.0	.27
21.6	4.85	3.55	177.5	.24

[18] various MoO_3/Al_2O_3 ($238m^2/g$ Rhone Poulenc) dry overnight 110°C; calcined 2 h @500°C

-sulfided a) 2 h @400°C 9.1 mol% H_2S/H_2 (60 ml/min); purge 1/4 h He @400°C and cooled to 60°C in 1/2 h in He (30 ml/min).

b) presulfided as above then run in reactor 2 h @400°C in 6.2 mol% thiophene/H_2(50ml/min); purged.

c) 20 h @420°C in 7.9 mol% thiophene/H_2(30 ml/min); purged.

-O_2 measured using pulse technique @60°C.

-data taken from graph.

a) & b) sulfiding

wt%Mo	#Mo/nm^2	mole/g	O/Mo
4.2	1.18	45	.21
5.3	1.52	50	.18
9.4	2.86	60	.12
15.0	5.10	55	.07

c) sulfiding

4.2	1.18	90	.41
5.3	1.52	130	.47
9.4	2.86	180	.37
15.0	5.10	175	.22

The two sets of data [6,18] show that sulfiding the catalyst in H_2S/H_2 results in much less O_2 uptake than sulfiding 20 h in thiophene/H_2S. This may be due to coke formation on the catalyst which is shown below to result in increased O_2 uptake.

[4] 8% Mo/Al_2O_3 (Topsøe catalyst)

- sulfided a) 9% H_2S @400°C 2-4 h/1-2 h He flush
  b) sulfided and thiophene/H_2 @350°C overnight
- O_2 measured by flow gravimetric technique. (temp?-78°C?)
- sample ~ 2.5 Mo/nm^2

sample	O_2 micromole/g	O/Mo
H_2/H_2S sulfided	30.3	.07
H_2/thiophene coked	80	.19

Here we see that O_2 uptake is increased 2-1/2 times in agreement with the above results [18] which show 2-3 fold increases.

Additionally, Zmierczak et al [4] show the temperature dependence of O_2 chemisorption on sulfided MoO_3/Al_2O_3 catalysts as did Bachelier et al [17].

One final set of data by Nag [14] shows the lowered O_2 uptakes occurring at -78°C for sulfided samples.

[14] various %MoO_3/Al_2O_3 (204 m^2/g Harshaw) dry 16 h @120°C; calcined 16 h @540°C.

- sulfided 2 h @400°C in CS_2-saturated H_2 @25°C; evacuated 2 h @10^{-6} torr @400°C; evacuated 2 h @-78°C.

- O_2 measured by difference between two isotherms; the data are taken from a graph and the conversions are made assuming a loading expressed as micromol/original Al_2O_3 surface area.

micromol/nm^2	#mol/nm^2	O_2 10^2 micromole/m^2	O_2 micromole/m^2	O/Mo
1	.60	6	11.7	.10
2.5	1.51	9	17.1	.075
3.5	2.11	12	22.3	.07
4.2	2.53	16	29.1	.065
6.3	3.79	19	32.7	.06
8.2	4.94	20	33.0	.04

A value at this temperature taken from [4] is as follows,

about 2.5 #Mo/nm^2 30 micromole/g 0.073 O/Mo

for an H_2S/H_2 sulfided sample.

All of the data are plotted on the next page. It should be noted that these catalysts should be fully sulfided since they fulfil the basic conditions for complete sulfidation as shown in the literature survey section on MoS_2.

Several observations can be made:

1. All the curves, regardless of sulfidation method, coking or temperature of O_2 chemisorption show a levelling off of O_2 uptake at about 3 Mo/nm^2 loading.
2. Below 3 Mo/nm^2 loading, O_2 chemisorption increases with increased loading.
3. Deposition of carbon (or coking) results in increased chemisorption of O_2 for all loadings above .6 Mo/nm^2.
4. The leveling off of O_2 chemisorption at about 3 Mo/nm^2 seems to occur at the point at which MoO_3 can be detected by laser Raman spectroscopy in oxidic samples, namely $\geq$ 3.4 Mo/nm^2 as shown in the literature survey section on MoO_3/Al_2O_3.

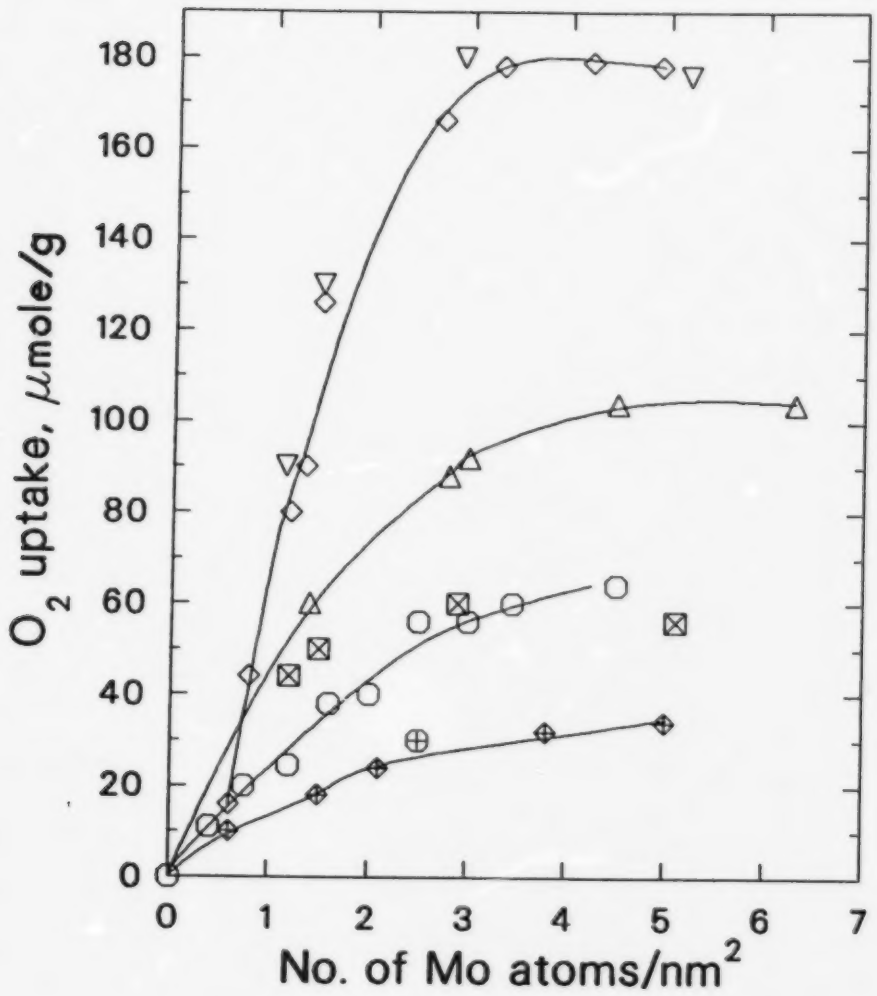

Correlation of O_2 uptakes on sulfided MoO_3/Al_2O_3 from various sources:

- ○ [5] 27°C, H_2S/H_2
- △ [5] Room Temp., H_2S/H_2
- ◇ [6], ⊕ [17] 60°C, thiophene 24 h
- ▽ [18] 60°C, thiophene 24 h
- ⊠ [18] 60°C, H_2S/H_2
- ⊕ [14] -78°C, CS_2/H_2 and [4]-78°C, H_2S/H_2

REFERENCES

1. J.M. Bridges, D.S. MacIver and H.H. Tobin, Actès Congr. Int. Catal. 2nd, 1960, p.2161 (1961).
2. N-Y. Topsøe and H. Topsøe, J. Catal. 75, 354 (1982).
3. H-C Liu and S.W. Weller, J. Catal. 66, 65 (1980).
4. W. Zmierczak, G. MuraliDhar and F.E. Massoth, J. Catal. 77, 432 (1982).
5. H.J. Jung, J.L. Schmitt and H. Ando, in "Proc.Climax 4th Intern. Conf. on Chemistry and Uses of Molybdenum" (H.F.Barry and P.C.H. Mitchell, Eds.), Climax Molybdenum Co., Ann Arbor, Michigan, p.246 (1982).
6. J. Bachelier, M.J. Tilliette, J.C. Duchet and D.Cornet, J.Catal. 76,300 (1982).
7. W.S. Millman and W.K. Hall, J.Catal. 59, 311 (1979).
8. J. Valyon and W.K. Hall, J.Catal. 84, 216 (1983).
9. W.K. Hall and M. LoJacono, Proc. VIth Int.Cong.Catal.1,246 (1977)
10. B.S.Parekh and S.W. Weller, J. Catal. 47, 100 (1977).
11. R.Srinivasan, H-C Liu and S.W. Weller, J.Catal. 57, 87 (1979).
12. H-C Liu, L.Yuan and S.W. Weller, J.Catal.61, 282 (1980).
13. A Lopez Agudo, F.J. Gil Llambias, P.Reyes and J.L. Garcia Fierro, Appl.Catal. 1, 59 (1981).
14. N.K. Nag, J.Catal. 92, 432 (1985).
15. R.Burch and A. Collins, in "Proc. Climax 4th Intern.Conf. on Chemistry and Uses of Molybdenum", (H.F.Barry and P.C.H. Mitchell, Eds.), Climax Molybdenum Co., Ann Arbor, Michigan, p.379 (1982).
16. A Lopez Agudo, F.J. Gil Llambias, J.M.D. Tascón and J.L.G. Fierro, Bull.Soc.Chim.Belg. 93, 719 (1984).

References - continued

17. J.Bachelier, J.D. Duchet and D. Cornet, Bull.Soc.Chim.Belg. 90, 1301 (1981).

18. J.P.R. Vissers, J.Bachelier, H.J.M. ten Doeschats, J.C. Duchet, V.H.J. deBeer, and R.Prins, in "Proc.8th Int.Congr.Catal." (Berlin 1984), p.II-387, Verlag Chemie 1984.

The effects of CO exposure on MoO_3/Al_2O_3 catalysts will now be reviewed.

CO on oxidic MoO_3/Al_2O_3

CO was not found to chemisorb measurably on oxidized molybdena-alumina catalysts [19]. Using IR spectroscopy, Peri [20] found no CO chemisorption on the oxidized catalysts even after evacuation temperatures as high as 600°C. Bachelier et al.[21] also found no IR evidence for CO uptake at 30°C. Only upon reduction or sulfidation did CO chemisorption occur.

CO on reduced MoO_3/Al_2O_3

Work on CO chemisorption by reduced MoO_3/Al_2O_3 has been done by Yao [22].

[22] various %Mo/Al_2O_3($180m^2/g$ Dispal-M gamma-Al_2O_3); $(NH_4)_2$ Mo_2O_7 soln; drying; calcination at 400-600°C in air for 2,4 or 20 h.

- reduction in flowing H_2 1 h @500°C; degassed at 500°C (1 h?)
- difference between two isotherms @25°C.

wt%Mo	#Mo/nm^2	CO micromol/m^2	CO micromole/g-cat	CO/Mo
0.75	.26	.0026	.47	.005
1.50	.53	.016	2.4	.015
2.86	1.04	.125	18.3	.063
4.07	1.51	.22	31.4	.075
7.19	2.81	.41	56.9	.078
10.10	4.14	.42	56.7	.055
18.24	8.71	.41	~49	.029

CO chemisorption increases as a function of catalyst loading up to about 3 Mo/nm^2 and then levels off.

CO on sulfided MoO_3/Al_2O_3

For sulfided MoO_3/Al_2O_3, Bachelier et al [17] found that no CO was retained above 120°C but that adsorption was observed at 60°C and rapidly increased with decreasing temperature. At low temperature, a large fraction of the adsorbed CO was fixed by the support itself, although for $T \geq 0$°C no CO was held. For this reason, CO uptake was studied at 0°C at which temperature the alumina support had no effect. CO chemisorption was also found to be reversible.

Desorption was fast and complete at 150°C in flowing He.

[17] various %MoO_3/Al_2O_3 (238m^2/g Rhône Poulenc, gamma-alumina) dry 110°C, calcination 2 h @500°C.

- sulfided 24 h @420°C in thiophene (60 torr) and H_2 (700 torr), 30 ml/min; flushed 2 h @420°C with Ar; cooled.
- pulse technique with CO in He @0°C.

wt%MoO_3	#Mo/nm^2	$10^4 N_{CO}$(mole/g)	CO micromole/g	CO/Mo
3.1	.56	-	-	-
4.5	.83	.11	11	.035
7.0	1.33	.31	35	.072
8.0	1.53	.39	39	.070
13.3	2.69	.65	65	.070
15.7	3.27	.67	67	.061
19.3	4.20	.69	69	.051
21.6	4.85	.67	67	.045

Using the same catalyst preparation, sulfidation procedure, and measurement technique at 0°C Bachelier et al [23] found 27 micromole/g CO uptake for 6.9% MoO_3/Al_2O_3 (1.31 Mo/nm^2) and 67 micromole/g CO uptake for 15.7% MoO_3/Al_2O_3 (3.27 Mo/nm^2). In another paper [21), they found 26 micromole/g CO uptake for a sulfided 6.3% MoO_3/Al_2O_3 (1.18 Mo/nm^2) sample with CO/Mo = .059.

The results for the reduced and sulfided MoO_3/Al_2O_3 catalysts are plotted on the following page. In both cases CO chemisorption increases with increased Mo loading up to about 3 Mo/nm^2 and then levels off. It should be noted that coke formation on the sulfided catalysts is quite likely, but whether or not it results in increased CO uptake as it did for O_2 is unknown due to a lack of available data.

Comparing the CO results with the O_2 ones, it is seen that a levelling off in uptake occurs at about 3 Mo/nm^2 in both cases, but that the CO/Mo are smaller than the O/Mo ratios by a factor of about six.

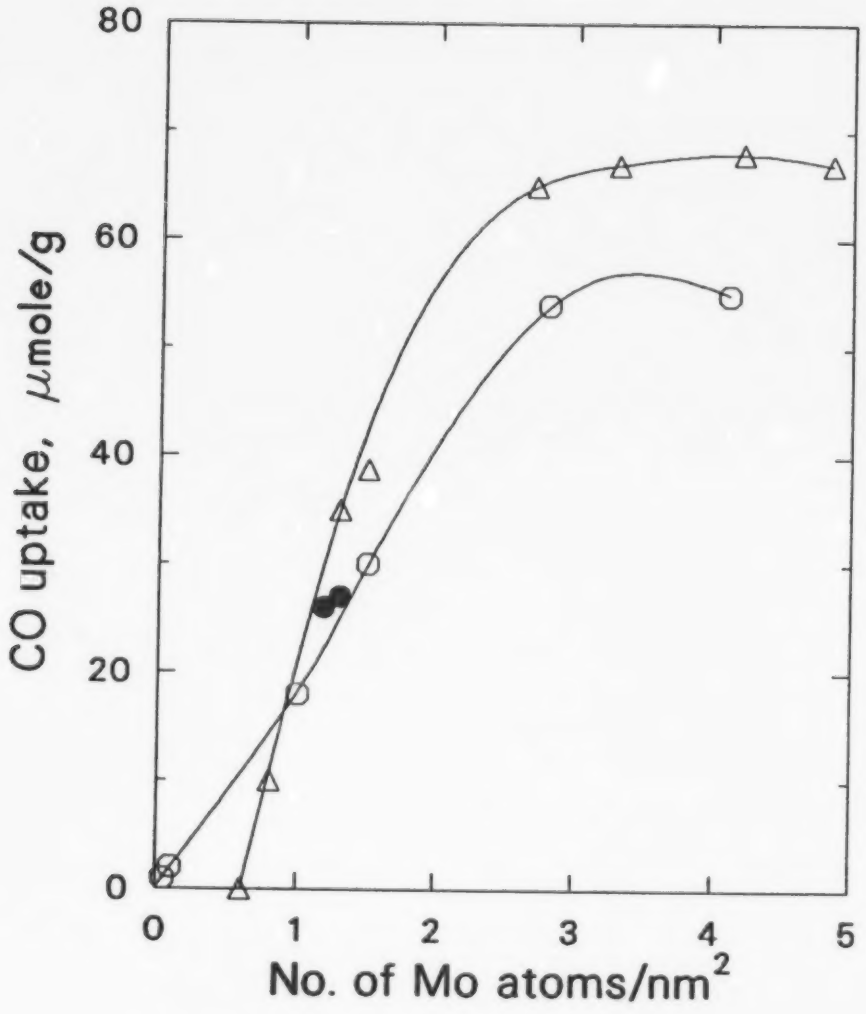

CO uptake on reduced and sulfided MoO_3/Al_2O_3:

○ [22] , reduced, 25°C

△ [17] , sulfided, 0°C

● [21,23] , sulfided, 0°C

Finally, we look at NO chemisorption on MoO_3/Al_2O_3 catalysts.

NO on oxidic MoO_3/Al_2O_3

No uptake of NO on oxidic 8% Mo/Al_2O_3 (2.97 Mo/nm^2) was found by Hall and coworkers [8,19,24]. Using IR spectroscopy, Peri [20] did not find NO chemisorption on the oxidized catalysts even after evacuation at temperatures up to 600°C. Topsoe and Topsoe [2] observed that NO chemisorption did not occur upon oxidic 8% Mo/gamma-Al_2O_3 (2.48 Mo/nm^2) degassed at only low temperature. They stated that since Mo is present in calcined catalysts in the form of Mo^{6+} which has a d^0 structure, it is not expected to adsorb NO strongly. However,IR adsorption bands were observed when the sample was evacuated at 450°and 500°C. An uptake (at room temperature) of 3.7 micromoles/g NO (NO/Mo =.004) was measured for a sample evacuated at 500°C, thus showing that the catalyst surface could be modified to adsorb NO, although only in small amounts.

NO on reduced MoO_3/Al_2O_3

Several studies of NO chemisorption on the reduced catalysts have been performed. The first one considered is by Yao [22]:

[22] various %Mo/Al_2O_3 (180m^2/g Dispal-M, gamma-Al_2O_3); $(NH_4)_2$ Mo_2O_7 soln; dried; calcination at 400-600°C in air for 2, 4 or 20 h.

- reduction in flowing H_2, one h @500°C; degassed at 500°C (1 h?)

-difference between two isotherms at 25°C.

wt% Mo	#Mo/nm^2	NO (micromole/m^2)	NO micromole/g	NO//Mo
0.75	.26	.18	32.4	.34
1.50	.53	.39	57.7	.37
2.86	1.04	1.24	181	.62
4.07	1.51	1.85	264	.63
7.19	2.81	3.25	452	.62
10.10	4.14	3.40	458	.45
18.24	8.71	3.75	450	.26

We see that NO chemisorption increases with increased Mo loading and then levels off at about 3 Mo/nm^2.

[19] On partially reduced catalysts we have the following results.

8% Mo (2.97 Mo/nm^2) - calcined overnight in O_2 flow @ 500°C.

- after 40 min evacuation @500°C, reduction was carried out in H_2 (or CO) of a given amount and then evacuated 90 min.
- volumetric measurement of NO uptake

e/Mo	NO(cm^3/g)	NO (micromole/g)	NO/Mo
.9	1.15	51.4	.06
1.35	2.5	112	.13

[24] 8% Mo/Al_2O_3 (192m^2/g Ketjen CK-300 alumina) (2.97 Mo/nm^2)

- calcined overnight in O_2 @500°C followed by a 40 min evacuation
- after 5 min evacuation to remove He, NO at 20°C was admitted and NO chemisorption was determined from gravimetric measurements
- extrapolation to t=0 from single uptake vs time curve.

The maximum uptake was about 248 micromole NO/g at the maximum reduction shown which is not well defined. This corresponds to .3 NO/Mo.

[8] 8% Mo/Al_2O_3 (192 m^2/g Ketjen CK-300, gamma-alumina)(2.97 Mo/nm^2).

- calcined overnight in flowing O_2 @ 400 - 700°C
- reduction in H_2 ($70cm^3/min$) for 0.5-2 h @ 400-700°C.
- uptake measured at room temperature as in [24] and also by a pulse technique at - 78°C.

At maximum reduction (which was greater than in [24]) the pulse technique gave a NO/Mo ratio of 0.41 or about 338 micromole/g NO uptake, while the volumetric method at 25°C gave NO/Mo roughly equal to 0.45 corresponding to 371 micromole/g NO uptake.

A graph of all the results is shown on the next page for NO on reduced MoO_3/Al_2O_3 catalysts. Uptake is seen to be dependent upon Mo loading as well as the extent of reduction of the catalyst.

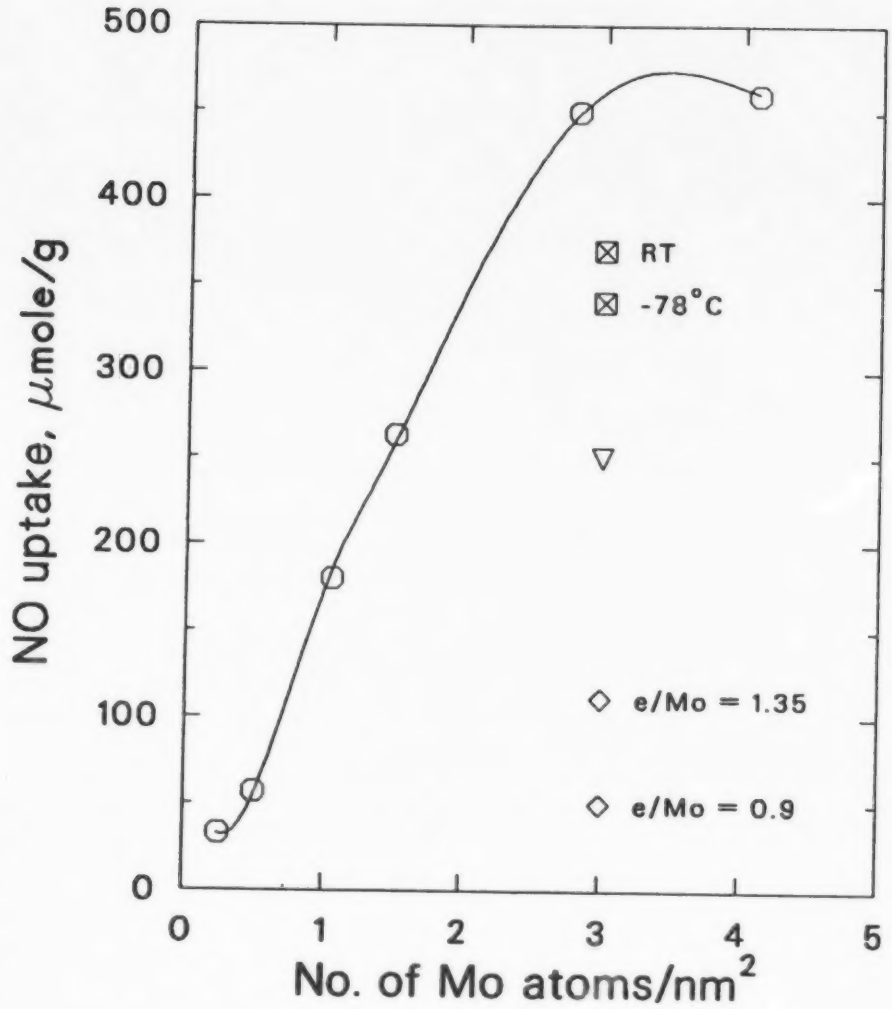

NO Uptakes on reduced MoO_3/Al_2O_3 :

- ○ [22], same reduction, 25°C
- ◇ [19], various reductions, room temp.
- ▽ [24], more reduction than in [19], room temp.
- ⊠ [8], more reduction than in [24], room temp. and -78°C

NO on sulfided MoO_3/Al_2O_3

Several works dealing with the chemisorption of NO on sulfided MoO_3/Al_2O_3 catalysts have been published.

[5] various %MoO_3 (231 m^2/g American Cynamid) dry; calcined 1 h @600°C

- sulfided 1 h @400°C, 10% H_2S/H_2 (50cc/min); purged 1/2 h He @400°C.
- measured with pulse technique at 27°C.

% MoO_3	#No/nm^2	NO micromole/g-cat	NO/Mo
0	0	9.8	-
4	.75	54	.19
8	1.57	83	.15
12	2.47	113	.14
16	3.44	158	.14
20	4.53	158	.11

NO uptake increases with Mo loading up to about 3 Mo/nm^2 and then levels off.

[25] 8% Mo/Al_2O_3 (230 m^2/g gamma-Al_2O_3)(2.48 Mo/nm^2); dry; calcined 2 h @500°C in air

- sulfided in flow 1.7% H_2S/H_2 2 h. @400°C; flush with N_2 16 h @400°C; cool to RT and evacuated to 10^{-5} torr.
- difference between two isotherms at room temperature or extrapolating to zero pressure (results for the latter procedure are given).

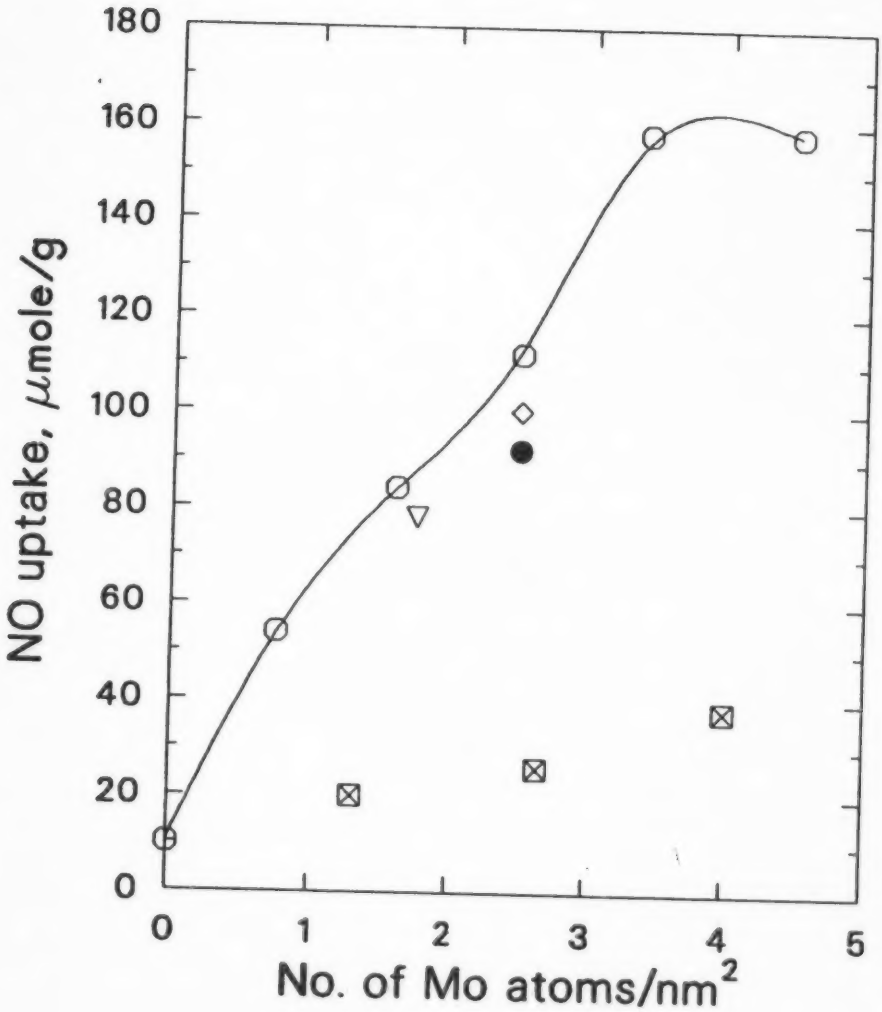

NO Uptake on sulfided MoO_3/Al_2O_3 :

- ○ [5], 27°C
- ◇ [25], room temp.
- ● [26], room temp.
- ▽ [16], room temp.
- ⊠ [27], room temp.

From the given graphs, the NO uptake is about 100 micromole/g or NO/Mo=0.12 although in the reference a ratio of 0.17 is stated.

[26] 8.6% Mo/Al_2O_3 (250 m^2/g gamma-Al_2O_3)(2.48 Mo/nm^2) dry; calcined 2 h @500°C in air.

- sulfided in flow about 2% H_2S/H_2, 4 h @400°C; flush with N_2 16 h @400°C; cool to RT
- isotherm extrapolation to zero pressure at room temperature.

NO uptake was 94 micromole/g or NO/Mo = 0.105 for this sample.

16] 8% MoO_3/Al_2O_3 (188 m^2/g Girdler T-126 gamma-alumina) dry 77°C; heat 2-1/2 h @370°C; calcined 4-1/2 h @550°C (1.78 Mo/nm^2).

- sulfided 2 h @400°C, 2% H_2S/H_2 (160 cm^3/min); 1/2 h flush He @400°C; outgas one h @500°C; cool to RT
- difference between two isotherms @ RT

The NO uptake was 0.079 mmole/g-cat = 79 micromole/g giving NO/Mo = 0.15.

All the above values are within the same range, whereas the next set of data gives uptakes much lower than expected.

[27] various % MoO_3/Al_2O_3 (156 m^2/g Nishio Ind. Type AE-11 gamma-alumina) dry 100°C 16 h; calcined 5 h @550°C in air.

- sulfidation H_2S/H_2 (1/10, 100 Torr) @400°C for ten-2(min. exposures (200 min) followed by evacuation for 1 h @400°C.
- NO measured volumetrically at RT.

%MoO_3	#Mo/nm^2	NO (10^{-5}mol/g-cat)	NO Micromole/g-cat	NO/Mo
4.8	1.35	2.00	20.0	.060
9.1	2.66	2.68	26.8	.043
13.0	4.00	3.85	38.5	.040

These values of NO uptake are much smaller than the other results on sulfided samples. All samples should be completely sulfided (as determined in the literature survey section on MoS_2). The only major difference is the lack of flushing the sample with He or N_2 @400°C for at least 1/2 h before cooling to room temperature and doing the NO uptake measurement. Residual H_2S/H_2 may therefore still have been on the sample and perhaps interfered with the measurement.

Some work on sulfided samples has been carried out by Valyon andHall [8]. Unfortunately, the samples were reduced prior to sulfidation (as described earlier in this report) and an uptake of 300 micromole/g NO was described for a sulfided sample (4 h @350°C in 10% H_2S/H_2). This value is rather high compared to the other results and because of the non-standard reduction-sulfidation procedure will not be included with the other data.

On the next page a graph of the NO uptake on sulfided MoO_3/Al_2O_3 catalysts is shown as a function of Mo loading. As before, NO uptake reaches a maximum near 3-3.5 Mo/nm^2 and then levels off.

To sum up, the following observations are made.

1) CO and NO uptakes on reduced and sulfided MoO_3/Al_2O_3 catalysts level off at about 3 Mo/nm^2. This is similar to the behavior of O_2 on sulfided samples.
2) Below 3 Mo/nm^2 loading, CO and NO chemisportion increases with increased loading.
3) In all cases, NO chemisorption was several times greater than CO chemisorption.

4) In terms of O/Mo, CO/Mo and NO/Mo ratios, the data for O/Mo on reduced samples are very scattered. CO/Mo and NO/Mo on reduced samples both show a maximum at about 2Mo/nm^2. O/Mo and NO/Mo ratios on sulfided samples decrease as Mo loading increases with the exception of the sulfided/coked data in which O/Mo shows a maximum at roughly 2 Mo/nm^2. CO/Mo on sulfided/coked samples also shows a maximum at near 2 Mo/nm^2. CO/Mo data are not available for uncoked/sulfided samples nor are NO/Mo data for sulfided/coked catalysts. Using these data, it would be interesting to see if the same trends exist for the three gases, O_2, CO and NO.

REFERENCES

1. J.M. Bridges, D.S. MacIver and H.H. Tobin, Actès Congr. Int. Catal., 2nd, 1960, p.2161 (1961).
2. N-Y Topsøe and H. Topsøe, J. Catal. 75, 354 (1982).
3. H-C Liu and S.W. Weller, J.Catal. 66, 65 (1980).
4. W.Zmierczak, G. MuraliDhar and F.E. Massoth, J.Catal.77, 432 (1982).
5. H.J.Jung, J.L. Schmitt and H. Ando, in "Proc. Climax 4th Intern.Conf. on Chemistry and Uses of Molybdenum", (H.F Barry and P.C.H Mitchell, Eds.),Climax Molybdenum Co., Ann Arbor, Michigan, p.246 (1982).
6. J.Bachelier, M.J. Tilliette, J.C. Duchet and D. Cornet, J.Catal., 76, 300 (1982).
7. W.S. Millman and W.K. Hall, J.Catal. 59, 311 (1979).
8. J. Valyon and W.K. Hall, J.Catal. 84, 216 (1983).
9. W.K. Hall and M. LoJacono, Proc. VIth Int.Cong.Catal., 1,246 (1977).

10. B.S. Parekh and S.W. Weller, J.Catal. 47, 100 (1977).

11. R. Srinivasan, H-C Liu and S.W. Weller, J.Catal. 57, 87 (1979).

12. H-C Liu, L. Yuan and S.W. Weller, J.Catal. 61, 282 (1980).

13. A. Lopez Agudo, F.J. Gil Llambias, P.Reyes and J.L. Garcia Fierro, Appl.Catal.1, 59 (1981).

14. N.K. Nag, J.Catal. 92, 432 (1985).

15. R. Burch and A. Collins, in "Proc. Climax 4th Intern.Conf.on Chemistry and Uses of Molybdenum", (H.F.Barry and P.C.H.Mitchell, Eds.),Climax Molybdenum Co., Ann Arbor, Michigan, p.379 (1982).

16. A.Lopez Agudo, F.J. Gil Llambias, J.M.D.Tascón and J.L.G. Fierro, Bull.Soc.Chim.Belg. 93, 719 (1984).

17. J.Bachelier, J.D.Duchet and D.Cornet, Bull.Soc.Chim.Belg. 90, 1301 (1981).

18. J.P.R. Vissers, J.Bachelier, H.J.M. ten Doeschats, J.C. Duchet, V.H.J. deBeer, and R. Prins, in "Proc. 8th Int.Congr. Catal." (Berlin 1984) p.II-387, Verlag Chemie, 1984.

19. E.A. Lombardo, M.LoJacono and W.K. Hall, J.Catal. 64, 150 (1980).

20. J.B. Peri, J.Phys.Chem. 86, 1615 (1982).

21. J.Bachelier, M.J. Tilliette, M. Cornac, J.C. Duchet, J.C.Lavalley and D.Cornet, Bull.Soc.Chim.Belg. 93, 743 (1984).

22. H.C. Yao, J.Catal. 70, 440 (1981).

23. J.Bachelier, J.C. Duchet and D. Cornet, J.Catal. 87, 283 (1984).

24. K-I. Segawa and W.K. Hall, J.Catal. 77, 221 (1982).

25. H-Y Topsøe and H. Topsøe, J.Catal. 84, 386 (1982).

26. R.Candia, B.S. Clausen, J.Bartholdy, N-Y Topsoe, B.Lengeler and H. Topsøe, in "Proc. 8th Int.Congr.Catal." (Berlin 1984) pII-374, Verlag Chemie, 1984.

27. Y. Okamoto, Y. Katoh, Y. Mori, T. Imanaka and S. Teranishi, J.Catal. 70, 445 (1981).

HYDRODELSULFURIZATION ON MoO_3/Al_2O_3 CATALYSTS

Some experimental results for the hydrodesulfurization (HDS) of thiophene over molybdena/alumina catalysts will be presented. Activities will be correlated with molybdenum loading.

Two papers [1,2] by Okamoto et al give % conversions of thiophene over a series of MoO_3/Al_2O_3 catalysts pretreated under various conditions. Procedures for both sets of results are essentially the same and are described below.

156 m^2/g gamma-Al_2O_3 (Nishio Ind.Co.Ltd. Type AE-11) was impregnated with ammonium heptamolybdate solution, dried 16 h at 100°C and calcined 5 h at 550°C in air.

A fixed bed flow reactor was used in which about 0.154 g catalyst was heated to 400°C in a stream of dry nitrogen and then subjected to one of the following pretreatments for 1 h at 400°C: 1) H_2 (50 ml/min), 2) CS_2/H_2 (1/9 molar ratio, H_2:27 ml/min) and 3) nonpretreatment.

The HDS reaction of thiophene was then carried out at 400°C and atmospheric pressure of hydrogen using a thiophene/benzene/H_2 (1/0.8/18, H_2 50 ml/min) mixture. Steady state was reached after about 2 h for presulfided samples and 3 h for prereduced and oxidic samples.

Data for the three pretreatments are given on the next page, with graphs on the following pages. While raw conversion increased with metal loading for reduced and nontreated samples, it remains constant for presulfided catalysts.

Prereduced in H_2		[1] raw conversion %	[1] intrinsic* activity	[2] raw conversion %	[2] intrinsic* activity
wt%MoO_3	#Mo/nm^2				
0	0	0			
2.4	.66	1.39	3.64	1.4	3.6
4.8	1.35	3.60	4.91	3.0	4.1
6.5	1.87	-	-	7.7	7.7
9.1	2.66	16.3	11.6	17.2	12.3
13.0	4.00	22.2	11.1	20.6	10.2
16.7	5.37	21.3	8.30	19.6	7.7
23.1	8.05	30.0	8.45	23.8	6.7
Nonpretreatment					
4.8	1.35	5.95	8.11	4.1	5.5
9.1	2.66	14.3	10.2	-	-
13.0	4.00	17.7	8.83	-	-
16.7	5.37	19.0	7.40	23.6	9.2
23.1	8.05	23.5	6.61	-	-
Presulfided					
0	0	0		-	
4.8	1.35	4.49	6.12	5.9	8.0
9.1	2.66	6.52	4.66	-	-
13.0	4.00	6.33	3.15	6.7	3.4
16.7	5.37	6.70	2.61	-	-
23.1	8.05	3.95	1.97	8.8	2.5

* intrinsic activity = (raw conversion (%)/g of MoO_3) x 10^{-2}

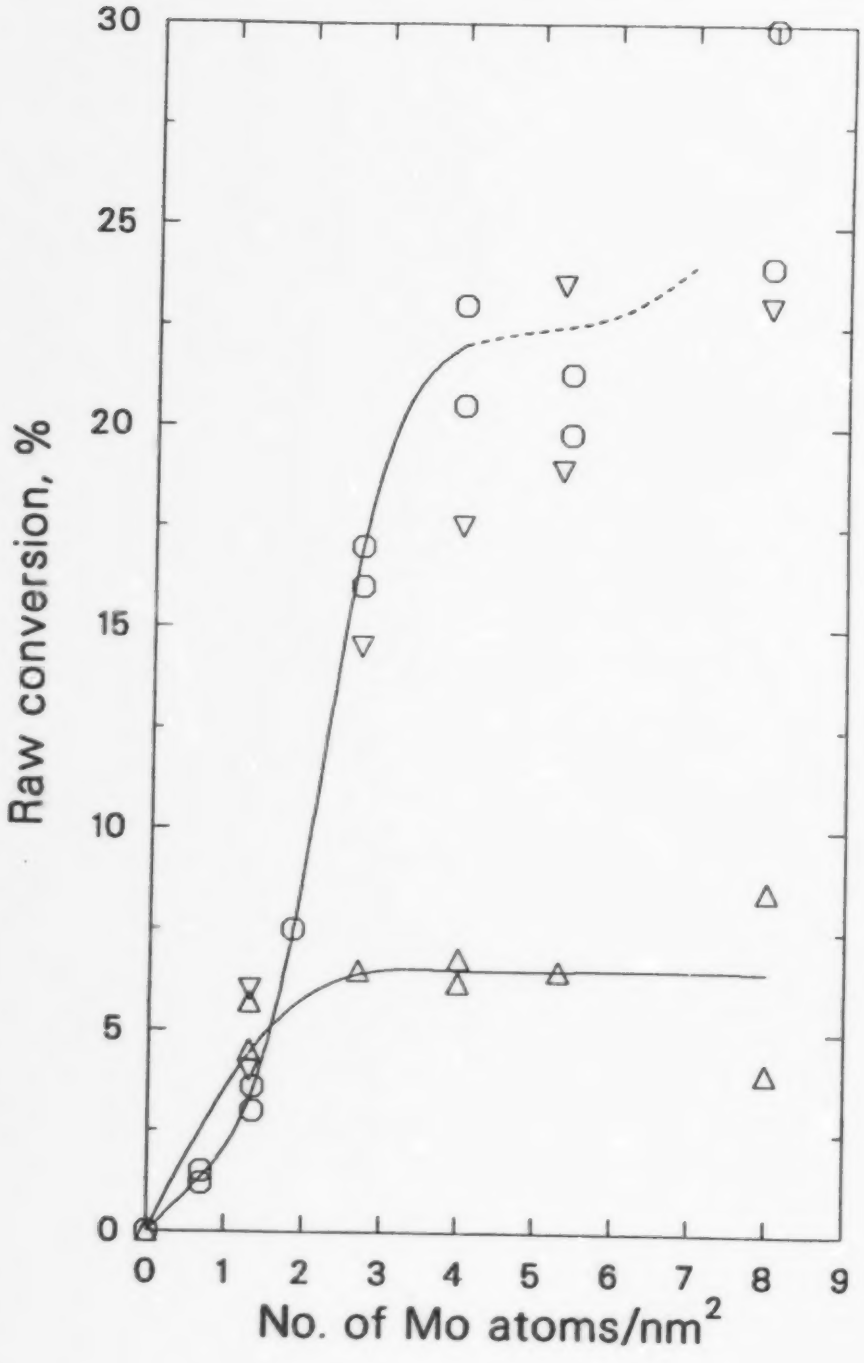

Conversion of thiophene :

○ Pre-reduced
△ No pretreatment
▽ Presulfided

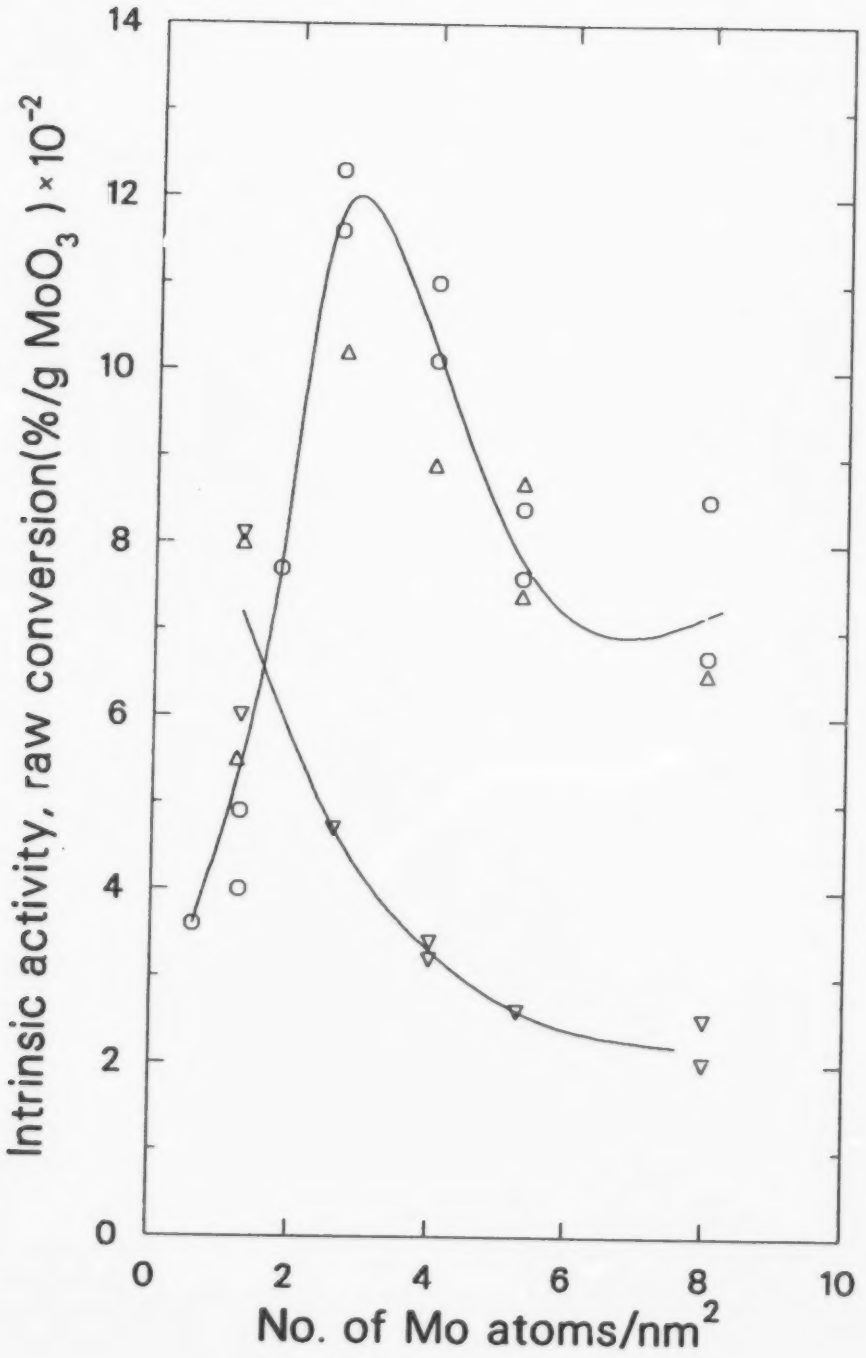

Effect of Mo loading on intrinsic activity :

- ○ Pre-reduced
- △ No pretreatment
- ▽ Presulfided

Using various preparation methods for MoO_3/Al_2O_3 catalysts, Thomas et al. [3] examined the variation of reaction rate constant with respect to molybdenum loading for thiophene hydrodesulfurization. Catalysts for wet and "dry" impregnation were prepared using aqueous ammonium heptamolybdate on 213 m^2/g gamma-Al_2O_3 (Ketjen 000-1,5E). Catalysts were dried 16 h at 120°C and calcined under fluidizing conditions in dry air for 2 h at 550°C. References for other preparations are given.

HDS experiments were carried out in a micro-flow reactor at atmospheric pressure. The sample (about 0.5g) was presulfided in 10 mol% H_2S/H_2 (42 micromol^{-1} flow rate) at 400°C for 2 h. After this, hydrogen and thiophene (thiophene mole fraction of 6.2 mol%) were fed into the reactor at a rate of 35 micromol^{-1}. HDS activity was calculated from data obtained after runs of 2 h length.

Catalyst	#Mo/nm^2	k'_1 m^3 thiophene converted, (mol metal)$^{-1}$.s^{-1}.10^{-3}
MoO_3/Al_2O_3	.09	.47
"dry" impreg-	.22	.34
nation	.46	.45
	.99	.70
	2.16	.83
	4.48	1.05
MoO_3/Al_2O_3	.10	-
wet impreg-	.22	.10
nation	.42	.31
	.95	.63
	1.61	.91
	3.25	1.10
MoO_3/Al_2O_3		
adsorption pH=9	.05	-
pH=6	1.39	.79
pH=1	4.68	.90
MoO_3/Al_2O_3		
Ketjen 120-3E	1.96	1.08
MoO_3/Al_2O_3	.75	.65
Impregnation of	1.42	.87
boehmite	2.27	1.08
	3.69	1.14

The data show that the "intrinsic" rate constant increases with Mo loading to a maximum of approximately 2.5-3.0 Mo/nm^2.

Work by Bachelier et al.[4] also explored HDS activity with respect to molybdenum loading. Catalysts were prepared by aqueous ammonium heptamolybdate impregnation of 238 m^2/g gamma-Al_2O_3 (GFS C Rhône Poulenc). After drying at 110°C for 12 h in air and calcination at 500°C for 2 h under air circulation, catalysts were again heated 2 h at 500°C in air immediately prior to use.

Oxidic catalysts (about 0.240 g) were then introduced into a reactor and sulfided with a H_2 (700 Torr) - thiophene (60 Torr) mixture at 420°C and flow rate of 30 cm^3/min. After 24 h on stream the product mixture was analyzed and activity expressed as the reaction rate r_{hds}, (mol $h^{-1}g^{-1}$) at initial conversion. For noninitial conversions, a first-order behavior was assumed to obtain r_{hds}. A correction for the activity of the support was made: r_{hds} 0.03×10^{-3} mol $h^{-1}g^{-1}$.

wt%MoO_3	#Mo/nm_2	$10^3 r_{hds}$, (mol $h^{-1}g^{-1}$)	"intrinsic" r_{hds} (mmol/mmol Mo/h)
3.1	.56	.31	1.44
4.5	.83	.95	3.04
7.0	1.33	2.63	5.40
8.0	1.53	3.51	6.32
13.3	2.69	5.32	5.64
15.7	3.27	5.96	5.47
19.3	4.20	7.27	5.42
21.6	4.85	7.60	5.06

Graphs of the data will be presented later in this section.

Vissers et al. [5] also did some work on HDS activities with respect to loading.

238 m^2/g gamma-alumina (Rhône-Poulenc) was impregnated with aqueous ammonium heptamolybdate, dried overnight at 110°C in air and calcined at 500°C for 2 h.

Catalysts were sulfided for 2 h at 400°C in an H_2S (9.1 mol%)/H_2 mixture of 60 ml/min flow rate. After the sulfiding (0.2 g sample), a mixture of 6.2 mol % thiophene in H_2 was fed to the reactor (50 ml/min) at 400°C. First order rate constants for t=2 h and t=0 h (initial activity) were calculated.

Catalysts (0.24g) were also sulfided for 20 h at 420°C in a mixture of 7.9 mol% thiophene/H_2 of 30 ml/min flow rate. Data obtained at the end of the 20 h sulfiding step were used to calculate a t=20 h HDS rate constant.

The results presented below were taken from a graph.

wt% Mo	#Mo/nm^2	$k_{hds}(t=0)$	$k_{hds}(t=2)$	$k_{hds}(t=20)$
2	.54	1.8	.9	0.5
4.2	1.18	3.5	2.1	3.5
5.3	1.52	6.2	3.2	6.2
9.4	2.88	10.5	5.8	9.6
15.0	5.08	16.2	8.9	13.6

k_{hds} [(m^3 total feed)/(kg-cat)(s)]10^{-4}

Conversion to "intrinsic" values are given below.

2	.54	1.30	.65	.36
4.2	1.18	1.20	.72	1.20
5.3	1.52	1.69	.87	1.69
9.4	2.88	1.61	.89	1.47
15.0	5.08	1.55	.86	1.31

$k_{intrinsic,\ hds}$, [m^3/(mol metal)(s)]10^{-3}

The data show that the rate constants increase with increasing loading, while the "intrinsic" rates peak at roughly 1.5 to 2.0 Mo/nm^2 (t=0, t=20) and at about 2.0 to 2.5 Mo/nm^2/(t=2). The t=2 data matches that of Thomas et al [3] quite well.

Reddy et al [6] investigated the HDS activity of thiophene with respect to catalyst loading. Catalysts were prepared by incipient wetting of a 204 m^2/g gamma-alumina (Harshaw Al-111-61 precalcined 16 h at 540°C) with pH 8 solutions of ammonium heptamolybdate of appropriate concentration. Samples were then air dried 16 h at 120°C and calcined in air at 540°C for 16 h. Using a differential flow microreactor operating at atmospheric pressure, 0.2 g catalyst samples samples were presulfided for 2 h at 400°C using a CS_2/H_2 mixture (about 40 cm^3/min). The reactor was then flushed with N_2 at 400°C for 1/2 h and the HDS reaction was then carried out in a stream of H_2 saturated with thiophene (80 Torr). Rates were measured under steady-state conditions. Data for the HDS rates were taken from their graph.

wt% Mo	#Mo/nm^2	r_{hds} (10^{-4} mol)/(g catalyst)(h)	"intrinsic" r_{hds}, (mmol/mmol metal·h)
2.0	.64	1.8	.87
4.0	1.31	3.6	.86
6.0	2.03	4.9	.78
8.0	2.79	6.7	.81
10.0	3.62	6.1	.59
12.0	4.50	6.1	.49

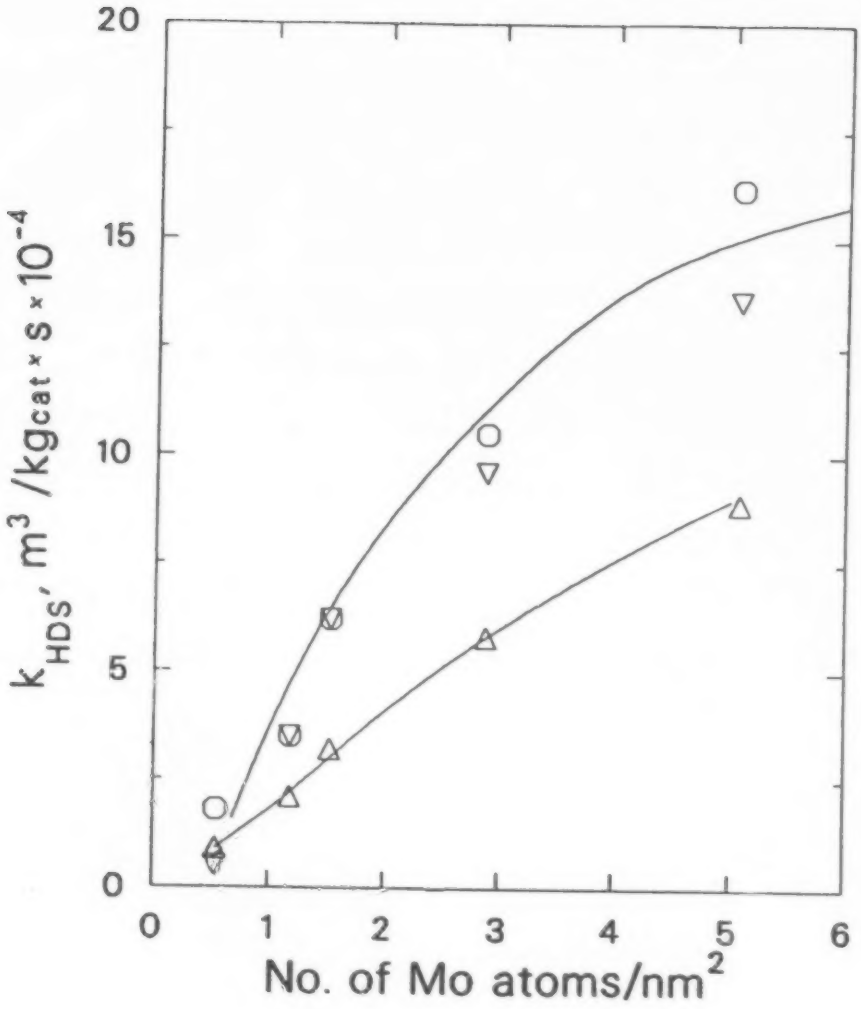

k_{HDS} versus Mo loading:

○ t=0

△ t=2

▽ t=20

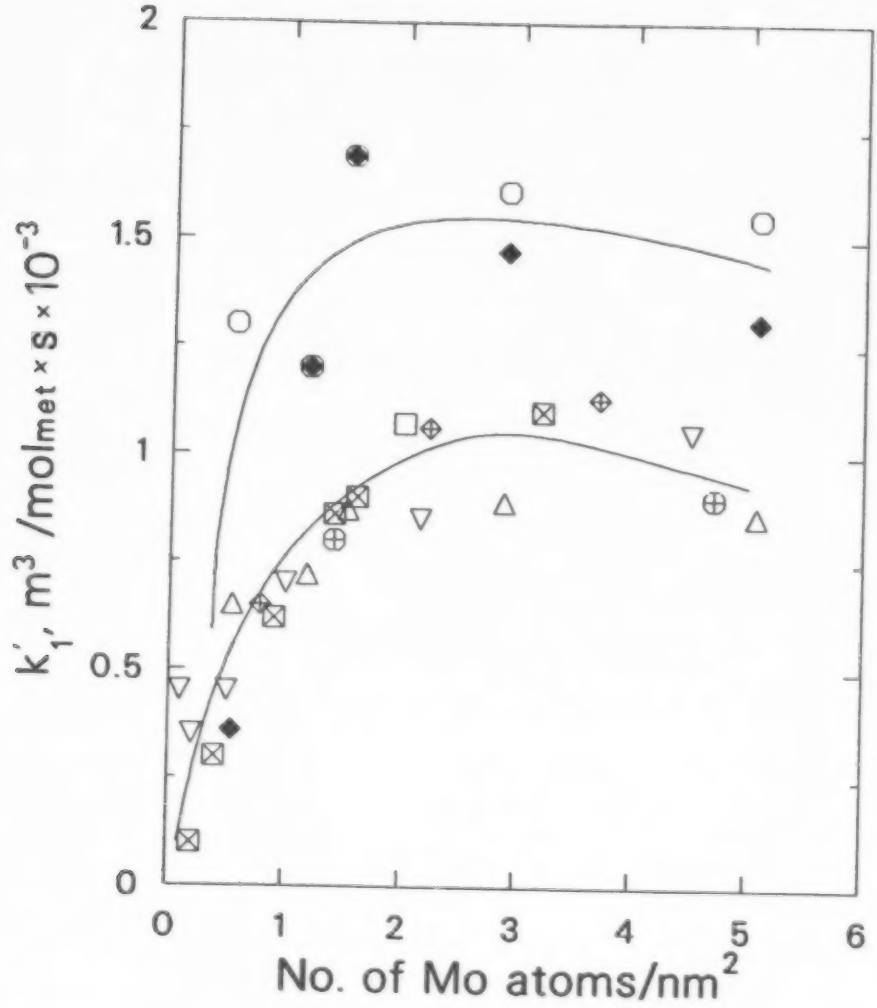

k_{HDS} (intrinsic) versus Mo loading:

○ t=0
△ t=2
◆ t=20
} Vissers et al. [5]

▽ ⊠ ⊕ ⊕ □ Thomas et al. [3]

These data were graphed in conjunction with related work of others.

Finally, Burch and Collins [7] present some activity data for the hydrodesulfurization of thiophene on MoO_3/Al_2O_3 catalysts of various loadings. Catalysts were prepared by wetting 244 m^2/g gamma-Al_2O_3(Ketjen 0003P) with aqueous ammonium heptamolybdate, drying at 120°C for 16 h and calcination at 500°C for 4 h. The catalysts were then presumably presulfided in a 10% v/v mixture of H_2S and H_2 (1200 cm^3/h) either at about 380°C for 1 h or the sequence of 2 h at about 210°C, 1/2 h at 320°C and finally 1-1/2 h at 380°C.

HDS activity of thiophene on the catalysts was determined in a glass microreactor operating under flow conditions at atmospheric pressure at 350°C. 10% v/v thiophene in hexane was injected (0.4 cm^3/h) into an H_2 flow (1200 cm^3/h) and passed through the catalyst sample. Rates were determined after 2 h on stream.

wt% Mo	#Mo/nm^2	rate, mmol/(h)(g-cat)	"intrinsic" rate mmol/h·mol Mo)
4.72	1.31	0.68	1.39
9.11	2.72	1.18	1.24
12.8	4.07	1.53	1.15
16.1	5.45	1.92	1.14

These data are also plotted on the next two pages along with that of Bachelier et al. [4] and Reddy et al. [6].

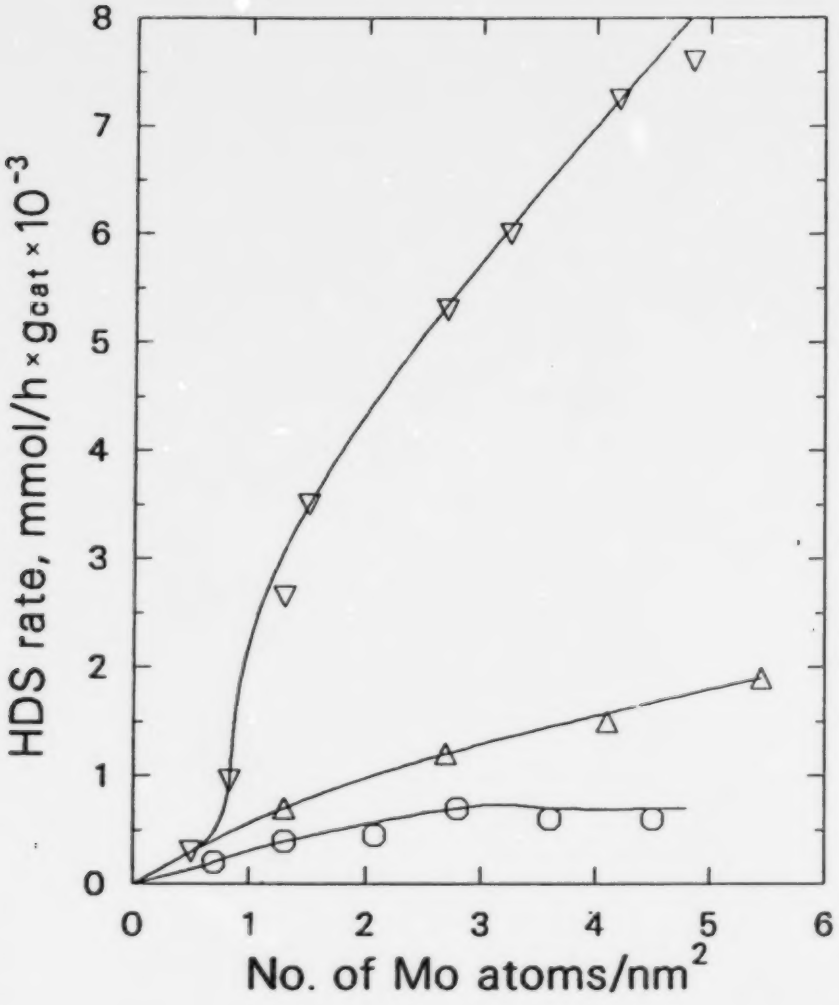

HDS of thiophene at various conditions:

- ○ Reddy et al. [6]
- △ Burch and Collins [7]
- ▽ Bachelier et al. [4]

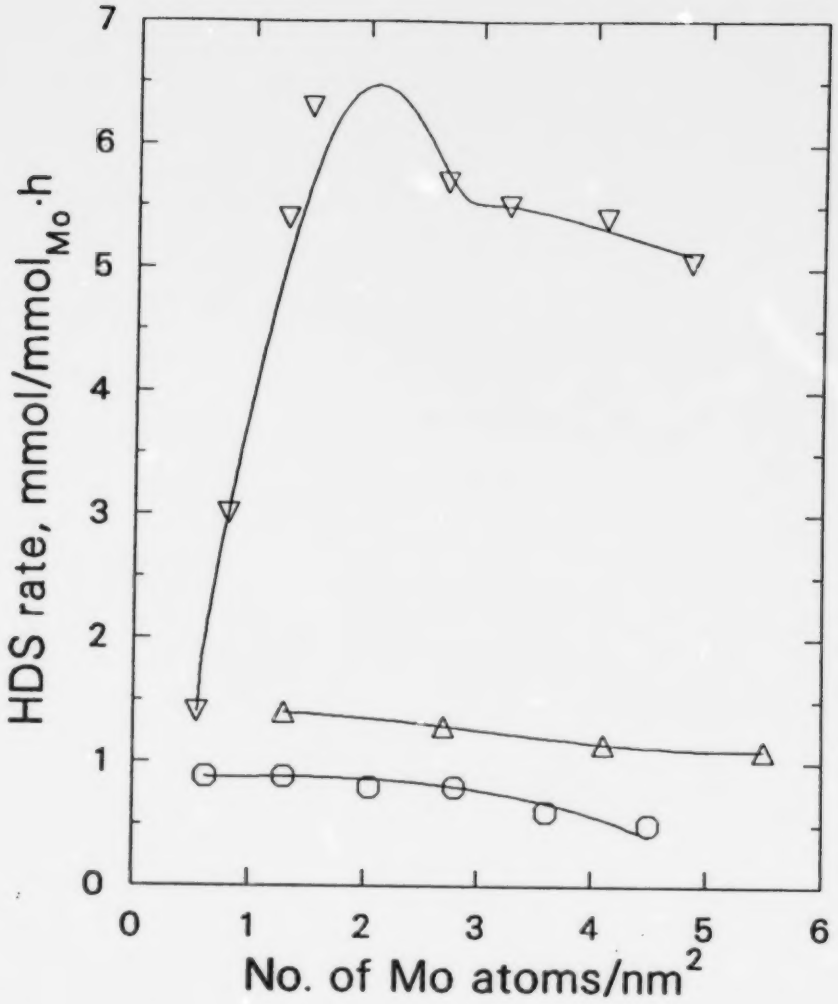

HDS of thiophene related to Mo loading:

○ Reddy et al. [6]

△ Burch and Collins [7]

▽ Bachelier et al. [4]

As shown in the first graph, the HDS rate tends to increase with increasing Mo loading. While a similar trend is shown, the values of rate constant at a given loading are quite different (except below about 0.6 Mo/nm^2). This is likely partly due to the different conditions under which the various HDS of thiophene were measured.

In the case of the "intrinsic" or "specific" rates Bachelier et al. [4] see a maximum at about 1.5 to 2.5 Mo/nm^2 while the other two groups [6,7] find a decreasing trend over the range of Mo loadings examined.

To draw conclusions from these sets of data is rather difficult since HDS activities have been studied under widely varying conditions and constraints, and have been expressed in various ways: raw conversion, rate ($-r_{hds}$), and rate constant (k_{hds}).

In general HDS activity tends to increase as Mo loading increases. Intrinsic rate constants are seen to reach a maximum at about 2 to 3 Mo/nm^2, while the intrinsic rate, r_{hds}, reaches a maximum near 2 Mo/nm^2 in one case [4] after a long time (24 h) on stream, but remains relatively constant in others [6,7] with shorter times on stream.

REFERENCES

1. Y.Okamoto, H.Tomioka, Y. Katoh, T. Imanaka and S. Teranishi, J.Phys.Chem. 84, 1833 (1980).

2. Y.Okamoto, H.Tomioka, T.Imanaka and S. Teranishi, J. Catal, 66, 93 (1980).

3. R. Thomas, E.M. vanOers, V.H.J. DeBeer, J. Medema and J.A. Moulijn, J.Catal. 76, 241 (1982).

4. J.Bachelier, M.J. Tilliette, J.C. Duchet and D. Cornet, J.Catal. 76, 300 (1982).

5. J.P.R. Vissers, J.Bachelier, H.J.M. tenDoeschate, J.C. Duchet, V.H.J.deBeer and R. Prins, in "Proc.8th Int.Congr.Catal." (Berlin 1984), p.II-387, Verlag Chemie 1984.

6. B.M.Reddy, K.V.R. Chary, V.S. Subrahmanyam and N.K. Nag, J.Chem. Soc., Faraday Trans. I, 81, 1655 (1985).

7. R.Burch and A. Collins, Appl.Catal. 17, 273 (1985).

INFRARED SPECTROSCOPY AND $MoO_3.Al_2O_3$ CATALYSTS

This section examines the use of infrared spectroscopy in understanding hydrodesulfurization catalysts, in particular MoO_3/Al_2O_3.

An IR study of the nature of molybdenum species on alumina is difficult due to the very high absorbance of alumina in the region where molybdenum-oxide absorption bands occur. For HDS, this limits study in general to the region above 1000 cm^{-1} where bands due to water and hydroxyl groups are usually the only ones present. Bands below 1000 cm^{-1} have been accessed by Raman spectroscopy as shown previously in the section on the characterization of MoO_3/Al_2O_3.

Some IR results have been reported on the changes of the hydroxyl stretching bands with respect to molybdenum loading for MoO_3/Al_2O_3 catalysts:

[1] eta-alumina, (220 m^2/g) 2 h @500°C in air.

wt% Mo	#Mo/nm^2
3.0	0.90
8.0	2.59

IR spectra were taken after evacuation for 16 h @500°C to remove weakly bound water and hydroxyl groups. Similar spectra were observed after 16 h @380°C. Spectra for samples sulfided 2 h @380°C in 1.7% H_2S/H_2 followed by flushing with N_2 for 16 h @380°C are also shown. Bands were observed at 3770, 3725 and 3670 cm^{-1}.

[2] gamma-alumina (192 m^2/g), equilibrium adsorption, calcination time and temperature not given. (incipient wetness method - 8% Mo).

Mo/g catalyst	#Mo/nm^2
1.1×10^{20}	0.6
2.8×10^{20}	1.3
4.6×10^{20}	2.6
5.0×10^{20}	3.0
7.3×10^{20}	4.6

Samples were calcined 12 h in O_2 and evacuated 1/2 h @500°C before spectra were recorded. Bands are present at about 3780, 3770, 3725, 3680 and near 3640 cm^{-1}. These are similar to those of [1], but with improved resolution, FT-IR being used.

[3] gamma-alumina (238 m^2/g) overnight calcination at 500°C in a muffle furnace.

wt% MoO_3	#Mo/nm^2
4	0.73
8	1.53
12	2.39
20	4.40

Samples were evacuated 20 min @400°C, calcined in O_2 for 1 h @400°C and evacuated again 15 min @400°C. Using FT-IR, bands were observed at 3765, 3725 and 3760, with a shoulder at 3600 cm^{-1}.

Resolution of the bands diminishes with Mo loading increases; a large diminution of the 3770 cm^{-1} band near 1.5 Mo/nm^2 and near loss at 2.5 Mo/nm^2. Loss of this band as well as the one at 3725 cm^{-1} is complete at a loading of 4.4 Mo/nm^2.

Work by Ratnasamy and Knözinger [4] for a 3.17 Mo/nm^2 on alumina (with 650 ppm Na) showed a result similar to those above.

We now examine thiophene, which is a model compound commonly used in studying hydrodesulfurization reactions. Little IR work has been done using thiophene with the MoO_3/Al_2O_3 system; therefore, results from other systems will be reviewed.

To begin, the vibrational modes for thiophene [5] are shown on the following page.

Skeletal modes - vibrational frequency (intensity)

1590 (8)

1404 (35)

1358 (Ra)

1252 (50)

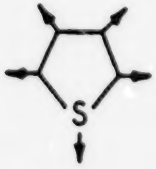

832 (95)

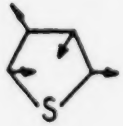

872 (3)

604

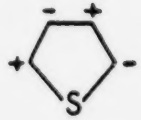

565

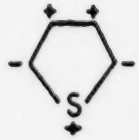

453

Out-of-plane hydrogen modes 835(95), 710 cm^{-1}.

Majority of 835(95) intensity probably due to the ring breathing mode.

In-plane hydrogen deformation modes

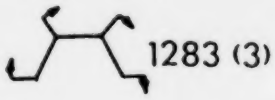

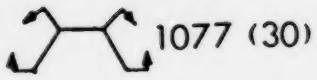

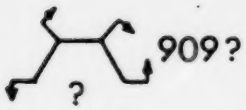

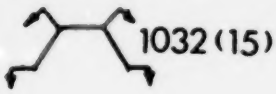

C-H stretching modes occur in the 3100 cm^{-1} region as shown below in the list of peak positions for thiophene vapor and liquid [6]. Mode assignments are inserted (SKEL=skeletal mode, IP=in-plane hydrogen, OP=out-of-plane hydrogen mode).

Vapor	Assignment	Liquid
605	skel	605
710	OP	710
836	skel, OP (95)	836
872	skel (3)	870
909	IP?	904
1035	IP (15)	1035
1077	IP (30)	1080
1252	skel (50)	1255
...	IP (3)	1290
1405	skel (35)	1405
		1479
		1565
	skel (8)	1590
3078	CH str.	3110
3108	CH str.	

Comparison of reference spectra for liquid or solid phase thiophene (API Research Project 44) indicate bands in addition to those listed above.

The interaction of thiophene with various solids will now be examined. An early work by Blyholder and Bowen [7] investigated thiophene chemisorption on silica-supported nickel (Ni/SiO_2). Thiophene was found to react with new bands formed at 2940, 2885 (shoulder), 1610 and 1460 cm^{-1}. The bands at 2940 and 2885 were attributed to C-H stretching of a saturated carbon atom, while the band at 1460 cm^{-1} was assigned to CH_2 or CH_3 bending vibrations. No assignment was proposed for the weak 1610 cm^{-1} band.

In work studying the interaction of thiophene with molybdenum sulfide and cobalt/molybdenum sulfide, Nicholson [6] found bands at 2960, 3005 and 3086 (his studies were in this region only), which he ascribed to CH vibrations of thiophene adsorbed on the surface in various orientations, as shown on the next page.

~3086

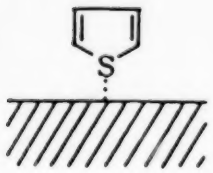

One-Point Form
or gas
or physically absorbed

3005

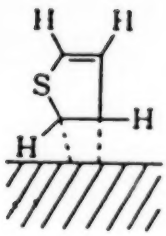

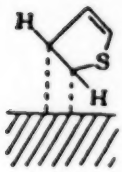

Two-point or side form

2960

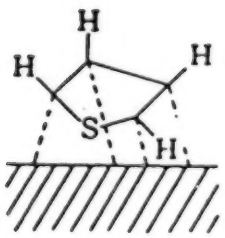

Four-point or flat form

Another work involving unsupported MoS_2 was reported by Ratnasamy and Fripiat [8]. Again, studying the C-H stretching region, they found chemisorbed bands at 3150, 3050 (weak) and 2920, 2850 (stronger). The 2920 and 2850 cm^{-1} bands seemed to relate to C-H stretching of saturated carbon atoms; and, possibilities for the other bands were suggested.

The above two papers [6] and [8] show that interaction of thiophene with MoS_2 seems to lead to saturation of carbon atoms of the molecule. Unfortunately, both studies leave out the spectral regions above and below the C-H stretch region which limits the amount of information gained and hence the possible interpretation.

Ratnasamy and Knozinger [4] looked briefly at the adsorption of thiophene on a commercial Harshaw Co-Mo/Al_2O_3 (similar to 2.5% CoO - 11.5% MoO_3/Al_2O_3) catalyst evacuated 4 h at 600°C. Desorption at 80°C (after 80°C adsorption) left bands at 3790, 3700, 3610, 3110, 1600, near 1480, 1390, 1360, 1215 and 1135 cm^{-1}. Regions of the spectrum were omitted, in particular, 3000 - 1700 cm^{-1} and 1300 - 1240 cm^{-1}. Some band assignments were given. They concluded that molecular thiophene was decomposed on the Co-Mo/Al_2O_3 surface, possibly at a Lewis-acid site, based on poisoning studies with pyridine.

Finally, Sultanov et al. [9] looked at the hydrogenolysis of thiophene on gamma-alumina. Thiophene was found to chemisorb on gamma-alumina with the formation of new bands at 2930, 2860 and 1470 cm^{-1}, attributed to stretching and deformation vibrations of the CH_2 group.

Their work shows that some of the original thiophene bands persist weakly after heating and evacuation. Hydrogenation of chemisorbed thiophene at high pressure resulted in the formation of new bands at 3018, 1360 and 1305 assigned to -CH=CH- stretch, CH_3 and -CH=CH- deformation vibrations, respectively, and suggestive of gas-phase butene.

In general, all the results have shown thiophene to be reactive with many systems (Ni/SiO_2, MoS_2, $Co\text{-}Mo/Al_2O_3$ and Al_2O_3) with resultant chemisorption, and saturation of carbon atoms. Details, however, seem to vary.

Pyridine, a weak base (pK_b=9) has been used in several IR studies to investigate the nature of acidic sites on alumina and molybdena/alumina. It has also been used as a model compound for hydrodenitrogenation. As a probe of surfaces, pyridine can exist in various forms: physically adsorbed, hydrogen bonded, coordinately bonded (Lewis-acid site), or as the pyridinium ion (Bronsted-acid site).

To begin, the vibrational mode assignments for pyridine and the pyridinium ion will be discussed. Pyridine contains 11 atoms and thus has 27 fundamental modes of vibration (3n-6). This planar molecule has a twofold axis of symmetry (C_{2v}) through the nitrogen atom and the gamma-carbon atom. Of the 27 modes, 19 are planar with 10 of class A1 (symmetrical with respect to the C_{2v}-axis) and 9 of class B1 (antisymmetrical with respect to the C_{2v}-axis), and 8 are non-planar (i.e. out-of-plane modes) with 5 of class B2 (antisymmetrical to the C_{2v}-axis) and 3 of class A2 (symmetrical to the C_{2v}-axis). All the vibrations are Raman-active while only those of classes A1, B1 and B2

are infrared-active. In the case of the pyridinium ion, 12 atoms are present resulting in 30 fundamental vibrations. Since the pyridinium in is expected to have C_{2v} symmetry, the fundamentals belong to the same classes as described above with 11 in class A1, 10 in class B1, 6 in class B2 and 3 in class A2. The modes are numbered 1-20 with suffixes a, b in some cases. Based on Wilson's [10] numbering system for benzene modes, Kline and Turkevich [11] show 27 modes of benzene as describing pyridine vibrational motions. These are shown on the following page.

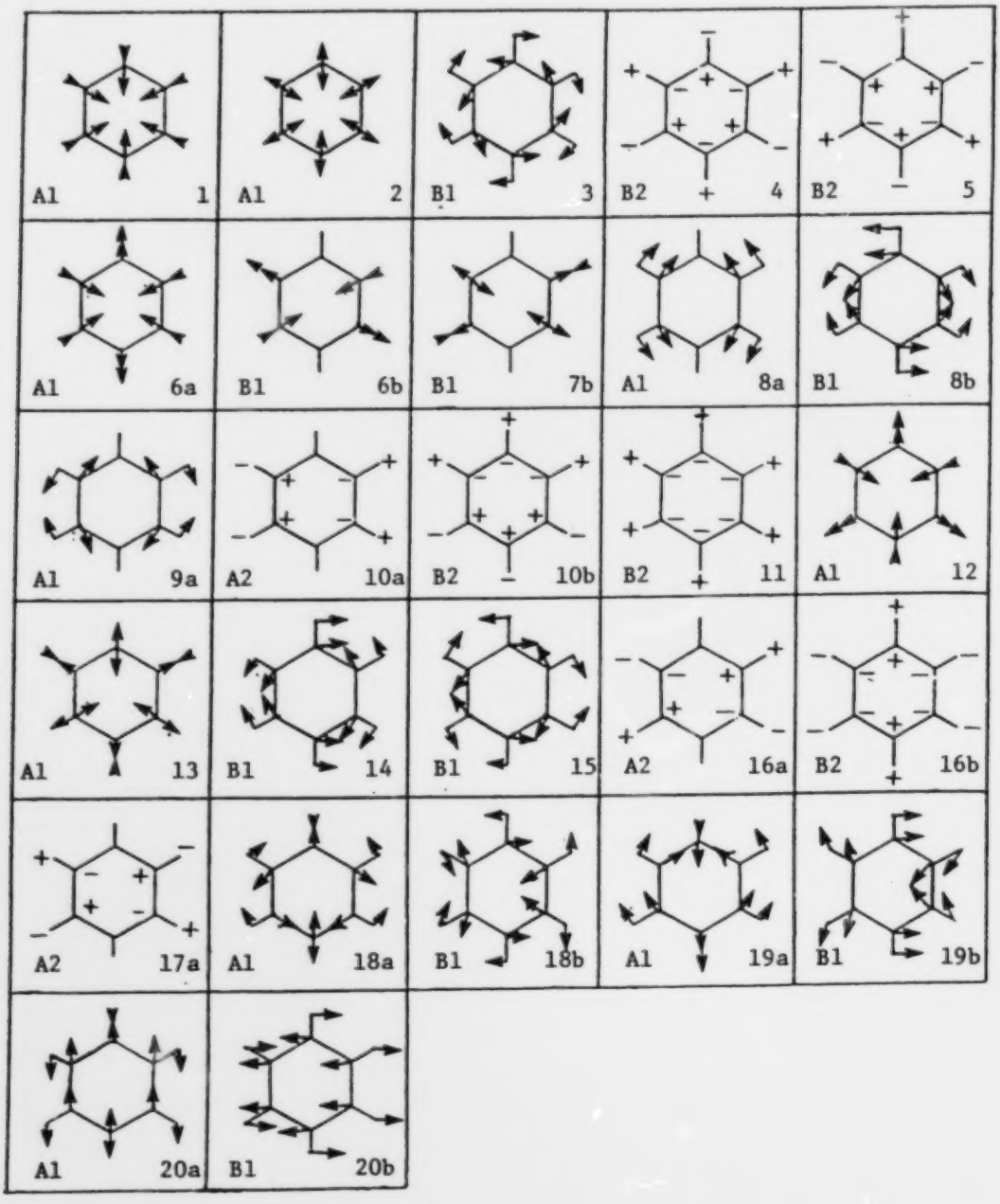

From Kline and Turkevich [11].

For pyridinium ion assignments, Cook [12] uses the above 27 modes, plus the following 3 for a total of 30.

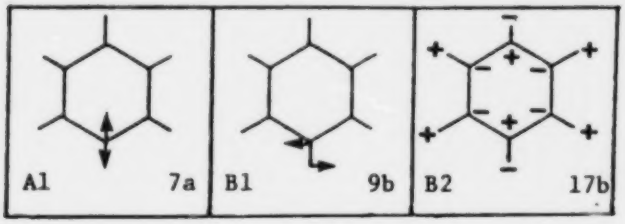

The modes can also be reclassified via the following scheme:

Pyridine and Pyridinium Ion

Class	Ring vibrations	Hydrogen vibrations
A1	1,6a,8a,12,19a	2,7a*,9a,13,18a,20a
B1	6b,8b,14,19b	3,7b,9b*,15,18b,20b
A2	16a	10a,17a
B2	4,16b	5,10b,11,17b*

---

*pyridium only

7a N-H stretch

9b N-H II bend (in-plane)

On the next page, observed and calculated frequencies for the various fundamental modes of pyridine are tabulated along with some frequencies for pyridine complexes and th pyridinium ion. Other references of interest are [5], [11] and [17-20].

		Pyridine			Pyridine Complexes	Pyridinium ion (with $SnBr_6^{2-}$)
Class	Mode	calc[13]	calc[14]	obs[15]	obs[16]	obs[12]
A1	1	981	984	992	1005-1016	1010
	2	3069	3050	3054		
	6a	605	603	605	622-641	
	8a	1597	1581	1583	1597-1610	1638
	9a	1178	1215	1218	1215-1221	1194
	12	1007	1063	1030	1035-1042	
	13	3075	3061	3054		3060
	18a	1030	1025	1068	1069-1082	1030
	19a	1486	1480	1482	1480-1490	1484
	20a	3052	3069	3036		
B1	3	1249	1298	1218		1326
	6b	615	651	652		
	7b	3044	3038	3036		3045
	8b	1575	1573	1572	1568-1575	1608
	14	1311	1224	1375	1379-1390	
	15	1154	1147	1148	1152-1165	1161
	18b	1056	1074	1085		1050
	19b	1420	1441	1435	1437-1449	1535
	20b	3078	3067	3083		
A2	10a	852	891	886		
	16a	401	372	374		
	17a	961	986	981		

		Pyridine			Pyridine Complexes	Pyridinium ion (with $SnBr_6^{2-}$)
Class	Mode	calc[13]	calc[14]	obs[15]	obs[16]	obs[12]
B2	4	756	744	749	750-769	738
	5	984	937	942	930-950	980
	10b	899	882	886		855
	11	712	705	700	680-713	671
	16b	438	404	405	410-426	
						3236 (7a A1)
						1235 (9b B1)

Although the calculated and observed frequencies, as well as the mode assignments for each agree fairly well, agreement is not complete. For example, the theoretical [14] and observed [15] assignments for modes 12 and 18a look like they should be interchanged (which is what Berezin [14] did when comparing the results of others), while calculated and observed results for 3 and 14 differ widely.

Vibrational mode diagrams for the pyridine molecule itself are drawn by Long et al. [13] and correspond fairly well with those drawn for benzene by others, such as Kline and Turkevich [11]. The diagrams drawn for modes 8a, 8b, 9a, 14, 15, 18a, 19a and 19b look like they should be for 9a, 9b, 8a, 15, 14, 19a, 19b, 18a and 18b, respectively.

An infrared reference spectrum for pyridine is available and may be compared to that for the pyridinium ion [12].

Egerton and Hardin [21] recorded both infrared and Raman spectra for liquid pyridine.

Their data show that formation of the pyridinium ion results in intense new bands at about 3240, 1640, 1535, 1325 and 1235 cm^{-1} which are absent in the spectrum of pyridine as well as coordinated pyridine.

In studies of surfaces, only the region of 1400 to 1700 cm^{-1} is generally examined when distinguishing the various forms of pyridine bonding to the surface. A table of major band positions in this region is given for the pyridinium ion as well as hydrogen bonded, coordinatively bonded and free pyridine, based on work by Cook [12], Gill et al. [19] and Parry [22].

	19b	19a	8b	8a
Free or physically bonded:	1435-1440	1478-1482	1572	1578-1582
Hydrogen bonded:	1440-1447	1485-1490	1580-1600	1580-1600
Coordinatively bonded:	1445-1460	1478-1503	1570-1580	1595-1633
Pyridinium ion:	1525-1542	1478-1490	1600-1620	1630-1640

Parry's work [22] illustrates the various bands in this region.

Next, the interaction of pyridine with alumina as studied by infrared spectroscopy will be reviewed. Parry [22] used a sample pre-treatment involving heating at 450°C for three hours after which the sample was cooled to room temperture before recording the IR

spectrum. After the various treatments, spectra were recorded at room temperature.

Parry showed that coordinately bonded (Lewis-acid sites) pyridine is present at all desorption temperatures, while physically and hydrogen-bonded pyridine are seen only below 150°C. As indicated by the absence of a band at 1535 cm^{-1}, pyridinium ion (Bronsted acid sites) is not present.

Work by Hughes and White [23] also showed only the presence of Lewis acidity on alumina, as well as that by Pichat et al. [24], for desorption temperature of 150°C.

Kiviat and Petrakis also looked at pyridine on alumina [25]. Their sample pretreatment included evacuation at 500°C for 16 h, optional reduction in H_2 (20 cc/min) at 500°C for 4 h followed by further evacuation at 500°C for 4 h. Twelve Torr of pyridine was then added in vapor form at 150°C for 1 h, followed by 2 h evacuation at the same temperature. The spectrum usually showed hydrogen-bonded pyridine which subsequently vanished after further evacuation for 16 h at 150°C, leaving only chemisorbed pyridine (coordinately bonded). The addition of HCl resulted in pyridinium ion formation.

Bands for the undoped eta-alumina occurred at 1453, 1496, 1578, 1618 and 1625 (150°C) and at 1457, 1496, 1578 and 1625 cm^{-1} (500°C).

Similar results were obtained by Segawa and Hall [2] using FT-IR. Their procedure included, oxidation or reduction, after which catalysts were evacuated at 500°C for 1 h and cooled to 200°C before exposure to 4 Torr of pyridine vapor for 1 h. The catalyst was then evacuated for 2 h at this or higher temperatures. The IR spectrum was subsequently taken (presumably at room temperature).

The results are similar to those of Parry [22], and Kiviat and Petrakis [25], with respect to the evacuation temperature-dependent band shifts and behavior of the near 1616, 1624 doublet. Furthermore, no Bronsted acidity (pyridium ions) was detected in agreement with the previous results.

Fransen et al. [26] observe only Lewis type acidity on Al_2O_3 and find that even the presence of water vapor before pyridine adsorption will not create Bronsted acidity.

Using photoacoustic FT-IR, Riseman et al. [27] studied the uptake of pyridine on sulfided Al_2O_3. Calcined catalysts were treated at 525°C for 4 h in an O_2 flow followed by overnight evacuation. Sulfidation was accomplished in a 9.7% H_2S/H_2 gas flow at 400°C for 2 h followed by overnight evacuation. Catalysts were then exposed to 18 Torr of pyridine at 150°C for 1 h, after which the catalyst was purged in flowing helium at 150°C for 16 h to remove as much physically adsorbed pyridine as possible. The sample was then cooled to room temperature. The pyridine spectrum for sulfided Al_2O_3 appeared to be the same as that for unsulfided alumina, with evidence for only coordinately bonded pyridine.

Knozinger and Kaerlein [28] using pyridine on delta-alumina revealed hydrogen bonded and coordinately bonded pyridine. As desorption temperature was raised, the bands for the hydrogen bonded species diminished.

To summarize, work on pyridine uptake on eta- and gamma-alumina, whether sulfided or unsulfided, has shown no evidence for Bronsted acidity (pyridinium ion formation). Pyridine is instead either

physically adsorbed, hydrogen bonded, or coordinately bonded (Lewis acidity). Pumping and prolonged heating at 150°C is sufficient to remove the physically held and hydrogen bonded species leaving behind the coordinately bonded pyridine. Due to the doublet at about 1618 and 1625 cm^{-1}, present at 150°C which becomes a single peak (1625 cm^{-1}) by the time 500°C is reached, Kiviat and Petrakis suggested the presence of both strong and weak Lewis-acid sites. Examining the other data suggests that pyridine bonded to the weaker sites is desorbed between 230 and 300°C, while the strongly bonded pyridine remains at a temperature of 565°C.

We now look at the uptake of pyridine on molybdena/alumina. IR work by Kiviat and Petrakis [25] showed evidence for pyridinium ion formation. The MoO_3/Al_2O_3 catalysts were prepared by ammonium heptamolybdate (aqueous) impregnation, drying at 100°C for 2 h, followed by 500°C calcination at 18 h in air current. Sample pretreatment included evacuation at 500°C for 16 h, optional reduction in H_2 (20 cc/min) at 500°C for 4 h followed by further evacuation at 500°C for 4 h. Twelve Torr of pyridine vapor was then added at 150°C for 1 h followed by a 2 h evacuation at the same temperature. Further evacuation was done at 150°C for 16 h. Spectra were recorded at room temperature. Coordinately bonded pyridine appeared to be present in all spectra. Additionally, the presence of pyridinium ion (Bronsted acidity), signalled by the presence of bands at about 1540 and 1640 cm^{-1}, was seen for 6% and 9% MoO_3/eta-Al_2O_3 and for 10% MoO_3/gamma-Al_2O_3. Although the exact loading (#Mo/nm^2) is unknown, since the alumina surface area was not given, the relative areas of

the 1540 cm^{-1} and 1640 cm^{-1} peaks increase with MoO_3 loading for the catalyst samples, suggesting that an increase in molybdenum on the surface results in more pyridinium ion formation. The 2% MoO_3/eta-Al_2O_3 sample does not show Bronsted acidity, either due to low concentration or the nature of the molybdenum bonding at low loading.

A further experiment using 10 wt% eta-Al_2O_3 or MoO_3 in KBr wafers showed pyridine chemisorption on the eta-Al_2O_3 but not on MoO_3. Segawa and Hall [2] also investigated pyridine on molybdena/gamma-alumina. The alumina used had a surface area of 192 m^2/g and catalysts were prepared either by incipient wetness (8% Mo/Al_2O_3 sample) or by equiiibrium adsorption. Calcination data were not given. Sample treatment for FT-IR included the following. After oxidation or reduction, catalysts were evacuated at 500°C for 1 h and cooled to 200°C before exposure to 4 Torr by pyridine vapor for 1 h. Catalysts were then evacuated at this or higher temperatures for two hours. Subsequently, unless further treatment was performed, the IR spectrum was recorded.

Pyridinium ion formation was seen for an oxidized 8% Mo/Al_2O_3 (3.0 Mo/nm^2) sample before and after addition of water vapor. Coordinately bonded pyridine was also observed. Reduction of the sample in H_2 for 1 h at 500°C, however, eliminated the ability to form pyridinium ions.

For oxidized catalysts, Lewis acidity decreased with increased molybdenum loading, particularly above roughly 2.6 Mo/nm^2 (near $4.5x10^{20}$ Mo/g), while Bronsted acidity being absent at about 0.7 Mo/nm^2 ($1.3x10^{20}$ Mo/g), then appeared to increase linearly above this "threshold" up to a last measured value of 4.6 Mo/nm^2 ($7.3x10^{20}$ Mo/g). The values for Lewis and Bronsted acidities were taken as the

areas under the 1455 and 1540 cm^{-1} peaks, respectively.

Work by Fransen et al. [26] also looked at MoO_3/Al_2O_3. Although Bronsted acidity was found to be present in some cases, the details given with the results were not sufficiently clear to justify comment.

Using photoacoustic FT-IR, Riseman et al. [27] looked at pyridine adsorption on both calcined and sulfided Mo/Al_2O_3. Catalysts were prepared by incipient wetness impregnation using a 210 m^2/g eta-alumina. Calcined catalysts (unspecified calcination parameters) were treated at 525°C for 4 h in flowing O_2 followed by overnight evacuation. Sulfidation was carried out in a 9.7% H_2S/H_2 gas flow at 400°C for 2 h followed by overnight evacuation. Catalysts were then exposed to 18 Torr of pyridine at 150°C for 1 h, after which the catalyst was purged in flowing helium for 16 h at 150°C. The sample was then cooled to room temperature.

The spectrum of 7.6 Mo/Al_2O_3 (2.54 Mo/nm^2) calcined only, included a band at 1541 cm^{-1}, indicating the presence of pyridinium ion, as well as coordinately bonded pyridine. On the sulfided sample (2.54 Mo/nm^2), only coordinately bonded pyridine is observed. The 1541 cm^{-1} band for pyridinium ion appears to be absent.

A similar result was observed by Mone [29] for sulfided Mo/Al_2O_3. Catalysts were prepared by ammonium molybdate impregnation of 153 m^2/g gamma-Al_2O_3 followed by overnight drying and calcination at 650°C. Pretreatment for IR work included outgassing at 420°C to a final pressure of $<10^{-5}$ Torr followed by pyridine adsorption at room temperature and desorption at 150 and 250°C. Sulfidation was carried out in a 20% H_2S/H_2 mixture for 1.5 h at 200°C followed by 1.5 h at 320°C. The sample was then cooled to room temperature and stripped

with H_2. Evacuation for 2 h at 350°C followed, and after this, pyridine adsorption.

Although unspecified, the loading was probably 12-15 wt% MoO_3/Al_2O_3 (2.3 to 2.9 Mo/nm^2). For the oxidic sample, both Bronsted and Lewis acidity are seen for 150°C desorption on Mo/Al_2O_3, while only Lewis type remains for the 250°C desorption. In the case of the sulfided sample, however, no Bronsted acidity is seen, even with the 150°C desorption temperature.

Also, according to Ratnasamy and Knözinger [28], no pyridinium ion is observed for sulfided Harshaw catalyst ($Co-Mo/Al_2O_3$) with sulfidation of 250°C for 4 h in a 10:1 H_2/CS_2 mixture.

In summary, we find that Mo/Al_2O_3 catalysts exhibit Bronsted, as well as Lewis acidity for loadings above 0.7 Mo/nm^2 with catalysts in oxidic form, and that Bronsted acidity increases with increased molybdenum loading. Once the Mo/Al_2O_3 catalyst is reduced or sulfided, pyridinium ion formation is eliminated leaving only coordinately bonded pyridine (as well physically and hydrogen bonded pyridine for T<150°C).

REFERENCES

1. N. Topsoe, J.Catal. 64, 235 (1980).
2. K.-I. Segawa and W.K. Hall, J. Catal. 76, 133 (1982).
3. M. Cornac, A. Janin and J.C. Lavalley, Infrared Phys. 24, 143 (1984).
4. P. Ratnasamy and H. Knozinger, J. Catal. 54, 155 (1978).
5. A.R. Katritzky, Quart. Rev. Chem. Soc. 13, 353 (1959).
6. D.E. Nicholson, Anal. Chem. 34, 370 (1964).
7. G. Blyholder and D.O. Bowen, J. Phys. Chem. 66, 1288 (1962).
8. P. Ratnasamy and J.J. Fripiat, Trans. Faraday Soc. 66, 2897 (1970)
9. A.S. Sultanov, U.B. Khakimov, G.Sh. Talipov and J.M. Shchekochikhin, React. Kinet. and Catal. Lett. 2, 243 (1975).
10. E.B. Wilson, Jr., Phys. Rev. 45, 706 (1934).
11. C.H. Kline, Jr. and J. Turkevich, J.Chem. Phys. 12, 300 (1944).
12. D.Cook, Can.J.Chem. 39, 2009 (1961).
13. D.A. Long and E.L. Thomas, Trans. Faraday Soc. 59, 12, 783 (1963).
14. M.A. Kovner, Yu.S. Korstelev and V.I. Berezin, Optics and Spectroscopy 10, 233 (1961); V.I.Berezin, Optics and Spectroscopy 15, 167 (1963).
15. J.K. Wilmshurst and H.J. Bernstein, Can. J. Chem. 35, 1183 (1957).
16. A.T. Balaban, G.D. Mateescu and M. Elian, Tetrahedron, 18, 1083 (1962).
17. L. Corrsin, B.J. Fax and R.C. Lord, J.Chem. Phys. 21, 1170 (1953).
18. N.N. Greenwood and K. Wade, J.Chem. Soc. 1130 (1960).
19. N.S. Gill, R.H. Nuttall, D.E. Scaife and D.W.A. Sharp, J.Inorg. Nucl. Chem. 18, 79 (1961).

References-continued

20. Y. Kakiuti, M. Akiyama, N. Saito and H. Saito, J. Mol. Spectrosc. 61, 164 (1976).

21. T.A. Egerton and A.H. Hardin, Catal. Rev.-Sci. Eng. 11, 71 (1975).

22. E.P. Parry, J.Catal. 2, 317 (1963).

23. T.R. Hughes and H.M. White, J.Phys. Chem. 71, 2192 (1967).

24. P.Pichat, M-V. Mathieu and B. Imelik, Bull.Soc.Chim.Fr. 2611 (1969).

25. F.E. Kiviat and L. Petrakis, J.Phys.Chem.77, 1232 (1973).

26. T.Fransen, O.van der Meer and P. Mars, J.Phys.Chem. 80, 2103 (1976).

27. S.M. Riseman, S. Bandyopadhyay, F.E. Massoth and E.M. Eyring, Appl. Catal. 16, 29 (1985).

28. H. Knözinger and C.-P. Kaerlein, J.Catal. 25, 436 (1972).

29. R.Moné, "Preparation of Catalysts", B. Delmon, P.A. Jacobs and G. Poncelet (Eds.), Elsevier, Amsterdam, 1976, p.381.

B. PREPARATION OF CATALYSTS

B-1. Use of gamma-alumina in preparing catalysts for infra-red spectroscopic "in situ" studies.

B-2. Preparation and analyses of various Mo loadings on alumina.

B-3. Miscellaneous observations.

B-1. USE OF γ-ALUMINA SUPPORTS

Since this research program was intended to rely heavily upon infrared spectroscopic techniques applied to heterogeneous catalysis, the catalysts to be studied must exhibit adequate transparency to infrared radiation over the spectral regions of interest between 4000 and 1000 cm^{-1}. The molybdena-based catalysts were prepared using an impregnation technique with γ-alumina as the support material.

Preliminary experiments used ALON (a commercial finely particulate form of fumed γ-alumina) because of its high surface area and simplicity in forming very thin wafers simply by dry compression. Its usefulness was questioned because of analytical results indicating as much as 1% Cl content by weight. Steam leaching successfully hydrolyzed more than 90% of the chloride present but very slowly, even inefficiently. Alternative leaching experiments using 0.1 M HNO_3 as solvent plus centrifugation to remove aluminum metal particles enabled purification to <0.02% by wt chloride ion. Alternative γ-alumina supports were prepared using aluminum isopropoxide and other commercial aluminas. Of these forms, only the dechlorinated ALON remained in sufficiently fine-sized particles that IR-transparent wafers could easily be prepared. All other alumina forms necessitated excessive time-consuming grinding in an agate mortar-and-pestle (no contamination by the grinder) to ensure a fine-size powder adequate for IR needs.

Chloride, molybdenum and nickel contents of various catalysts were determined by neutron activation analysis using a SLOWPOKE nuclear reactor. (The details of the ALON preparation are summarized in the attached page from the University of Alberta SLOWPOKE facility.)

The Use of "Alon" Gamma-Alumina as a Catalyst Support in the Preparation of Hydrodesulphurization Catalysts

Przystajko W., Konkin M. and Dalla Lana I.G., *Department of Chemical Engineering, University of Alberta.*
Ng D., *UASF.*

"Alon" is a special kind of alumina having excellent transmission for IR. Therefore, it is useful as a catalyst support in laboratory experiments when IR measurements are necessary. Since commeercial "Alon"is contaminated by a relatively high amount of chlorine (about 1.5 wt.%), a purification procedure is required to remove chlorine.

The method of washing with acidic solutions and subsequent heat treatment has been used for "Alon" purification. The washing procedure reduces the chlorine content to 0.97 wt.% and 0.17 wt.%, respectively, after treatment 0.001M and 0.1M nitric acid. Subsequent heating to 550 degrees Celsius lowers these values to 0.20 wt.% and 0.018 wt.% for the two acid concentrations. The latter contamination level is acceptable for use of "Alon" as a support. All quantitative analyses of chlorine content have been made using neutron activation analysis on the SLOWPOKE.

The dechlorinated "Alon" has been applied to the preparation of molybdenum and nickel-molybdenum catalysts. A quantitative analysis of nickel and molybdenum content is required for further investigations. The standard chemical methods require dissolved samples. It is very difficult to dissolve alumina catalysts and, therefore, neutron activation analysis is an especially useful technique for this purpose because it permits omission of the dissolution procedure.

For the instrumental neutron activation analysis (INAA) samples of approximately 100 mg were irradiated for 5 minutes at $1.0 \times 10^{11} n.cm^{-2}s^{-1}$ and counted for 8 minutes inside a lead cave after an 8 minute cool time. Results were compared with standards which were prepared from compounds and elements of known composition.

B-2. PREPARATION OF Mo/Al_2O_3 CATALYSTS

Preliminary preparation of $Ni\text{-}Mo/Al_2O_3$ catalysts, at various metal loadings at constant Ni-to-Mo ratio, indicated that IR measurements by transmission of the beam through the catalyst wafer were only possible at the lower metal loadings, especially after sulfidation of the catalyst. The literature survey had early indicated that studies of Mo/Al_2O_3 catalysts were necessary if a sound scientific approach were to be followed. Accordingly, the experimental study was directed to examining the H_2S uptake of catalysts with varying Mo content supported on dechlorinated ALON gamma-alumina.

The preparation of dechlorinated ALON, the impregnation with ammonium hexamolybdate solutions, and the analysis for Mo content have been described in earlier reports. Representative samples of these catalysts were also provided to Dr. C. Fairbridge for his use.

B-3. MISCELLANEOUS OBSERVATIONS

The literature survey suggested that laser Raman spectroscopy was a more sensitive indicator of the presence of different "crystalline" faces than was possible via X-Ray diffraction measurements. Considerable effort was directed towards this end. To obtain LRS measurements, equipment presently in the Department of Chemistry at the University of Alberta was employed. This research was delayed very considerably because of the consecutive demises of the laser sources in both Raman spectrometers. At the end of 1985, only partial completion of the experiments had been attained.

Early in 1986, samples were mailed to Professor R. Kydd at the University of Calgary for LRS measurements. Over a period of about three months, ending in March, 1986, these LRS analyses were completed. These data have not yet been reported.

C. CONSTRUCTION OF EXPERIMENTAL EQUIPMENT

As a part of this research project, equipment was to be constructed enabling catalysts to be treated (oxidized, reduced, contacted with adsorbate molecules, etc.) within a closed cell enabling IR measurements by transmission spectroscopic means. This cell was to have the capability of being switched into an open mode permitting continuous flow of reactant molecule(s) into and product molecule(s) from the IR cell. While in the open mode, the activity of the catalyst as a function of stage of pretreatment could be evaluated using a model test reaction. Infrared spectral scans could also be completed in either closed or open modes of operation to provide information about the catalyst and the surface reaction upon it.

It was further proposed to construct an apparatus which could be connected to the above reactor/IR cell, or which could operate on a stand-alone basis for temperature-programmed desorption experiments. Some funding for the IR cell-reactor and for the TPD apparatus was obtained as part of this research contract, as well as via support from the University of Alberta and the National Science and Engineering Research Council.

Descriptions of the following equipment items are listed in this section:

1. Sketch of the novel IR cell-reactor, and a flow diagram indicating the closed or open modes of operation;
2. Description of the seal developed between the IR crystal windows and the polished face of the cell body;

3. Layout of equipment for temperature-programmed-desorption studies, including the new clean turbopump vacuum installation.

1. IR CELL-REACTOR

Figure 1 shows a sketch of the cell exterior. The catalyst, in the form of a thin wafer mode from compression of fine powder, is placed within a metal holder which slides vertically downwards into the cell along machined grooves. The holder positions the wafer transverse to the IR beam. At this location, with the cell in the closed mode, the pretreatment or dosing with measured amounts of an adsorbate gas is conducted via the existing vacuum port shown in figure 2. Figure 2 also shows the layout of the apparatus whereby it may be switched from the closed mode to open mode for kinetics measurements. The IR cell-reactor is maintained at a desired reaction temperature, the recirculation lines are heat-traced electrically, and the recirculation pump is kept at a temperature sufficiently high to prevent condensation of any recirculating gaseous/vapour component. The capabilities of the apparatus are only limited by the integrity of the seal between the IR crystal windows and the side-faces of the cell body, assuming the stainless steel cell body remains catalytically inert at the elevated temperatures.

To facilitate operation varying from several atmospheres to 10^{-9} mbar vacuum, and from room temperature to some upper temperature (say $500^{o}C$ +), a novel pressure seal was developed. This will now be described in more detail.

FIGURE 1 : VIEWS OF IR CELL

EXTERIOR

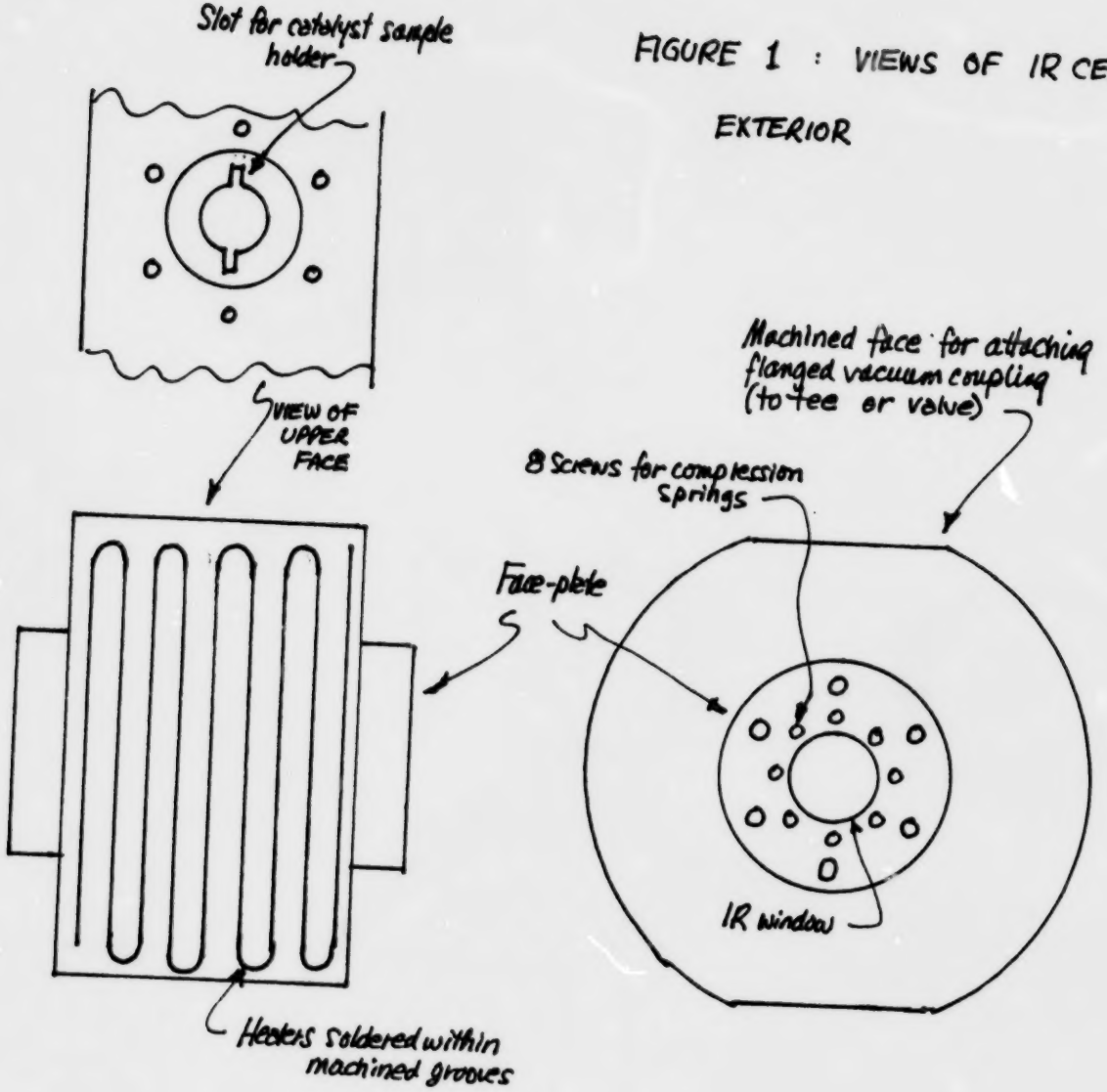
Slot for catalyst sample holder
VIEW OF UPPER FACE
Machined face for attaching flanged vacuum coupling (to tee or valve)
8 Screws for compression springs
Face-plate
IR window
Heaters soldered within machined grooves

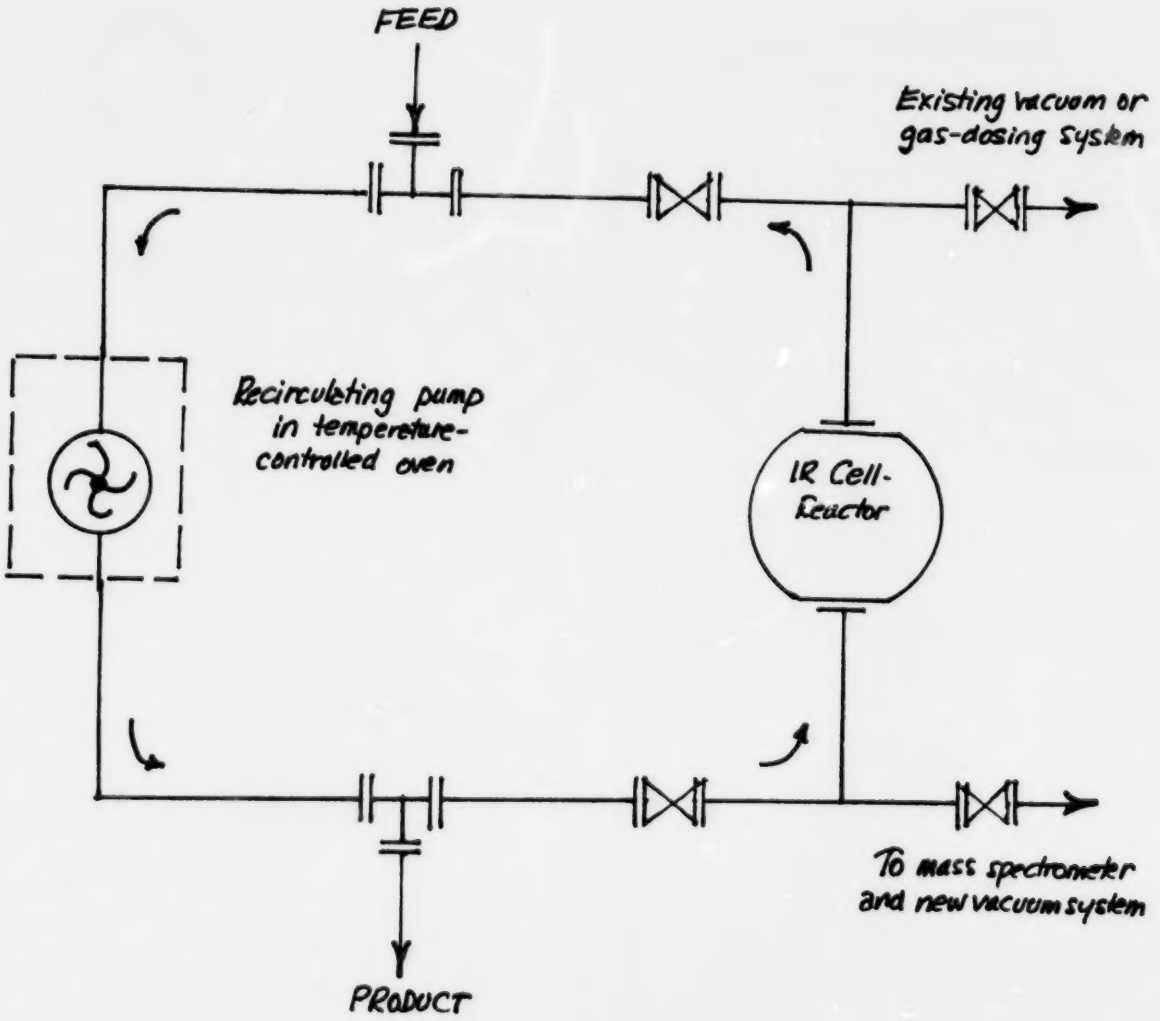

FIGURE 2 : Open or closed operational modes

2. DESIGN OF "PRESSURE-PLATE" VACUUM SEAL

Considerable effort was directed at developing a means of attaching IR-transparent windows made of polished crystals (NaCl, CaF_2, etc.) so as to cover an aperture in a cell body through which and IR beam could pass. The specifications for this crystal to metal joint was that it should maintain high vacuum (10^{-9} mbar) or moderate pressures (> 1 atm) even though the cell might be heated (or cooled) between room temperature and some elevated temperature (as high as physically possible). The differences in coefficients of expansion between the crystal windows and the metal body prevented use of cements (such as epoxy resins). Cementing created sufficient stresses in the windows to crack them even though the epoxy bond was maintained. Use of AgCl cements to bond window edges to a cylindrical recess to contain the window also was considered and discarded because of the complexity involved.

After a number of designs were tested, the mechanical seal system described in figure 3 was developed to meet the specifications cited. The seal incorporates a spring-loaded pressure plate which accommodates stresses on the crystal window which might arise during heating or cooling operations. Eight circumferential screws tighten onto heavy-duty springs which force a pressure plate onto the surface of the crystal window. The force exerted by each compressed spring is identical providing a uniform pressure onto the crystal surface irrespective of the operating temperature or internal pressure of the system.

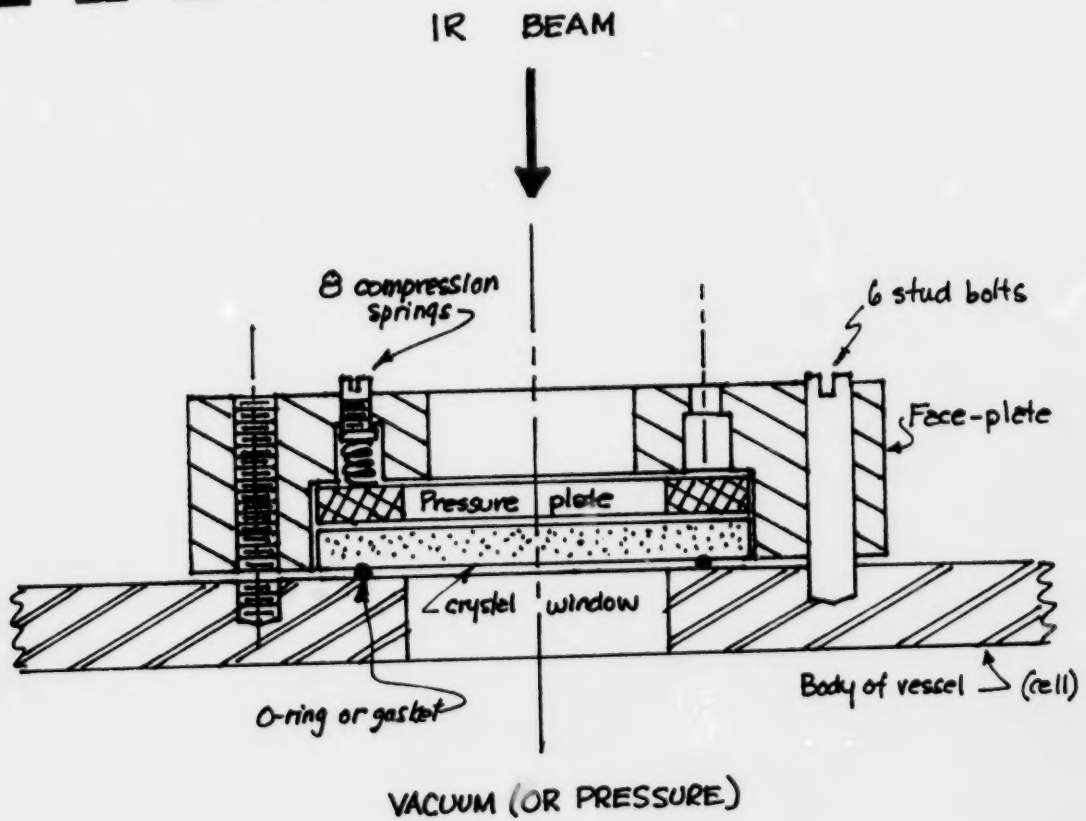

FIGURE 3 : Novel mechanical seal

The actual vacuum (or pressure) seal is effected between the polished surfaces of the crystal window and the cell body by using either gaskets or "O"-rings. Katrez (a DuPont perfluoro-elastomer) rings effectively provided seals up to 300°C temperatures. For operation above the elastomer's limiting temperatures, gold gaskets or a ring-shaped welded gold wire enabled much higher temperatures to be attained. It was necessary to obtain a mirror-quality polished face on the cell body and use of high-purity soft gold free of scratches, etc. to ensure seals of high integrity.

This type of seal may be useful in a variety of research applications in addition to its use in the construction of an IR cell-reactor. Patenting of this design concept may have some merit?

3. A TEMPERATURE-PROGRAMMED-DESORPTION APPARATUS

Figure 4 provides a schematic layout of the equipment components and connecting lines whereby temperature-programmed-desorption of a chemisorbed substituent from a solid adsorbent may be studied. This scheme embodies desorption into a vacuum environment maintained by the turbopump system, and which must be sufficiently low that a quadrupole mass spectometer may be directly connected to the TPD chamber. The MS repetitively scans preselected mass numbers in sequence (up to 8) in very short time cycles (10 to 15 seconds) during the about 10-15°C/min heating-rate. The TPD may entail heating from room temperature to 600°C, or so, thus requiring approximately 45 min to one h total time and about 250 MS scans. A small dedicated computer monitors the MS and is programmed to plot the signal height for any mass number as a function of time (or temperature).

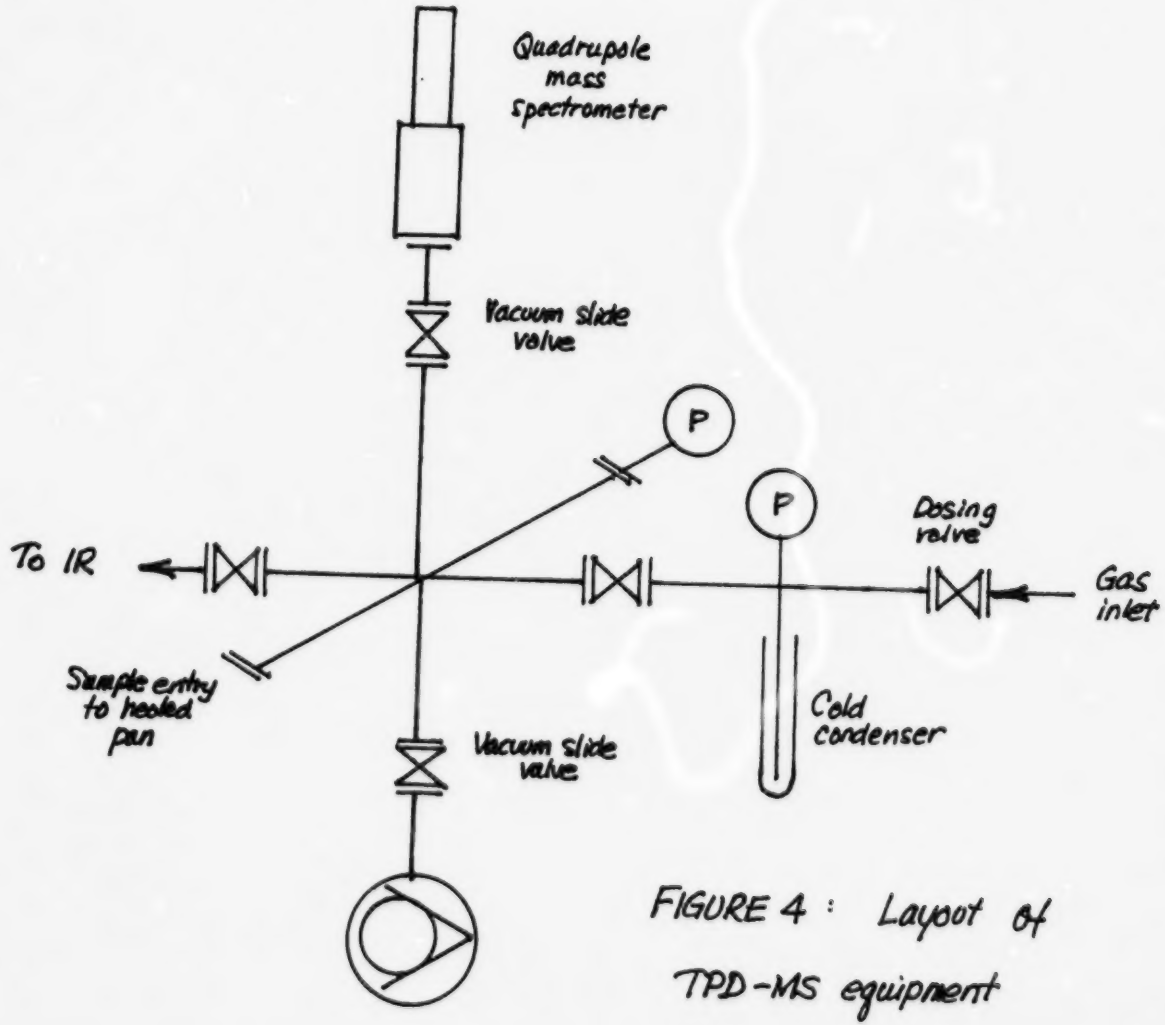

FIGURE 4 : Layout of TPD-MS equipment

The apparatus enables quantitative measurement of both physical and chemical adsorption of a gas upon the solid by using pressure (volume of gas) measurements in an entry manifold of calibrated total volume, along with a liquid-N_2 cooled condenser. The apparatus will also be connected to the IR cell-reactor equipment to enable species identification via the quadrupole mass spectrometer. Additional capabilities such as temperature-programmed-reduction, etc. are also being considered in future studies.

D. PROGRESS ON FUNDAMENTAL RESEARCH ON THE CHARACTER OF MoO_3/Al_2O_3 CATALYSTS

The initial focus of this work involved a systematic quantitative study of H_2S uptake upon oxidized MoO_3/ALON wafers, along with both IR and LRS spectral scans of various relevant samples. The quantitative work was directed at the measurement of H_2S uptakes on catalysts of varying Mo loading during their sulfidation. Additional measurements (estimates in some cases) of the water formed were also intended.

Blank test results indicated that H_2S uptake within the apparatus was also occurring, and to some extent, uptake of H_2 when the sample oven was at elevated temperatures. Considerable effort was directed towards elimination of this problem. The use of copper gaskets in the all-metal vacuum flange connections caused considerable H_2S chemical interaction. By testing a number of alternative gasket materials:

1) covering copper by sputtered gold technique
2) covering copper with gold by dipping into appropriate solutions of gold salts
3) electroplating gold onto copper gaskets
4) machining gaskets from alternative materials such as nylon, teflon, etc.

it was found that the problem could be reduced to a low-level background H_2S uptake, which could be largely reproduced. The electroplated gold onto copper gaskets were the sole copper form found to be reliable at higher temperatures. However, very adequate vacuum seals were also obtained by using gaskets nearly identical in size (perhaps slightly thicker than copper gaskets) but machined from teflon. The combination of the above, finally resulted, late in

1985, in some experimental data being obtained on H_2S uptakes.

With the completion of the LRS spectral, some H_2S uptake measurements in this work, plus some parallel information on O_2 and NO uptakes on the catalysts, the analysis of the data and preparation of a paper for publication were undertaken. This work was being done by Dr. M. Konkin after the completion of the contracted period, ending in February, 1986. Her new professional duties have prevented quick completion of this paper but it is anticipated that this analysis will be completed this summer. Since this forthcoming paper will utilize all of the fundamental data eventually obtained, this report will not elaborate on this item.